

NAVAL POSTGRADUATE SCHOOL

Monterey, California

AD-A205 101



THESIS

COMPUTATION OF MONOPOLE ANTENNA CURRENTS
USING CYLINDRICAL HARMONIC EXPANSIONS

by

Robert C. Hurley

December 1988

Thesis Advisor:

Michael A. Morgan

Approved for public release; distribution is unlimited

DTIC
ELECTE
MAR 13 1989
S H D

89 3 13 032

UNCLASSIFIED

SECURITY CLASSIFICATION OF THIS PAGE

REPORT DOCUMENTATION PAGE				Form Approved OMB No 0704-0188	
1a REPORT SECURITY CLASSIFICATION UNCLASSIFIED			1b RESTRICTIVE MARKINGS		
2a SECURITY CLASSIFICATION AUTHORITY			3 DISTRIBUTION / AVAILABILITY OF REPORT Approved for public release; distribution is unlimited		
2b DECLASSIFICATION / DOWNGRADING SCHEDULE			4. PERFORMING ORGANIZATION REPORT NUMBER(S)		
6a NAME OF PERFORMING ORGANIZATION Naval Postgraduate School			6b OFFICE SYMBOL (If applicable) 62		7a NAME OF MONITORING ORGANIZATION Naval Postgraduate School
6c ADDRESS (City, State, and ZIP Code) Monterey, California 93943-5000			7b ADDRESS (City, State, and ZIP Code) Monterey, California 93943-5000		
8a NAME OF FUNDING / SPONSORING ORGANIZATION		8b OFFICE SYMBOL (If applicable)		9 PROCUREMENT INSTRUMENT IDENTIFICATION NUMBER	
8c ADDRESS (City, State, and ZIP Code)		10 SOURCE OF FUNDING NUMBERS			
		PROGRAM ELEMENT NO	PROJECT NO	TASK NO	WORK UNIT ACCESSION NO
11 TITLE (Include Security Classification) COMPUTATION OF MONOPOLE ANTENNA CURRENTS USING CYLINDRICAL HARMONIC EXPANSIONS					
12 PERSONAL AUTHOR(S) HURLEY, Robert C.					
13a TYPE OF REPORT Master's Thesis		13b TIME COVERED FROM _____ TO _____		14 DATE OF REPORT (Year, Month, Day) 1988 December	
				15 PAGE COUNT 122	
16 SUPPLEMENTARY NOTATION The views expressed in this thesis are those of the author and do not reflect the official policy or position of the Department of Defense or the U.S. Government					
17 COSATI CODES			18 SUBJECT TERMS (Continue on reverse if necessary and identify by block number)		
FIELD	GROUP	SUB-GROUP	antenna; current; cylindrical expansions; harmonic expansions; monopole; numerical computation		
19 ABSTRACT (Continue on reverse if necessary and identify by block number) This thesis investigates the viability of a new method for numerically computing the input impedance and the currents on simple antenna structures. This technique considers the antenna between two ground planes and uses multiregion cylindrical harmonic expansions with tangential field continuity to obtain the surface currents and input impedance. The computed results are compared to the results obtained from the Numerical Electromagnetics Code for various physical parameters to assess computational accuracy.					
20 DISTRIBUTION / AVAILABILITY OF ABSTRACT <input checked="" type="checkbox"/> UNCLASSIFIED/UNLIMITED <input type="checkbox"/> SAME AS RPT <input type="checkbox"/> DTIC USERS			21 ABSTRACT SECURITY CLASSIFICATION UNCLASSIFIED		
22a NAME OF RESPONSIBLE INDIVIDUAL MORGAN, Michael A			22b TELEPHONE (Include Area Code) 408-646-2677		22c OFFICE SYMBOL 62Mw

DD Form 1473, JUN 86

Previous editions are obsolete

SECURITY CLASSIFICATION OF THIS PAGE

S/N 0102-LF-014-6603

UNCLASSIFIED

Approved for public release; distribution is unlimited.

Computation of Monopole Antenna
Currents Using Cylindrical Harmonic Expansions

by

Robert C. Hurley
Lieutenant, United States Navy
B.S.E.E, University of Missouri, 1979

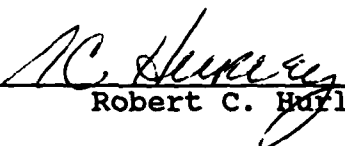
Submitted in partial fulfillment of the
requirements for the degree of

MASTER OF SCIENCE IN ELECTRICAL ENGINEERING


from the


NAVAL POSTGRADUATE SCHOOL
December 1988


Author:



Robert C. Hurley

Approved by:


Michael A. Morgan, Thesis Advisor


Richard W. Adler, Second Reader


John P. Powers, Chairman,
Department of Electrical and
Computer Engineering


Gordon E. Schacher,
Dean of Science and Engineering

ABSTRACT

This thesis investigates the viability of a new method for numerically computing the input impedance and the currents on simple antenna structures. This technique considers the antenna between two ground planes and uses multiregion cylindrical harmonic expansions with tangential field continuity to obtain the surface currents and input impedance. The computed results are compared to the results obtained from the Numerical Electromagnetics Code for various physical parameters to assess computational accuracy.

Accession For	
NTIS GRA&I	<input checked="checked" type="checkbox"/>
DTIC TAB	<input type="checkbox"/>
Unannounced	<input type="checkbox"/>
Justification	
By	
Distribution/	
Availability Codes	
Dist	Avail and/or Special
A-1	



Table Of Contents

I.	INTRODUCTION	1
	A. METHOD USED	3
	B. ASSUMPTIONS MADE	4
II.	COMPUTATIONAL PROCEDURE	6
	A. THEORETICAL TECHNIQUE	6
	B. SOFTWARE OVERVIEW	19
III.	VALIDATION	25
	A. THE NUMERICAL ELECTROMAGNETICS CODE	25
	B. COMPARISONS MADE	27
	C. RESULTS	29
IV.	CONVERGENCE CONSIDERATIONS	43
	A. MODAL TRUNCATIONS FOR REGIONS I AND II	43
	B. MODAL NEEDS FOR THE GAP REGION	44
	C. EFFECT OF REDUCING N_1 AND N_2	51
	D. EFFECT ON ACCURACY AS M_1 VARIES	53
V.	A SIMPLER APPROACH	60
	A. MODIFYING THE TECHNIQUE	61

B.	SOFTWARE MODIFICATIONS	62
C.	RESULTS	63
VI.	CONCLUSIONS AND RECOMMENDATIONS	68
A.	CONCLUSIONS	68
B.	RECOMMENDATIONS	70
APPENDIX A:	SOFTWARE FLOW CHART FOR MONO WITH GAP FIELD EXPANSION	72
APPENDIX B:	SOURCE CODE FOR MONO WITH GAP FIELD EXPANSION	74
APPENDIX C:	SOFTWARE FLOW CHART FOR MONO WITHOUT GAP FIELD EXAPNSION	89
APPENDIX D:	SOURCE CODE FOR MONO WITHOUT GAP FIELD EXPANSION	91
APPENDIX E:	SAMPLE INPUT/OUTPUT DATA FILES USED WITH MONO	103
APPENDIX F:	SAMPLE INPUT/OUTPUT DATA FILES USED WITH NEC	108
	LIST OF REFERENCES	113
	INITIAL DISTRIBUTION LIST	114

ACKNOWLEDGEMENT

I would like to express my appreciation to some of the highly motivated and professional people I have met here, and whose friendship and support have been most welcomed. First, Captain Martin J. Marbach, USMC, whose very presence during many long hours of study has helped to encourage that extra effort that has resulted in a better understanding of our highly technical world, hopefully for both of us. To Professor Michael A. Morgan whose assistance in the background theoretical development and many other areas has helped in the completion of this project.

And to my loving and patient wife and children who have had to endure a great deal on their own in support of my efforts over the past several months. Your encouragement, support and understanding were instrumental in the final completion of this effort.

I. INTRODUCTION

There are a number of methods in use today that numerically solve for the currents on simple wire antenna structures. The majority of these methods utilize an integral equation solution to Maxwell's Equations which also match the boundary conditions on the structure and satisfy the radiation conditions for the radiated fields. One of the most widely used implementations of the integral equation method is the Numerical Electromagnetics Code (NEC) [Ref 6]. This program has been proven to be highly accurate for antenna structures that can be modeled using individual wire segments or surface patch elements.

A new method is presented here which does not rely upon an integral equation formulation. This technique encloses the antenna structure between two parallel ground planes, as an approximation to the free space condition, to allow a partial field representation using a periodic Fourier series. In the initial investigation being reported here, the simple monopole radiator is being considered. In such a case, cylindrical regions are established around the structure and the harmonic expansions of the magnetic and electric fields are matched along the regional boundaries to solve for the unknown

expansion coefficients. These coefficients are then used to compute the current imposed on the surface of the antenna.

This project began as a search for the viability of computing the currents on a top loaded monopole between two ground planes using cylindrical harmonic expansions in three regions. After a number of weeks of inconclusive results, it was decided to look at the simpler case of the monopole antenna between two ground planes as presented in Chapter 2.

During the validation of the code, as presented in Chapter 3, it was found that the number of terms used in each region can be reduced by as much as 90% and still yield consistent results for the surface current and input impedance. However, the representation of the electric field along the surface of the antenna is highly inaccurate when the number of terms are insufficient to adequately represent the field. This phenomenon will be discussed in Chapter 4. Additional research revealed that a simpler method could be used that would remove the requirement for one complete expansion. This is presented in Chapter 5. Finally, conclusions and recommendations are presented in the last chapter. In addition, Appendices are used to contain much of the detailed descriptions of the computer algorithms and resultant programming for this effort.

A. METHOD USED

The general approach is to place the antenna structure being analyzed between two perfectly conducting ground planes and divide the surrounding area into a number of cylindrical regions, using a cylindrical coordinate system, that coincide with the natural boundary interfaces of the antenna as shown in Figure 1. The upper ground plane is introduced to completely close the regions and produces multiple images, each identical to the previous image but with opposite polarity.

Once the regions are defined, we start by obtaining the solution to the complex scalar Helmholtz equation. Then, by

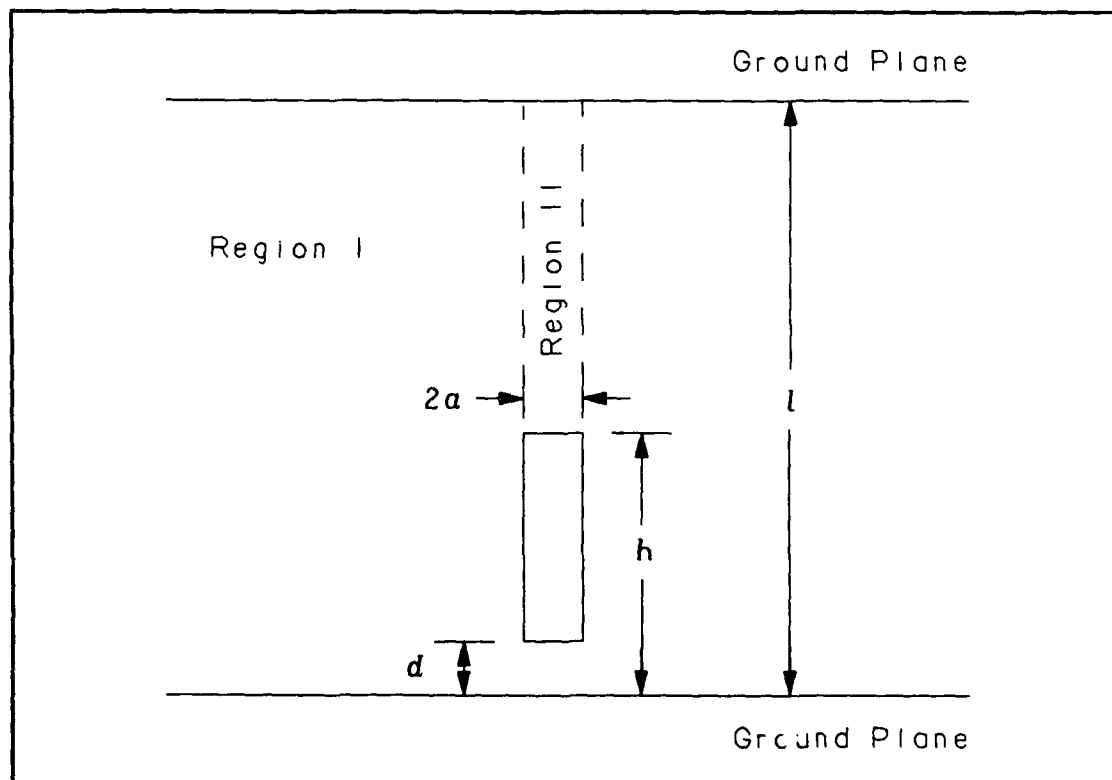


Figure 1 The Unloaded Monopole Antenna Structure

using an harmonic expansion of the resulting scalar wave function, ψ , we write an expression for the vector electric and magnetic fields in each region. The tangential component of the electric field, as approximated by the truncated expansion in Region I, is set equal to the "known" field in the gap and set equal to zero along the cylindrical surface of the perfectly conducting monopole. The tangential electric and magnetic field expansions are then matched across the boundary interface between Regions I and II. The resulting set of equations is reduced to a system of one equation with one unknown by sifting out some of the coefficients using the orthogonality principle of Fourier moment integrations. The resulting system is then solved for the remaining set of unknown coefficients. These coefficients are then used to compute the current distribution along the surface of the antenna. To validate the source code, the results are then compared to those obtained from the Numerical Electromagnetics Code (NEC) to ascertain computational accuracy.

B. ASSUMPTIONS MADE

In order to simplify the derivations, assumptions were made regarding the electric characteristics along the ground planes and the surface of the antenna structure, and the electric field produced by a driving source of constant frequency. First, the ground planes are modeled as perfectly

conducting ground planes of infinite dimension. In reality, a ground plane can be considered to have infinite dimension, for purposes of antenna current calculations, if it is larger in dimension than about 10 times the size of the antenna [Ref. 1]. Additionally, the electric field produced by the driving source is considered to be of constant magnitude within the gap region. This is a standard source model employed in integral equation modeling of antenna structures, [Ref. 1].

II. COMPUTATIONAL PROCEDURE

This chapter will present the mathematical background required to solve for the currents and the input impedance on a simple monopole antenna structure using cylindrical harmonic expansions. The final solution will be reduced to a system of one set of unknowns which will be solved using a digital computer system. An overview of the software code used, including error detection, hardware requirements and a brief discussion of the input and output file structures will also be presented. Details of the algorithm implementation are relegated to Appendices.

A. THEORETICAL TECHNIQUE

The antenna structure shown in Figure 1 (page 3) is orientated within the cylindrical coordinate system as shown in Figure 2. We begin this development with the complex scalar wave equation, known as the Helmholtz equation, given in cylindrical coordinates as [Refs. 2, 3]

$$\nabla^2 \psi(\rho, z) + k^2 \psi(\rho, z) = 0 \quad (\text{Eq. 1-1})$$

where ψ is used to denote the electric type Hertz potential and not the magnetic flux [Ref. 3]. Expanding this equation, and noting that the structure and the fields are assumed to be axisymmetric, one obtains the following:

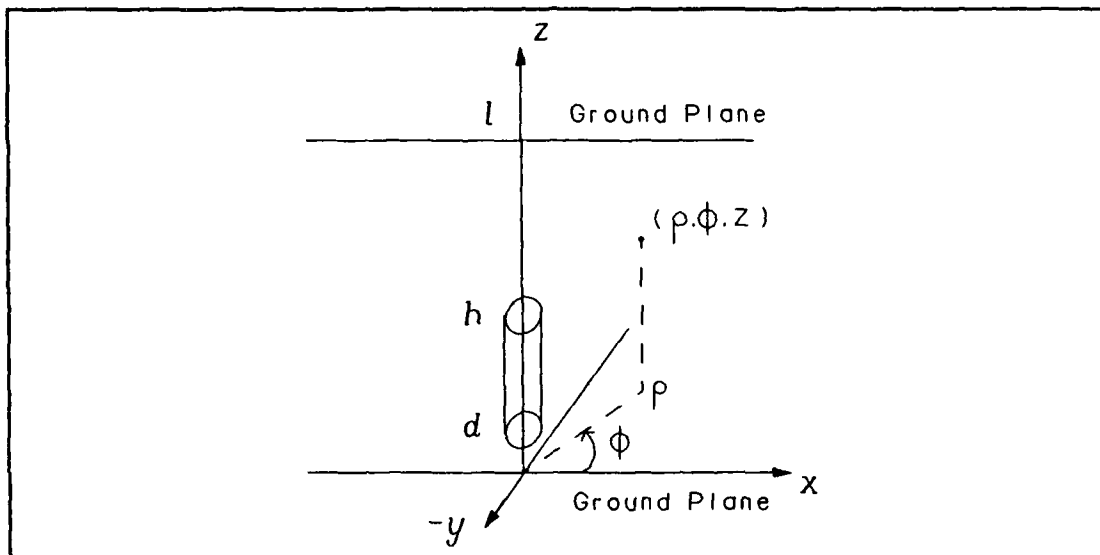


Figure 2 Cylindrical Coordinate System

$$\frac{1}{\rho} \frac{\partial}{\partial \rho} \left(\rho \frac{\partial \psi}{\partial \rho} \right) + \frac{\partial^2 \psi}{\partial z^2} + k^2 \psi = 0 \quad \text{(Eq. 1-2)}$$

Utilizing axisymmetry, the transverse magnetic (TM) solutions are given in cylindrical coordinates as [Ref. 3]

$$\begin{aligned} E_{\rho} &= \frac{1}{\hat{y}} \frac{\partial^2 \psi}{\partial \rho \partial z} & H_{\rho} &= 0 \\ E_{\phi} &= 0 & H_{\phi} &= - \frac{\partial \psi}{\partial \rho} \\ E_z &= \frac{1}{\hat{y}} \left(\frac{\partial^2}{\partial z^2} + k_0^2 \right) \psi & H_z &= 0 \end{aligned}$$

(Eq. 1-3)

where

$$\hat{y} = j\omega\epsilon_0$$

(Eq. 1-4)

The following boundary conditions must be satisfied:

- The electric field tangential to the ground planes must be zero ($E_\rho = 0$).
- The electric field tangential to the top of the antenna structure must be zero.
- The tangential electric field along the antenna structure must be zero ($E_z = 0$).
- The electric field along the gap distance d must be a constant value ($E_z = -V_0/d$).
- The electric and magnetic fields must be continuous across the boundary between the two regions above the antenna structures (E_z, H_ϕ).
- The radiated fields in Region I must be purely outbound at large distances from the antenna and must satisfy the radiation condition that $E_z = \eta_0 H_\phi$, where $\eta_0 = 377\Omega$.

Using separation of variables, where the product solution has the form $\psi = R(\rho)Z(z)$, one obtains the following equations: [Ref. 3]

$$\rho \frac{d}{d\rho} \left(\rho \frac{dR}{d\rho} \right) + \left[(k_\rho \rho)^2 - n^2 \right] R = 0$$

$$\frac{d^2 Z}{dz^2} + k_z^2 Z = 0$$

(Eq. 1-5)

The first equation is recognized as Bessel's equation of order n . The solutions to Bessel's equation are represented by any of several special functions, including [Ref. 3]

$$J_n(k_\rho \rho), Y_n(k_\rho \rho), H_n^{(1)}(k_\rho \rho), H_n^{(2)}(k_\rho \rho) \quad \text{(Eq. 1-6)}$$

where $J_n(k_\rho \rho)$ and $Y_n(k_\rho \rho)$ represent Bessel functions of the first and second kind of order n , and $H_n^{(1)}(k_\rho \rho)$ and $H_n^{(2)}(k_\rho \rho)$ are Hankel functions of the first and second kind of order n , where $H_n^{(\frac{1}{2})} = J_n \pm j Y_n$. As any two of these functions are linearly independent of each other, the solution to Bessel's equation can be represented as a linear combination of any two of these functions. The solution to the Z equation is a linear combinations of harmonic functions of the form $e^{jk_z z}$ and $e^{-jk_z z}$.

Using these results, the desired solutions to the Helmholtz equation becomes

$$\psi(\rho, z) = \begin{pmatrix} J_0(k_\rho \rho) \\ H_0^{(2)}(k_\rho \rho) \end{pmatrix} \cdot \begin{pmatrix} \sin(k_z z) \\ \cos(k_z z) \end{pmatrix} \quad \text{(Eq. 1-7)}$$

where

$$\begin{aligned} k_\rho^2 + k_z^2 &= k_0^2 \\ &= \omega^2 \mu \epsilon \end{aligned} \quad \text{(Eq. 1-8)}$$

and where k_0 is defined as the wave number, ω the angular frequency, μ the permeability of a vacuum ($4\pi \times 10^{-7}$ H/m) and ϵ the permittivity of a vacuum (8.854×10^{-12} F/m). Acceptable quantized values of k_z are found by substituting the product solution into Equation 1-3 and setting $E_r = 0$ on the upper ground planes in Region I while enforcing $E_r = 0$ on the upper

ground plane and the top of the antenna in Region II. This gives, respectively,

$$k_{z_n} = \frac{n\pi}{l} \quad \text{in Region I} \quad \{\text{Eq. 1-9.a}\}$$

$$k_{z_n} = \frac{n\pi}{l-h} \quad \text{in Region II} \quad \{\text{Eq. 1-9.b}\}$$

It should be noted here that the trigonometric terms used in Equation 1-7 will uniquely satisfy the first three boundary conditions listed previously for each term in the series.

For large arguments, the Bessel and Hankel functions listed above closely resemble harmonic functions. As seen in Table I [Ref. 3], $J_n(k_\rho \rho)$ and $Y_n(k_\rho \rho)$ are analogous to cosine and sine functions respectively, while $H_n^{(1)}(k_\rho \rho)$ and $H_n^{(2)}(k_\rho \rho)$ are related to complex exponential functions. Therefore, Bessel functions can be used to represent standing waves, while the Hankel functions describe travelling waves; specifically $H_n^{(1)}$ represents inbound waves while $H_n^{(2)}$ represents outbound waves. Using these properties, the potential field in Region I can be written as the product of Hankel and cosine functions where the cosine term implicitly satisfies the tangential electric and magnetic field boundary conditions.

Because the higher spectral bandwidth of the potential field generated by the gap voltage was expected to require a larger number of terms in the Fourier series expansion than

Table I PROPERTIES OF SOLUTIONS TO BESSEL'S EQUATION

$H_n(k\rho)$	Alternative representations	Small-argument formulas ($k\rho \rightarrow 0$)	Large-argument formulas ($ k\rho \rightarrow \infty$)	Zeros	Infinities	Physical interpretation
$H_n(k\rho)$	$J_n(k\rho) + jN_n(k\rho)$	$1 - j \frac{2}{\pi} \log \left(\frac{2}{\gamma k\rho} \right)$ $n=0$ $\frac{(k\rho)^n}{2^{n-1}n!} - j \frac{2^{n(n-1)!}}{\pi(k\rho)^n}$ $n > 0$	$\sqrt{\frac{2j}{\pi k\rho}} e^{-j\pi/4}$	$k\rho \rightarrow j\infty$	$k\rho \rightarrow 0$ $k\rho \rightarrow -j\infty$	k real—outward-traveling wave k imaginary—evanescent field k complex—attenuated traveling wave
$H_n^{(1)}(k\rho)$	$J_n(k\rho) - jN_n(k\rho)$	$1 + j \frac{2}{\pi} \log \left(\frac{2}{\gamma k\rho} \right)$ $n=0$ $\frac{(k\rho)^n}{2^{n-1}n!} + j \frac{2^{n(n-1)!}}{\pi(k\rho)^n}$ $n > 0$	$\sqrt{\frac{2j}{\pi k\rho}} e^{-j\pi/4}$	$k\rho \rightarrow -j\infty$	$k\rho \rightarrow 0$ $k\rho \rightarrow j\infty$	k real—outward-traveling wave k imaginary—evanescent field k complex—attenuated traveling wave
$J_n(k\rho)$	$\frac{1}{2}[H_n^{(1)}(k\rho) + H_n^{(2)}(k\rho)]$	1 $n=0$ $\frac{(k\rho)^n}{2^{n-1}n!}$ $n > 0$	$\sqrt{\frac{2}{\pi k\rho}} \cos \left(k\rho - \frac{\pi}{2} - \frac{\pi}{4} \right)$	Infinite number along the real axis	$k\rho \rightarrow +j\infty$	k real—standing wave k imaginary—two evanescent fields k complex—localized standing wave
$N_n(k\rho)$	$\frac{1}{2j}[H_n^{(1)}(k\rho) - H_n^{(2)}(k\rho)]$	$-\frac{2}{\pi} \log \left(\frac{2}{\gamma k\rho} \right)$ $n=0$ $-\frac{2^{n(n-1)!}}{\pi(k\rho)^n}$ $n > 0$	$\sqrt{\frac{2}{\pi k\rho}} \sin \left(k\rho - \frac{\pi}{2} - \frac{\pi}{4} \right)$	Infinite number along the real axis	$k\rho \rightarrow 0$ $k\rho \rightarrow \pm j\infty$	k real—standing wave k imaginary—two evanescent fields k complex—localized standing wave

* When $k = -ja$, the functions $I_n(jk\rho) = I_n(a\rho) = j^n J_n(-ja\rho)$ and $K_n(jk\rho) = K_n(a\rho) = \frac{\pi}{2} (-j)^{n+1} H_n^{(1)}(-ja\rho)$ are used.

† When $k = 0$, the Bessel functions are I and $\log a$, $n = 0$, and ρ^n and ρ^{-n} , $n \neq 0$.

that of the quasi-singular field at the end of the antenna, the total field in Region I was separated into two parts as shown below

$$\begin{aligned}\psi(\rho, z) &= \sum_{n=0}^{\infty} a_n H_0^{(2)}(v_n \rho) \cos\left(\frac{n\pi z}{l}\right) + \sum_{m=0}^{\infty} b_m H_0^{(2)}(v_m \rho) \cos\left(\frac{m\pi z}{l}\right) \\ &= \psi_a + \psi_b\end{aligned}\tag{Eq. 1-10}$$

where

$$v_n = \sqrt{k_0^2 - \left(\frac{n\pi}{l}\right)^2}\tag{Eq. 1-11}$$

In Region II, the potential field is constrained as a standing wave and can be expressed as

$$\psi(\rho, z) = \sum_{n=0}^{\infty} c_n J_0(u_n \rho) \cos\left[\frac{n\pi}{q}(z-h)\right]\tag{Eq. 1-12}$$

where

$$u_n = \sqrt{k_0^2 - \left(\frac{n\pi}{q}\right)^2}\tag{Eq. 1-13}$$

and $q = l - h$.

Using Equation 1-3, the electric field component at the end of the antenna is approximated by the truncated expansion

$$E_{z_a}(a,z) = \frac{1}{y} \sum_{n=0}^{N_1} v_n^2 a_n H_o^{(2)}(v_n a) \cos\left(\frac{n \pi z}{l}\right)$$

$$= \begin{cases} 0, & \text{for } 0 \leq z \leq h \\ \frac{1}{y} \sum_{n=0}^{N_2} u_n^2 c_n J_o(u_n a) \cos\left[\frac{n \pi(z-h)}{q}\right], & \text{for } h \leq z \leq l \end{cases}$$

(Eq. 1-14)

and the electric field due to the gap voltage is given by

$$E_{z_b}(a,z) = \frac{1}{y} \sum_{m=0}^{M_1} v_m^2 b_m H_o^{(2)}(v_m a) \cos\left(\frac{m \pi z}{l}\right)$$

$$= \begin{cases} -\frac{V_o}{d}, & \text{for } 0 \leq z \leq d \\ 0, & \text{for } d \leq z \leq l \end{cases}$$

(Eq. 1-15)

where N_1 represents the number of terms to be used to in Region I, N_2 for Region II, and M_1 for the electric field component due to the gap voltage.

The last boundary condition to enforce is that the magnetic field be continuous across the interface of Region I and Region II. Again using Equations 1-8, 1-10 and 1-12, and setting $H_\phi^I(a,z) = H_\phi^{II}(a,z)$, an expression for the phi component of the total magnetic field can be written as

$$\begin{aligned}
H_{\phi}(a, z) &\approx \sum_{n=0}^{N_1} v_n a_n H_1^{(2)}(v_n a) \cos\left(\frac{n\pi z}{l}\right) \\
&+ \sum_{m=0}^{M_1} v_m b_m H_1^{(2)}(v_m a) \cos\left(\frac{m\pi z}{l}\right) \\
&\approx \sum_{n=0}^{N_2} u_n c_n J_1(u_n a) \cos\left[\frac{n\pi(z-h)}{q}\right]
\end{aligned}
\tag{Eq. 1-16}$$

Equation 1-16 can be reduced to one set of unknowns by solving for the coefficients b_m analytically and using this result to solve for the c_n in terms of b_m and the unknown a_n 's. This is accomplished by sifting out the desired coefficient using the orthogonal property of Fourier moment integrations which can be defined over the regions where the fields exist as

$$I_m^{(1)} = \int_0^l \cos\left(\frac{m\pi z}{l}\right) \cos\left(\frac{n\pi z}{l}\right) dz = \begin{cases} 0, & m \neq n \\ \frac{l}{2}, & m = n \neq 0 \\ l, & m = n = 0 \end{cases}
\tag{Eq. 1-17.a}$$

$$I_m^{(2)} = \int_h^l \cos\left(\frac{m\pi(z-h)}{q}\right) \cos\left(\frac{n\pi(z-h)}{q}\right) dz = \begin{cases} 0, & m \neq n \\ \frac{q}{2}, & m = n \neq 0 \\ q, & m = n = 0 \end{cases}
\tag{Eq. 1-17.b}$$

$$I_m^{(3)} = \int_0^d \cos\left(\frac{m \pi z}{l}\right) dz = \begin{cases} d, & m = 0 \\ \frac{l}{m \pi} \sin\left(\frac{m \pi d}{l}\right), & m \neq 0 \end{cases}$$

(Eq. 1-17.c)

Applying the integrations to both sides of Equation 1-15, the b_m coefficients can be solved for in terms of known functions resulting in an expression for the terms in the second summation of Equation 1-16, as shown below:

$$\begin{aligned} \sum_{m=0}^{M_1} v_m^2 b_m H_0^{(2)}(v_m a) \int_0^l \cos\left(\frac{m \pi z}{l}\right) \cos\left(\frac{n \pi z}{l}\right) dz \\ = -\hat{y} \frac{V_o}{d} \int_0^d \cos\left(\frac{n \pi z}{l}\right) dz \end{aligned}$$

(Eq. 1-18)

Therefore,

$$v_n^2 b_n H_0^{(2)}(v_n a) I_n^{(1)} = -\hat{y} \frac{V_o}{d} I_n^{(3)}$$

(Eq. 1-19)

which can be rearranged to give

$$v_n b_n H_1^{(2)}(v_n a) = -\frac{j \omega \epsilon_0}{v_n} \frac{V_o}{d} \frac{I_n^{(3)}}{I_n^{(1)}} \frac{H_1^{(2)}(v_n a)}{H_0^{(2)}(v_n a)} \quad \text{(Eq. 1-20)}$$

By applying the Fourier moment integrations to Equation 1-16 then substituting in the expression for b_m (Equation 1-20), the c_n term can be written as

$$u_n^2 c_n J_0(u_n a) = u_n \frac{J_0(u_n a)}{I_n^{(2)} J_1(u_n a)} \left\{ \sum_{k=0}^{N_1} v_k a_k H_1^{(2)}(v_k a) T_{k,n} - j\omega \epsilon_0 \frac{V_0}{d} \sum_{k=0}^{M_1} \frac{1}{v_k} \frac{I_k^{(3)}}{I_k^{(1)}} \frac{H_1^{(2)}(v_k a)}{H_0^{(2)}(v_k a)} T_{k,n} \right\}$$

(Eq. 1-21)

where

$$T_{k,n} = \int_h^l \cos\left(\frac{k\pi z}{l}\right) \cos\left[\frac{n\pi}{q}(z-h)\right] dz$$

$$= - \left\{ \frac{\left(\frac{k\pi}{l}\right)}{\left(\frac{k\pi}{l}\right)^2 - \left(\frac{n\pi}{q}\right)^2} \right\} \sin\left(\frac{k\pi h}{l}\right)$$

(Eq. 1-22)

We now have one equation with two unknowns. A second expression for the unknown a_n 's can be obtained by applying the moment integrations to the Equation 1-14 such that

$$\sum_{n=0}^{N_1} v_n^2 a_n H_0^{(2)}(v_n a) \int_0^l \cos\left(\frac{n\pi z}{l}\right) \cos\left(\frac{m\pi z}{l}\right) dz$$

$$= \sum_{n=0}^{N_2} u_n^2 c_n J_0(u_n a) \int_h^l \cos\left(\frac{n\pi(z-h)}{q}\right) \cos\left(\frac{m\pi z}{l}\right) dz$$

(Eq. 1-23)

which gives

$$v_m^2 a_m H_0^{(2)}(v_m a) I_m^{(1)} = \sum_{n=0}^{N_2} u_n^2 c_n J_0(u_n a) T_{m,n}$$

(Eq. 1-24)

Rewriting Equation 1-21 yields

$$u_n c_n J_1(u_n a) I_n^{(2)} = \sum_{k=0}^{N_1} v_k a_k H_1^{(2)}(v_k a) T_{k,n} \\ - j\omega \epsilon_0 \frac{V_0}{d} \sum_{k=0}^{M_1} \frac{1}{v_k} \frac{I_k^{(3)}}{I_k^{(1)}} \frac{H_1^{(2)}(v_k a)}{H_0^{(2)}(v_k a)} T_{k,n}$$

(Eq. 1-25)

Substituting this result into Equation 1-24 yields

$$v_m^2 a_m H_0^{(2)}(v_m a) I_m^{(1)} = \sum_{n=0}^{N_2} u_n \frac{J_0(u_n a) T_{m,n}}{I_n^{(2)} J_1(u_n a)} \left\{ \sum_{k=0}^{N_1} v_k a_k H_1^{(2)}(v_k a) T_{k,n} \right\} \\ - j\omega \epsilon_0 \frac{V_0}{d} \sum_{n=0}^{N_2} u_n \frac{J_0(u_n a) T_{m,n}}{I_n^{(2)} J_1(u_n a)} \left\{ \sum_{k=0}^{M_1} \frac{1}{v_k} \frac{I_k^{(3)}}{I_k^{(1)}} \frac{H_1^{(2)}(v_k a)}{H_0^{(2)}(v_k a)} T_{k,n} \right\}$$

(Eq. 1-26)

Collecting terms and rewriting yields

$$\begin{aligned}
& \sum_{k=0}^{N_1} v_k a_k H_1^{(2)}(v_k a) \left\{ \sum_{n=0}^{N_2} \frac{u_n J_0(u_n a) T_{m,n} T_{k,n}}{I_n^{(2)} J_1(u_n a)} \right\} - v_m^2 a_m H_0^{(2)}(v_m a) I_m^{(1)} \\
& = j\omega\epsilon_0 \frac{V_0}{d} \sum_{k=0}^{M_1} \frac{I_k^{(3)} H_1^{(2)}(v_k a)}{v_k I_k^{(1)} H_0^{(2)}(v_k a)} \left\{ \sum_{n=0}^{N_2} \frac{u_n J_0(u_n a) T_{m,n} T_{k,n}}{I_n^{(2)} J_1(u_n a)} \right\}
\end{aligned}
\tag{Eq. 1-27}$$

This can be written in matrix form as

$$\sum_{k=0}^{N_1} A_{m,k} a_k = B_m \quad \text{for } m = 0, N_1
\tag{Eq. 1-28}$$

where

$$\begin{aligned}
A_{m,k} &= v_k H_1^{(2)}(v_k a) P_{m,k} \quad m \neq k \\
A_{m,m} &= v_m H_1^{(2)}(v_m a) P_{m,m} - v_m^2 H_0^{(2)}(v_m a) I_m^{(1)} \\
B_m &= j\omega\epsilon_0 \frac{V_0}{d} \sum_{k=0}^{M_1} \frac{I_k^{(3)} H_1^{(2)}(v_k a)}{v_k I_k^{(1)} H_0^{(2)}(v_k a)} P_{m,k}
\end{aligned}
\tag{Eq. 1-29}$$

and

$$P_{m,k} = \sum_{n=0}^{N_2} \frac{u_n J_0(u_n a) T_{m,n} T_{k,n}}{I_n^{(2)} J_1(u_n a)}
\tag{Eq. 1-30}$$

The current as a function of distance along the antenna is then computed by

$$I(z) = 2\pi a H_0(a, z) \quad \text{for } d \leq z \leq h$$

$$= 2\pi a \left[\sum_{n=0}^{N_1} \left\{ v_n a_n H_1^{(2)}(v_n a) \cos\left(\frac{n\pi z}{l}\right) \right\} \right. \\ \left. - j\omega\epsilon_0 \frac{V_0}{d} \sum_{m=0}^{M_1} \left\{ \frac{I_m^{(3)} H_1^{(2)}(v_m a)}{v_m I_m^{(1)} H_0^{(2)}(v_m a)} \cos\left(\frac{m\pi z}{l}\right) \right\} \right] \quad \text{(Eq. 1-31)}$$

The input impedance is then given as the ratio of the gap voltage V_0 to the current at the end of the gap

$$Z_{in} = \frac{V_0}{I(z=d)} \quad \text{(Eq. 1-32)}$$

B. SOFTWARE OVERVIEW

The computer program was written in FORTRAN 77 and was designed to run on an MS-DOS compatible system with a numeric coprocessor and 460 kilobytes of available memory after the disk operating system is loaded. If the numeric coprocessor is not available, the source code could be recompiled to emulate the specific coprocessor calls. The user would notice a dramatic increase in run time, but as all calculations are done in single precision, the accuracy should not be affected.

The program code is divided into two separate programs. The first program, called MONO.FOR, is the main program that

calls a number of subroutines in SUBS.FOR. Variable names used in the program code closely follow those used in the theoretical development. Each variable is explicitly declared in each subroutine and array sizes are kept to a minimum to reduce required memory at run time.

The first section of code in MONO.FOR is used to input the physical parameters using either an unformatted ASCII data file as shown in Appendix E or by entering the values from the keyboard. In each case, measurements may be entered in either wavelength or meters. If a data file is used, the first line must be either a "w" or "m", and may be either upper or lower case, to distinguish between wavelengths or meters. Unit number zero was used for all READ statements, which allows use of the program in a batch mode where all inputs and screen directed outputs can be redirected by standard DOS methods. However, the use of compilers other than MicroSoft Fortran (Versions 4.01 or 4.1) may produce compiler errors when using this designation. The user should consult the specific compiler manual for details on unit designations.

Before prompting the user to identify the output file name, the program checks for two conditions that will produce inaccurate results. The first condition is when the upper plate height is a multiple of one half wavelength. Physically, this condition will allow resonant cavity modes between the plates, introducing instabilities in the numerical

solution. The mathematical basis for this can be easily shown. When the upper plate height is a multiple of half the wavelength, ν_n will become zero for certain values of n . As can be seen in Table I, the value of a Hankel function approaches $-j\infty$ as the argument approaches zero. This test occurs in the main program and supplies earlier error detection. The singularity is not checked for in the subroutine that computes the Hankel functions (HAN1) found in SUBS.FOR.

The second condition that is tested is when the distance of the top ground plane above the antenna, designated q , is an integer multiple of the antenna height. This is similar to the previous case in that a resonant area is present between the antenna and the upper ground plane. However, in this case, the value of u_n , which appears only in the $P_{m,k}$ matrix, becomes zero for multiples of the ratio h to q . Figure 3 illustrates the behavior of the Bessel function for a range of arguments [Ref. 4]. The zero order Bessel function, J_0 , is finite for small arguments; however the first order Bessel function, J_1 , (found in the denominator of Equation 1-30) rapidly approaches zero as the argument approaches zero, causing the errors.

In an effort to reduce computation time at the expense of memory requirements, several arrays are dynamically loaded so that the values may be easily extracted to fill the system matrix $A_{m,k}$ and the driving vector B_m . These include the

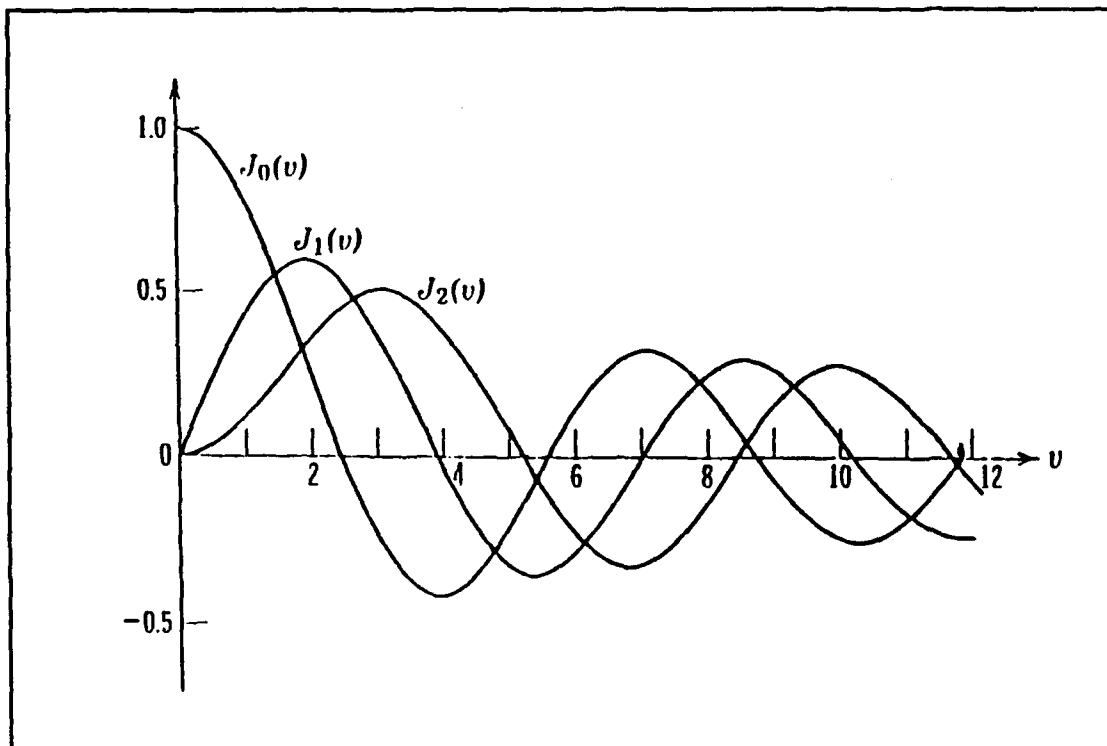


Figure 3 Bessel Functions of the First Kind

values for the Fourier moment integrations, the Bessel function values and the $P_{m,k}$ matrix. The T matrix has dimensions of $M_1 \times N_1$ and consists of terms from Equation 1-23. The I matrix has dimensions of $M_1 \times 3$ where the column positions correspond to the three equations in Equation 1-18. The Ja and $P_{m,k}$ matrices are loaded in the subroutine ALOAD and passed back to the main program. The Ja matrix is $M_1 \times 4$ in size where the column positions represent the following values:

<u>Column Position</u>	<u>Value</u>
1	$u_n * J_0(u_n a)$
2	$J_1(u_n a)$
3	$v_n * H_1(v_n a)$
4	$(v_n)^2 * H_0(v_n a)$

For large values of N_1 , N_2 and M_1 , about 60% of the total computation time is involved in filling the last temporary array, the $P_{n,k}$ matrix. This array is dimensioned to $N_1 \times M_1$ and uses values from all three arrays for each location. By filling these arrays first, the computation time was decreased by an average of 85%, however the memory required increased by 300%!

Once the system matrix and driving vector are stored in memory, it is a simple task to solve for the unknown a_n 's utilizing the back substitution method. First the matrix is upper triangulated by performing an L-U decomposition, with pivoting, on the $A_{n,k}$ matrix using the FACTOR subroutine. Once this is accomplished, the SOLVE subroutine calculates the eigenvalues by back substitution.

To maintain the convention that an outwardly travelling wave has a negative imaginary exponential argument, the CSR function was included in SUBS.FOR. Since not all compilers would return a negative imaginary value from the square root algorithm when the argument is a negative real value, the CSR

function insures the $-j$ component of the square root of a negative argument is returned.

The subroutines that compute the Bessel and Hankel functions for complex arguments and the matrix solution algorithms were supplied by Professor Michael A. Morgan of the Naval Postgraduate School. The Bessel and Hankel subroutines utilize the direct power series method for small values (less than or equal to five for the Bessel subroutine and six for the Hankel subroutine) and Hankel's asymptotic formula for larger values.

The output is directed to a user specified file on any drive or subdirectory as long as the entire string is less than 25 characters. Longer strings will truncate the extra characters without warning. Printed output includes all input variables including the number of coefficients chosen for Regions I and II and for the gap voltage expansion. Length measurements are reported in both meters and fractions of a wavelength. The system eigenvalues are then printed followed by the position number, distance from the end of the gap and magnitude and phase of the computed currents, up to the upper plate height. Finally the input resistance and reactance is computed and printed to the file. Sample input and output files are listed in Appendix E.

III. VALIDATION

In order to validate any computational algorithm, one must establish the accuracy obtained by comparing the computed results against either experimental data or another widely accepted software package that has been proven to be accurate. For this case, the logical choice was to use the Numerical Electromagnetics Code to calculate the input impedance and current distribution for a range of different physical structures and compare these results against those obtained by MONO. From this point, the program sensitivity will be examined for various ground plate spacings, antenna lengths and radii. Chapter 4 will investigate the effect that reducing the number of modal expansion terms has on this accuracy.

A. THE NUMERICAL ELECTROMAGNETICS CODE

The Numerical Electromagnetics Code (NEC) is widely accepted as an accurate method of computing the antenna currents, input impedance and radiation patterns of antennas that can be modeled using wire or patch structures. NEC calculates these values by solving integral equations for the currents imposed on the structure by a voltage source or an incident electromagnetic wave. The structure is best modeled

by straight wire segments that should be less than ten percent of the operating wavelength and conforms to the physical geometry using a best fit approach. [Ref. 6, p. 3]

The user supplies NEC with a formatted data file that specifies the location of the structure in the rectangular coordinate system, the number of segments used to compute the results, the driving source location and output parameters and the existence and characteristics of a ground plane in the XY plane. Because of the infinite number of images produced by a pair of perfect ground planes, the user must also construct enough images with the proper driving voltages that will yield consistent results. NEC then calculates the segment length, and uses this value as the gap distance between the ground plane and the base of the antenna. The currents are calculated at the midpoint of each segment vice at the ends as is done in MONO.

NEC uses two approximations in the calculation of the electric field, the thin-wire kernel and the extended thin-wire kernel. The thin-wire kernel can be used when the segment length to radius ratio is greater than 8, while the extended wire kernel is accurate when this ratio is at least 2. Since NEC sets the gap distance equal to the segment length and accuracy is improved if the segment lengths (especially across a boundary) are of equal size, setting the gap distance equal to the antenna diameter forces the segment

length-to-radius ratio to be equal to 2. Additionally, this gap distance is consistent with the requirement for a constant electric field potential inside the gap region. Therefore, the extended wire kernel, which uses a uniform surface current along the segment length and assumes no variation of the currents along the ϕ direction, will be used for all validation runs. These approximations also support the basic assumption of the TM mode dominating the currents on the monopole. For the conditions listed above, NEC's accuracy is within 1% of experimental results. [Ref. 6]

B. COMPARISONS MADE

The first goal will be to determine the minimum number of reflections that must be assembled in the NEC data set to obtain consistent results for a quarter wave antenna structure. From this data, an appropriate number of reflections will be used that represents consistent results while reducing the calculation time for all future runs. This will be followed by demonstrating consistent results for various ground plane spacings. The upper ground plane was introduced to establish a closed region. The upper plate should, if far enough away from the antenna, have little effect on the input impedance and antenna currents for distances that are not exact multiples of half the wavelength. Again a value of 1 will be selected that represents reliable results but reduces

the calculation time required for MONO. The antenna radius will then be adjusted over the range of 0.005λ to 0.02λ followed by variations in the antenna height for a selected radius.

For all MONO calculations, the number of modes used in Regions I and II (N_1 , N_2) will always be set to 60, while the number of modal expansion terms used for the gap field (M_1) will be set to two times the upper plate spacing to gap distance ratio. Chapter 4 will further investigate the accuracy of the results as a function of the number of modes used. A preliminary check for consistent results can be obtained by evaluating the differences in the input impedance results. But these values may differ slightly since NEC calculates the current at the midpoint of each segment instead of at the ends of the segment as is done in MONO. Additionally, since the first segment used in NEC is the gap distance, the input impedance is actually calculated for a point not on the monopole but in the center of the feed region. In comparison, MONO calculates the input impedance at the base of the antenna. The effect this has on the comparisons will be discussed later in this chapter. Additionally, these differences may be emphasized since the magnitude of the current at the end of the gap region can be quite small so that even small differences in the calculated values will yield relatively high differences. Therefore, to better

assess the accuracy of the results, the calculated current distribution along the antenna will be compared graphically with that obtained from NEC.

C. RESULTS

Since the ground planes used to divide the area into regions create an infinite number of reflections, one must first examine the minimum number of reflections required to obtain convergence to the half space case, having no upper ground plane. For this set of runs, the antenna is 0.24λ high with radius of 0.01λ and the upper ground plate was placed 1.4 wavelengths from the lower plate. Appendix F has a complete listing of some of the NEC data sets used for the validations. It should be noted that the distance between the lower plate and the center of the reflected dipole is equal to twice the plate spacing. This is due to the complete imaging, including the lower ground plane, of the physical structure from the upper ground plane. One can see from Figure 4 that adding a second reflection does not change the current distribution by any appreciable amount, therefore one reflection will be used for all further validations.

Now that a baseline data set has been decided upon, the effects of various plate spacing, antenna heights and radius will be examined. The first item to look at will be the effect the plate spacing has on the current distribution and

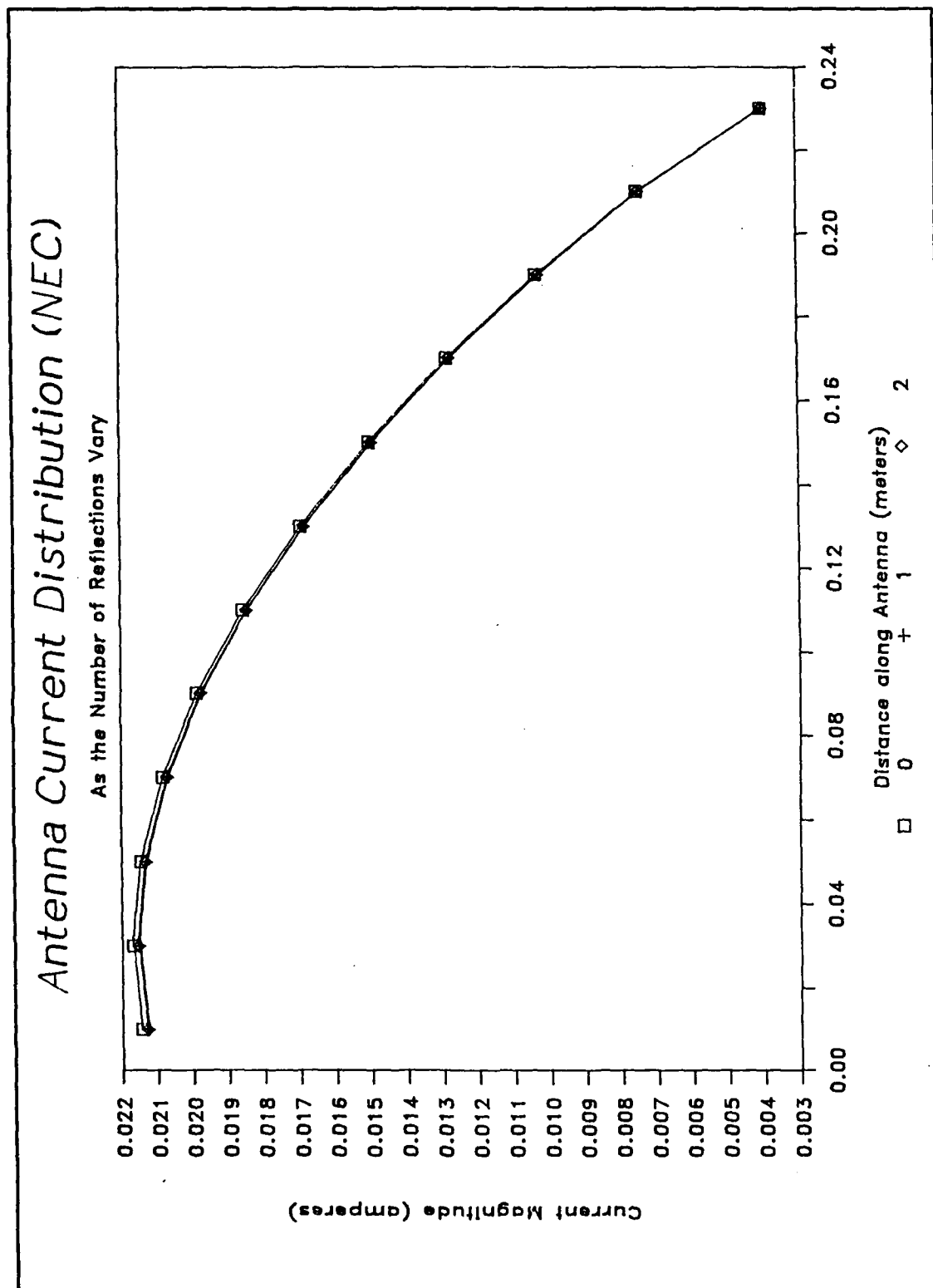


Figure 4 Antenna Current vs Number of Reflections

the calculated input impedance. Table II shows the numerical results for an antenna of height 0.24λ and radius of 0.01λ placed between ground planes that are spaced 3.1, 1.4 and 0.81λ

Table II RESULTS FOR VARIOUS UPPER PLATE SPACINGS

Plate Spacing	NEC		MONO		% Diff.	
	Rin	Xin	Rin	Xin	R	X
3.10 λ	44.63	13.35	42.65	13.14	4.64	1.60
1.40 λ	44.90	13.97	43.14	13.95	4.08	0.14
0.81 λ	43.51	14.84	44.67	13.84	2.66	6.74

wavelengths. Figures 5 through 7 show the current distribution for each of the above cases. While none of the results exceed acceptable limits, the case of $l=1.4\lambda$ is closer to the results computed by NEC and will be used as the baseline for further comparisons. It should be noted here that while the example values selected for the plate spacing have little effect on the result, the plate spacing can not be an integer multiple of a half wavelength. Likewise, the distance between the top of the antenna structure and the upper plate can not be a multiple of a half wavelength. Physically, these configurations would present the ability to support resonant modes that do not require a driving source. In reality, this condition will not exist as there is always a source of resistance which causes all modes to decay in time. However, the first condition will exist numerically where $H_0^{(2)}$ approaches negative infinity when ν_n (Equation 1-11) equals

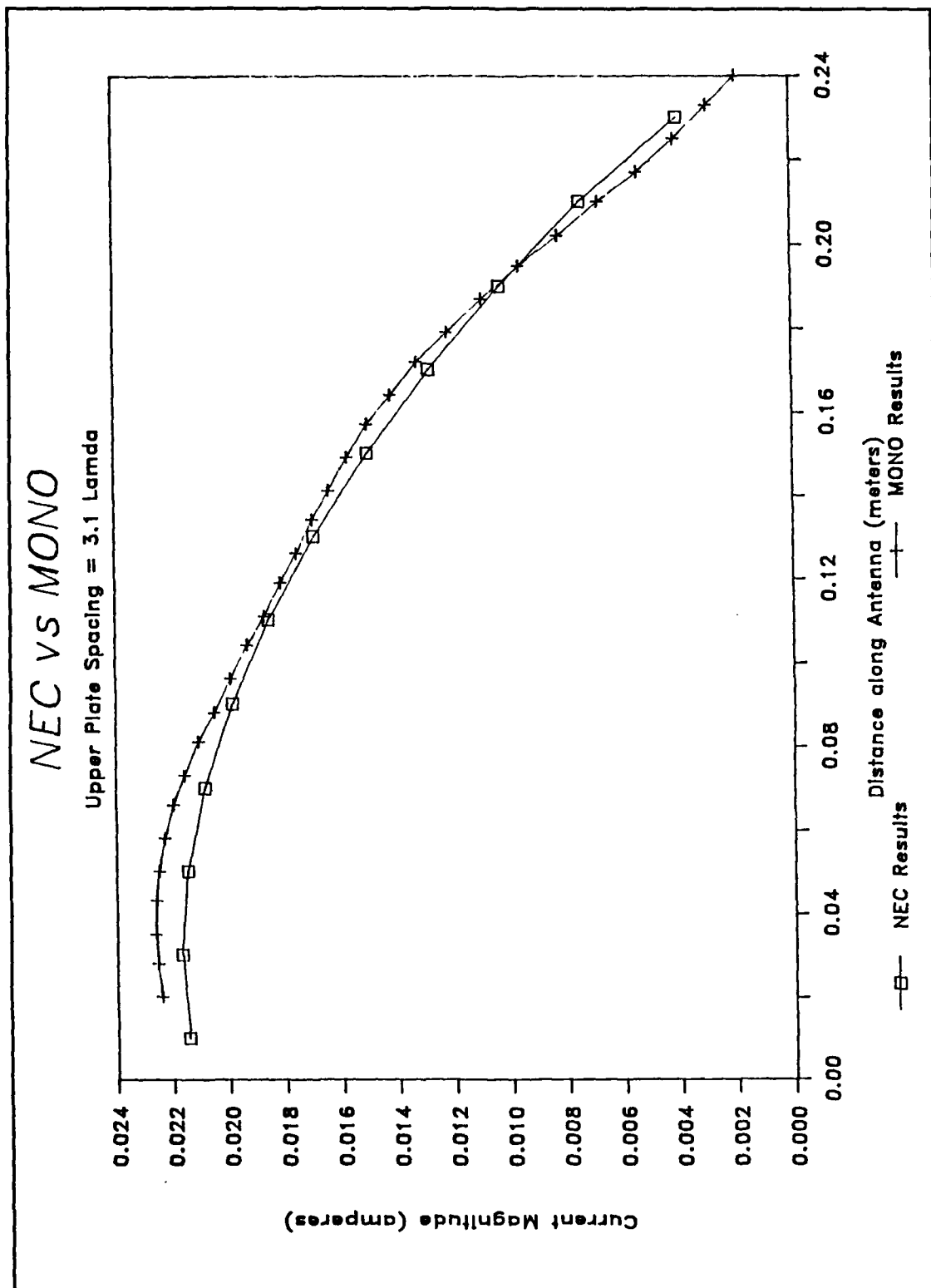


Figure 5 Comparison of NEC vs MONO when $l = 3.1\lambda$

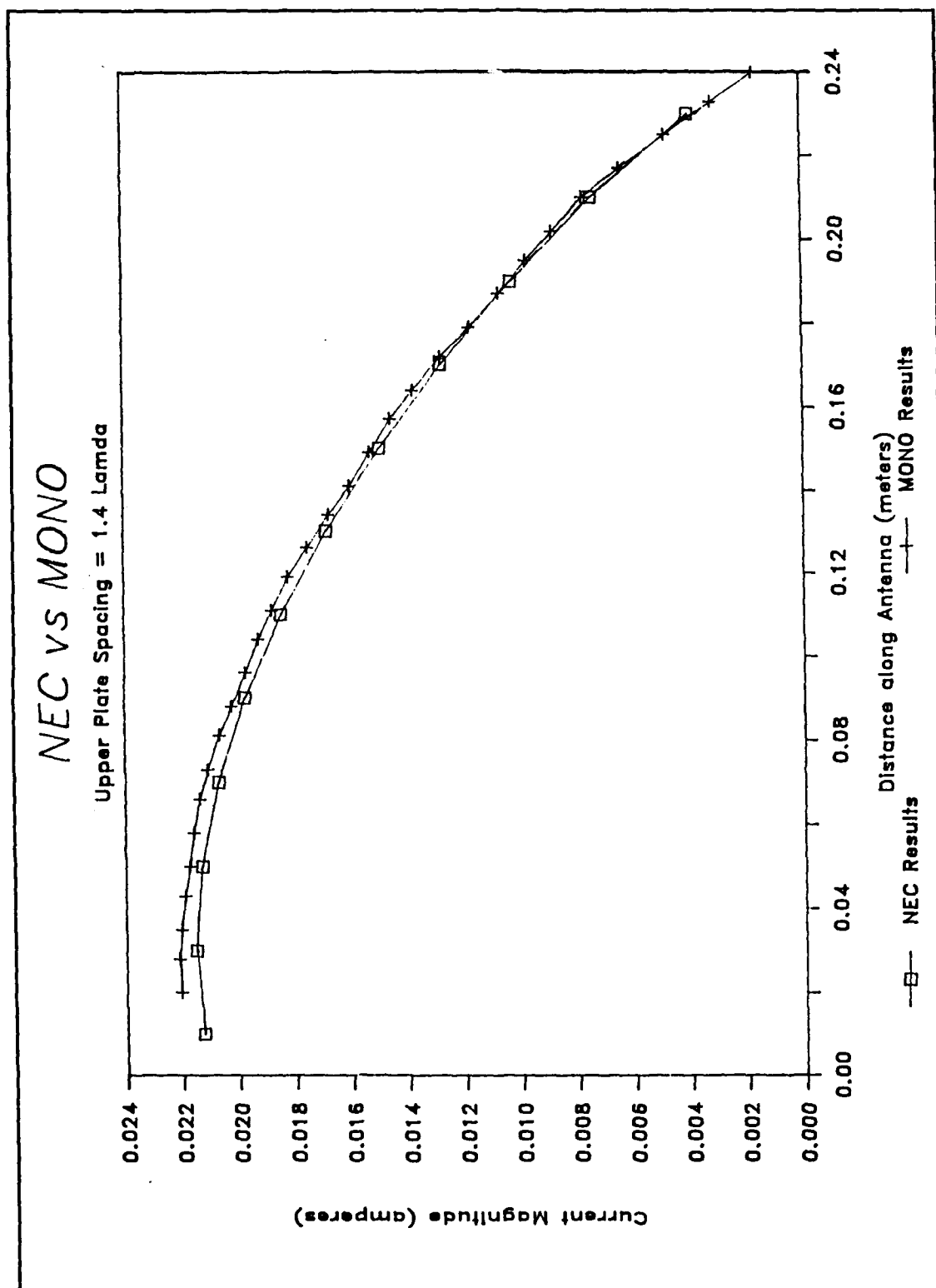


Figure 6 Comparison of NEC vs MONO when $l = 1.4\lambda$

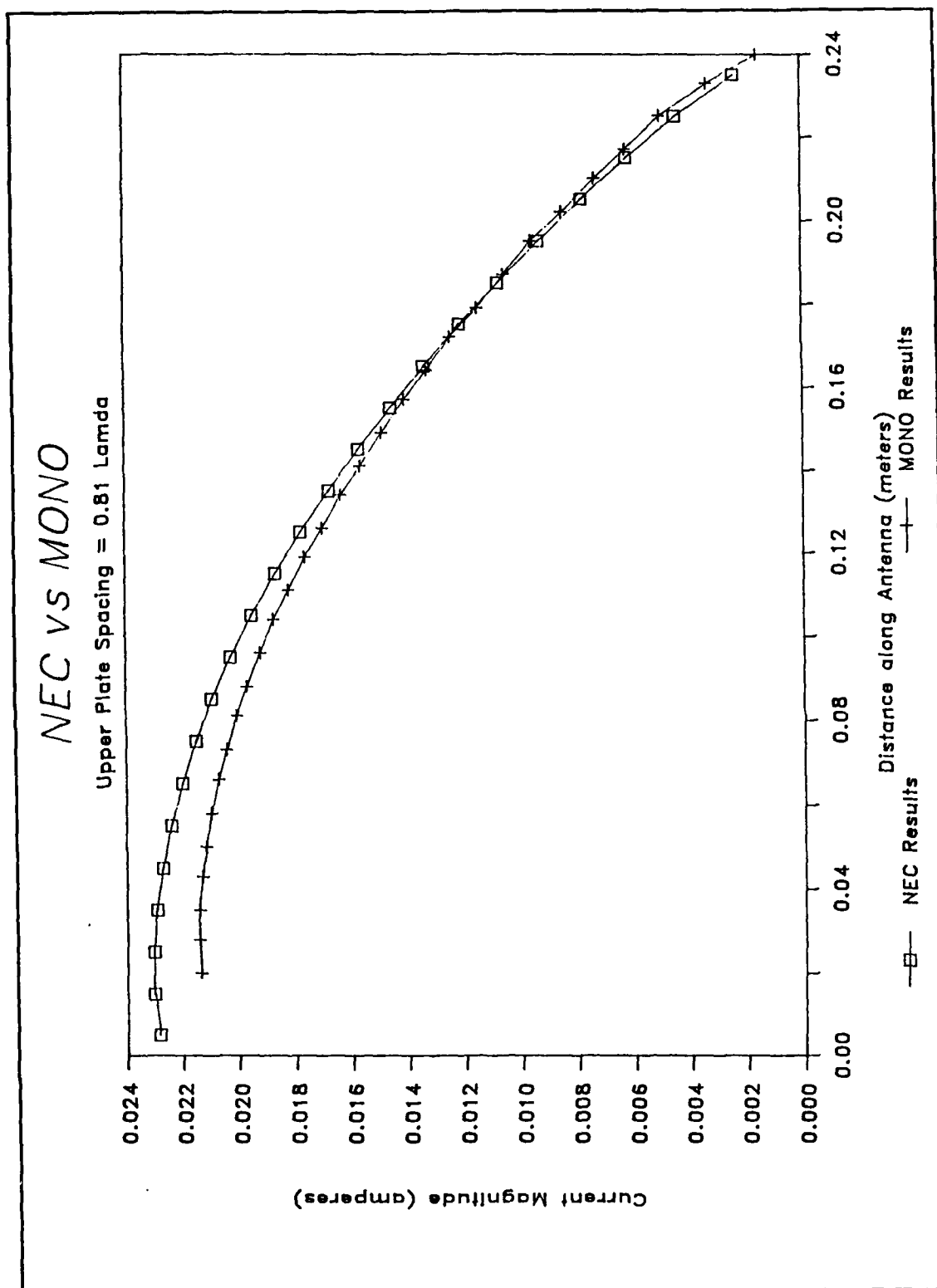


Figure 7 Comparison of NEC vs MONO when $l = 0.81\lambda$

zero. By replacing the wave number k_0 with $2\pi/\lambda$, then ν_n is zero when the plate spacing l is an integer multiple of a half wavelength. A similar condition will also occur when the distance between the top of the structure and the upper plate is a multiple of a half wavelength. In this case, J_1 found in the denominator of $P_{n,k}$ (Equation 1-30) is zero when ν_n is zero. The program code will alert the user to both conditions and halt execution.

The next variable to consider is the antenna height. For extremely short antenna structures, the current decays almost linearly along the wire from its initial value to zero. When the antenna is about one quarter wavelength long, the current distribution takes on the familiar cosine shape. As the antenna length approaches one half wavelength, the distribution approaches a sine wave shape and the input impedance approaches infinity as the current approaches zero.

Table III lists the results when the structure is placed between the two ground planes spaced 1.4λ apart for various antenna heights and radii. In the case where the antenna height approaches a half wavelength, the percent difference in the input impedance values appears to be large. This can be attributed to the differences in the location on the structure where the input impedance is actually calculated. This disparity combined with the low magnitudes in general can lead to alarming discrepancies with the NEC results.

Table III NEC, MONO RESULT COMPARISONS FOR VARIOUS h AND a

Antenna (λ)		NEC		Mono		% Diff	
h	a	Rin	Xin	Rin	Xin	R	X
.12	.005	6.6	-137.9	7.4	-148.7	10.7	7.3
.24	.005	42.0	12.4	40.6	10.8	3.3	14.8
.48	.005	254.8	-285.0	339.9	-281.7	25.0	1.2
.12	.01	7.7	-104.6	9.3	-118.2	17.8	11.5
.24	.01	44.9	14.0	43.1	14.0	4.0	0.1
.48	.01	177.7	-203.8	264.8	-199.9	32.9	2.0
.12	.02	9.8	-76.3	13.4	-92.2	26.5	17.2
.24	.02	47.9	13.4	46.1	15.9	4.0	15.5
.48	.02	129.6	-139.8	220.1	-120.9	41.1	15.6

Therefore, one must look at the current distribution to accurately determine the differences in the computed results. Figures 8 through 11 show that the differences in the magnitude of the current distribution are within two percent. Additionally, one could also compare the phase difference between the two methods to further establish an acceptable method of judging the accuracy. Figure 12 shows that the difference between the phase of the current as calculated by MONO and NEC is well within two percent along the entire length of the antenna.

Another point that can be observed is the effect that a change in the antenna radius has on the results. Once again a review of the current distribution is required to accurately assess the effect any errors would have on the far field pattern; however one detail is evident. As the antenna

becomes thinner the difference between the two results is reduced. This effect can be attributed to the increased resolution in the NEC results as the radii and, therefore, the gap distance are reduced. Additionally, the approximation to a TM current distribution along the surface of the structure becomes more accurate with a thinner structure.

In review, it has been shown that due to the differences in the methods, the best method to assess the accuracy of MONO using NEC is obtained by comparing both the current magnitude and phase distribution along the antenna surface vice the input impedance values. Using this criterion, MONO is consistently within two percent of the results obtained with NEC for a variety of structures. Chapter 4 will investigate the difference caused by reducing the number of expansion terms and attempt to identify a minimum number of terms required to obtain results that are consistent with those obtained here.

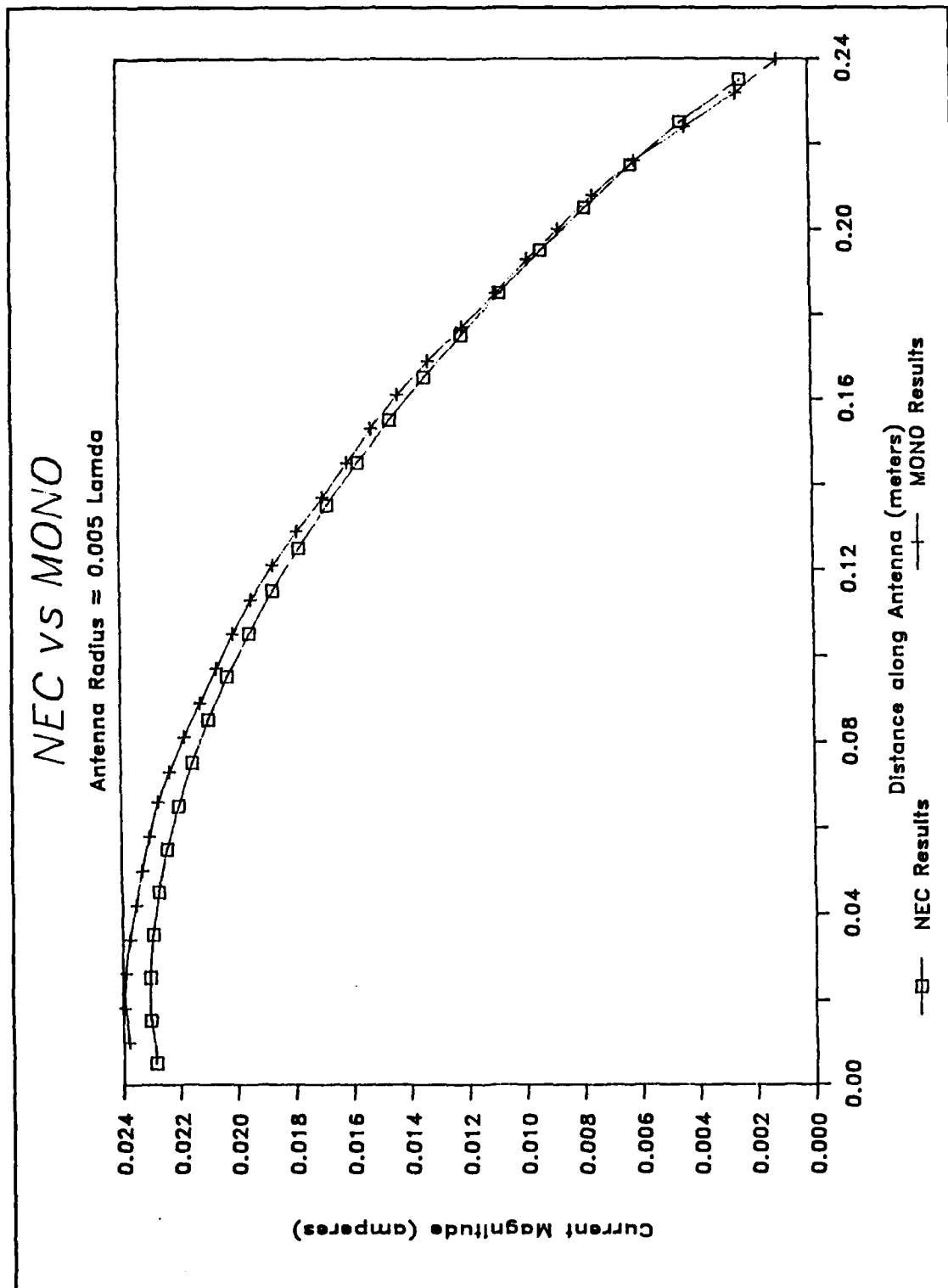


Figure 8 NEC vs MONO for Quarter Wave Monopole
(Radius = 0.005 λ)

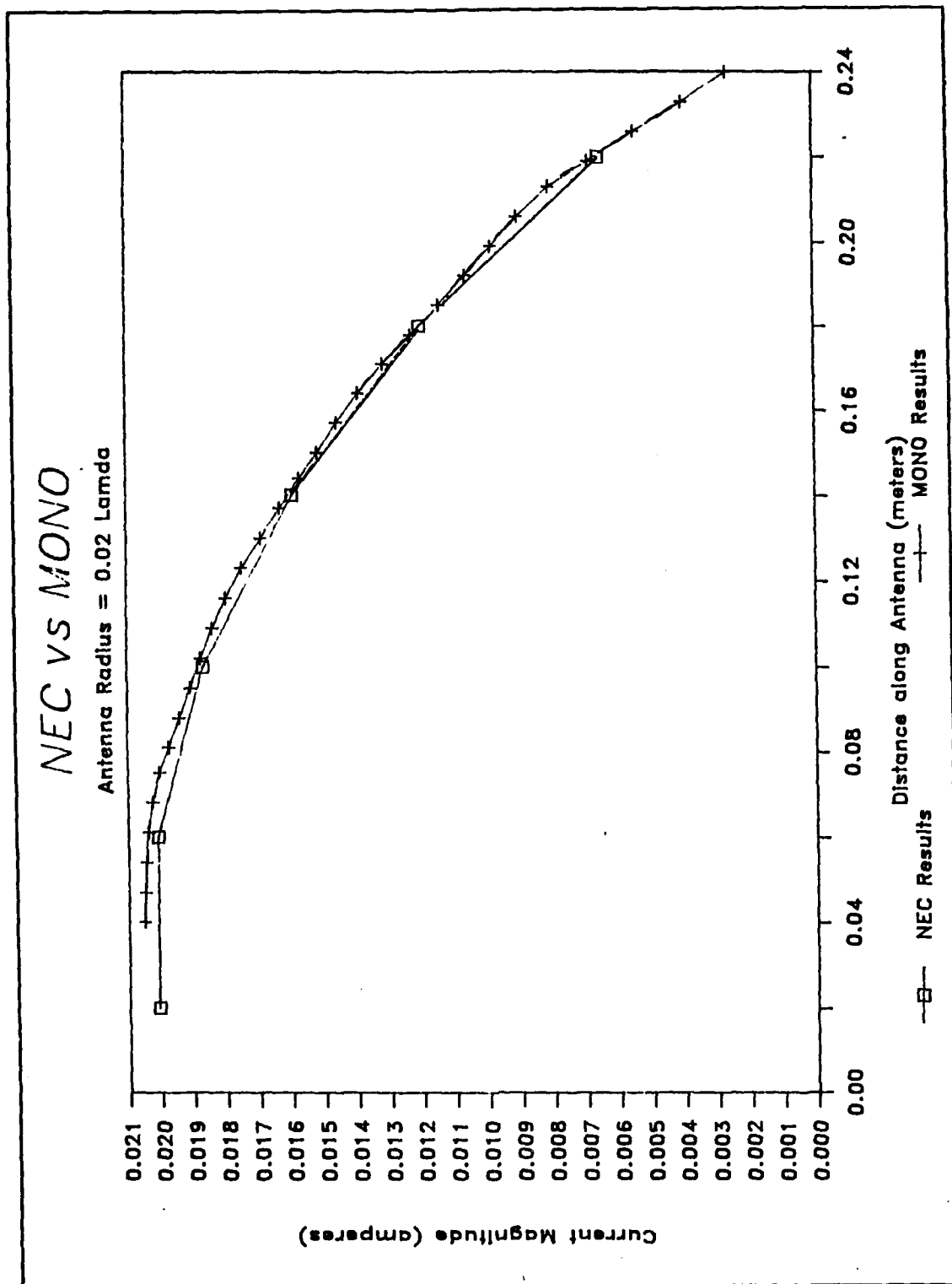


Figure 9 NEC vs MONO for Quarter Wave Monopole
(Radius = 0.02λ)

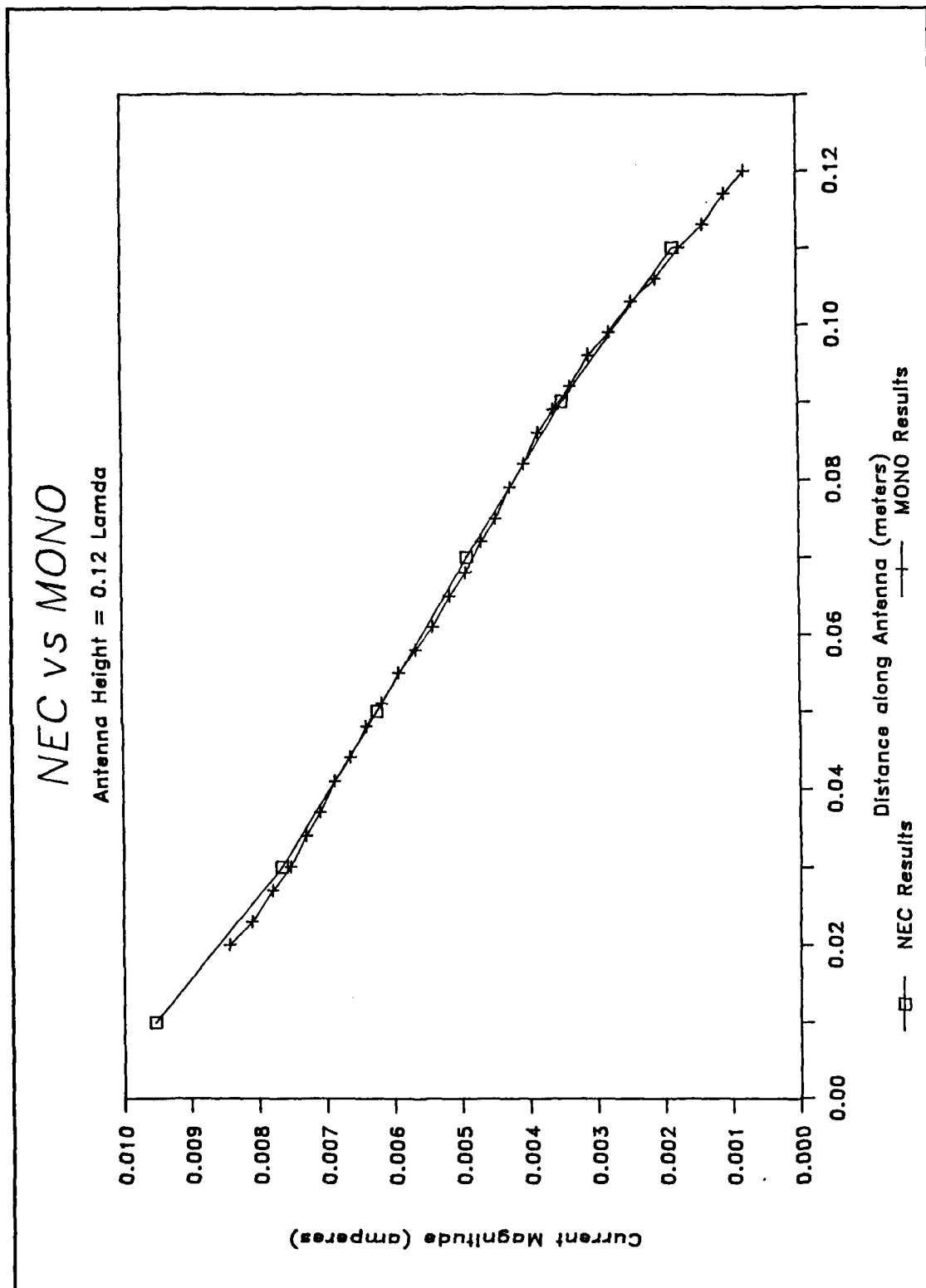


Figure 10 NEC vs MONO for Antenna Height = 0.12λ

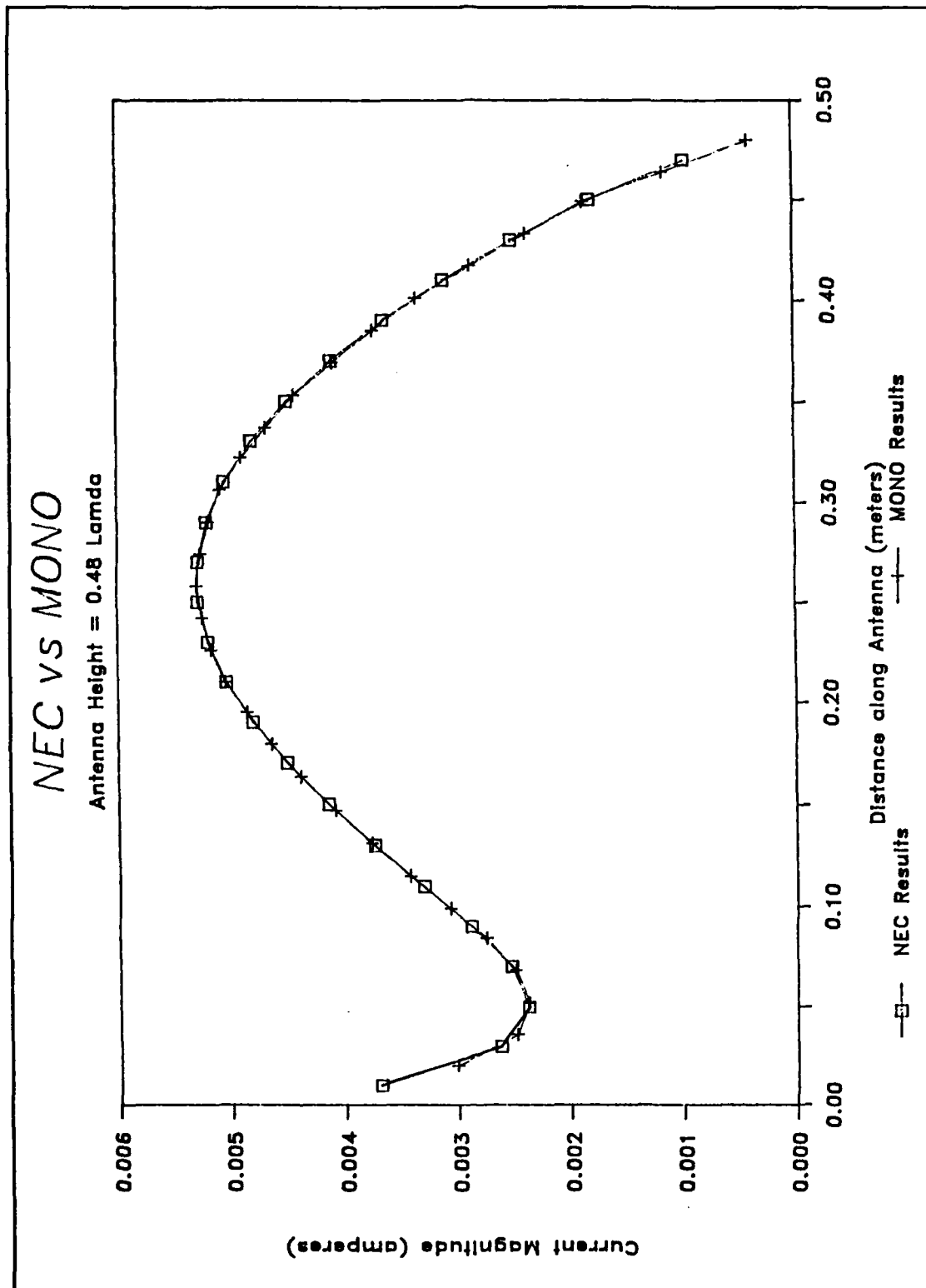


Figure 11 NEC vs MONO for Antenna Height = 0.48λ

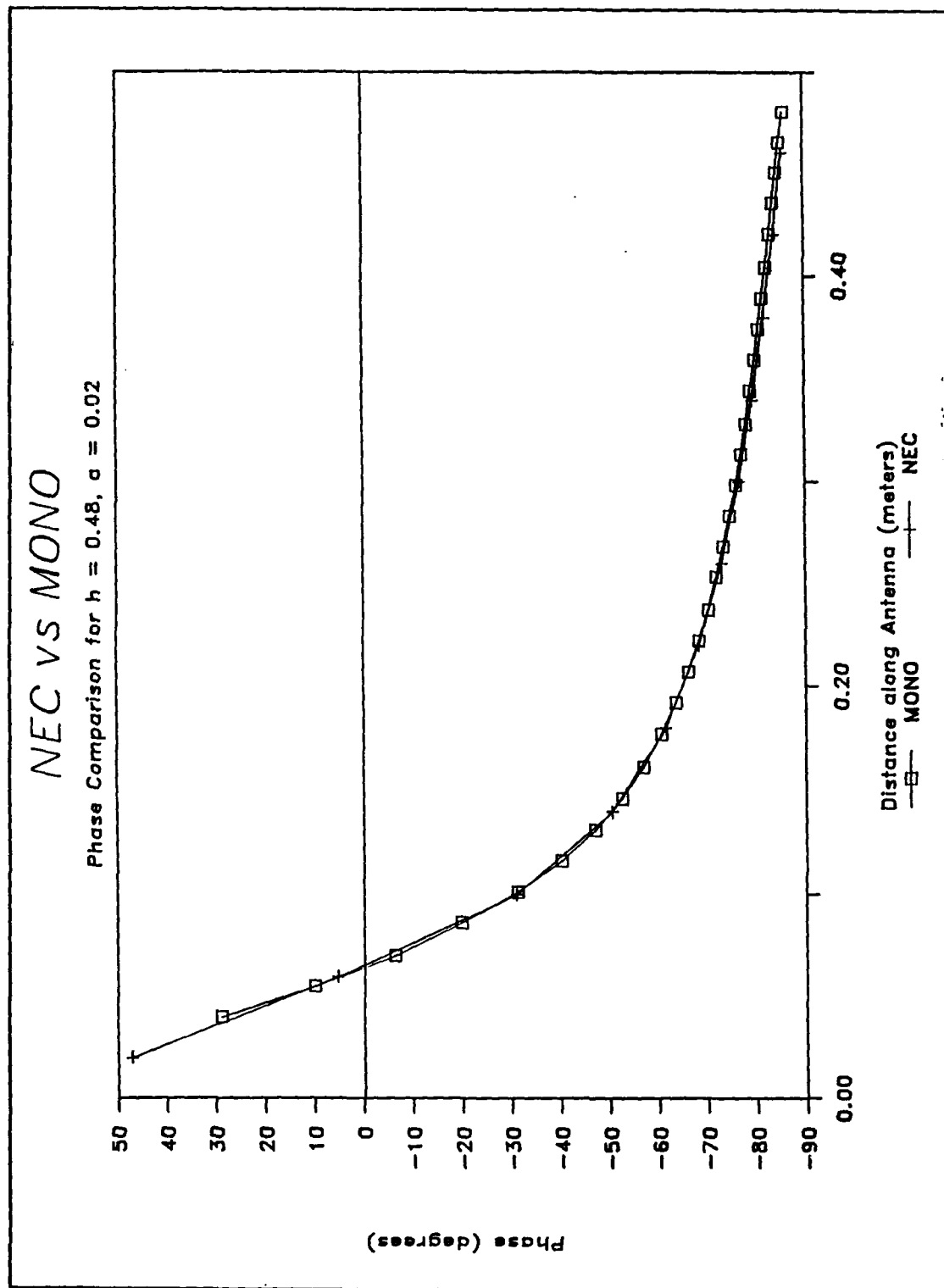


Figure 12 Phase Comparison between NEC and MONO
 $(h = 0.48\lambda, a = 0.02\lambda)$

IV. CONVERGENCE CONSIDERATIONS

In any realizable computing machine where there is a finite quantity of storage, the first question that must be answered is the number of terms required to obtain accurate results. If one uses too few terms, the results are erroneous. However, using too many terms can often lead to inaccuracies as well. If the additional terms are small enough to be approximately on the same order as the precision of the computer, then the additional terms may actually increase the error. To compound the problem, the additional terms require additional memory and increase the time required to compute the results. In investigating this question, we will first examine the number of terms required for Regions I and II (N_1 and N_2) followed by an analysis of the number of terms required to represent the electric field in the gap region (M_1).

A. MODAL TRUNCATIONS FOR REGIONS I AND II

In the previous chapter, the number of modes chosen for the two regions was the maximum allowed in the program, namely 60. But is that enough? One could say that since the results compare favorably with NEC, the solution has converged. A more accurate approach is to increase the number of modes and

compare the results. However, due to the memory limit of 640 kilobytes of addressable memory imposed by the compiler, the source code was recompiled on a 80386-specific FORTRAN compiler that allows for larger arrays and is only limited by the available memory of the computer being used. Figure 13 compares the current distribution of a quarter wave antenna that has the upper plate height set at a large value (3.1λ) for 60 modes and 100 modes. This additional information proves that the system has converged to an accurate solution with 60 modes and any additional modes are not required. The effect reducing this number has on the accuracy will be discussed later in this chapter.

B. MODAL NEEDS FOR THE GAP REGION

As mentioned earlier, the original approach was to expand the electric field along the surface of the antenna in one expansion between the ground planes as shown below

$$E_z(a,z) = \begin{cases} -\frac{V_o}{d}, & \text{for } 0 \leq z \leq d \\ 0, & \text{for } d \leq z \leq h \\ \frac{1}{y} \sum_{n=0}^{N_1} u_n^2 c_n J_0(u_n a) \cos\left[\frac{n \pi (z - h)}{q}\right], & \text{for } h \leq z \leq l \end{cases} \quad (\text{Eq. 4-1})$$

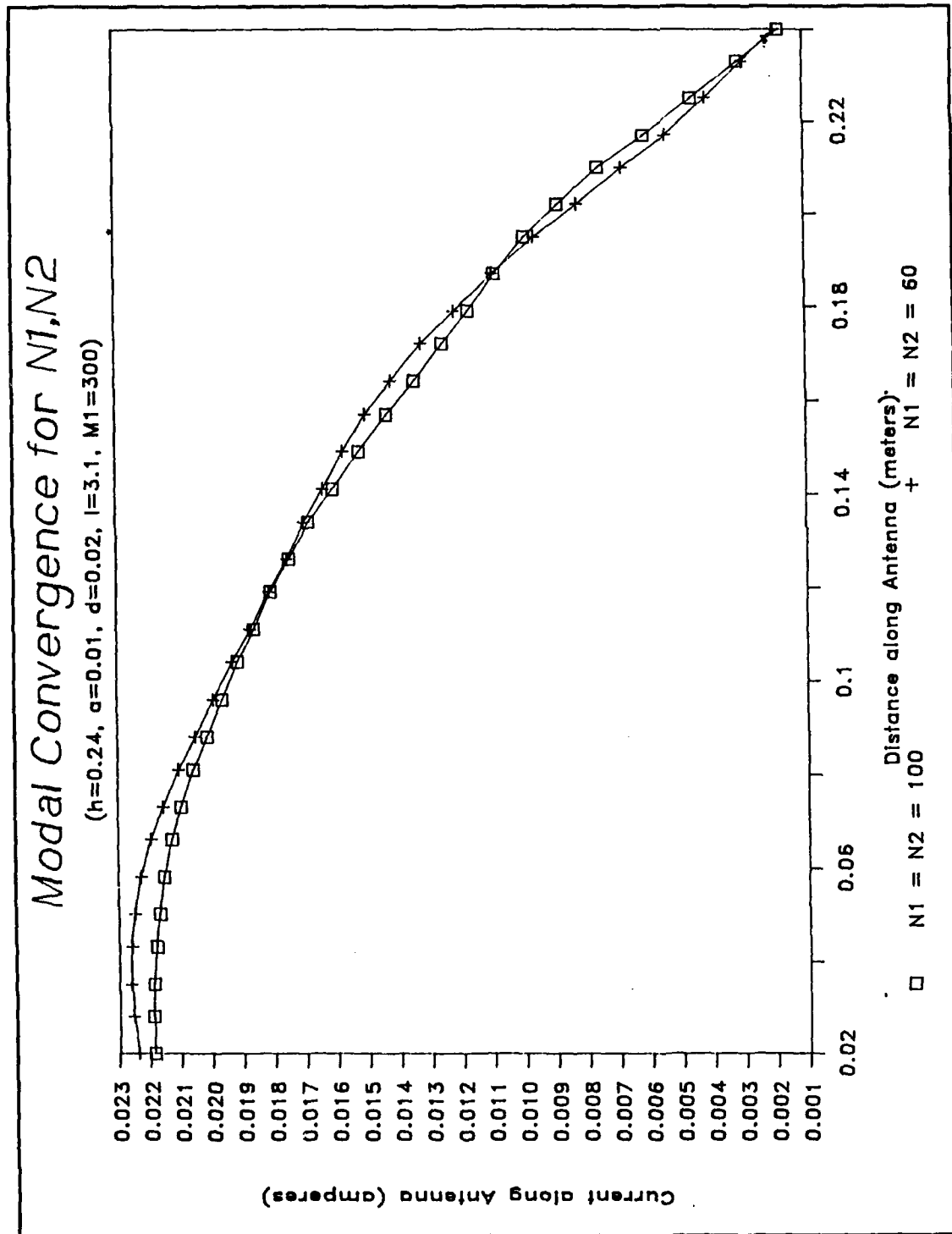


Figure 13 Results for $N_1 = N_2 = 60$ and 100 Modes

However, this approach failed to yield consistent results and a review of the source code showed no errors in the logical design. Upon an examination of the electric field in Region I, it was discovered that a very high value for N_1 would be required in order to obtain convergence to the known field in the narrow feed gap. It was believed that significant errors in the electric field would cause inaccuracies in the result. The errors in the results were thought to be caused by the lack of terms used to describe the electric field. The electric field in the gap region can be thought of as a step function of short duration. In the frequency domain, functions of this type occupy a large spectral bandwidth, requiring many terms for the description. The large expected value of N_1 would necessitate the inversion of a very large matrix, thus making this approach inefficient. To avoid this problem, a separate expansion for the constant electric field was added to Equation 4-1 to form Equation 1-14.

Once again the number of terms required was the main question. However, this field is known prior to the computation and the number of terms can be estimated using standard Fourier analysis. The Fourier transform of a step function is known to be a sinc function with zero crossings at multiples of $1/d$, where d is the duration of the pulse. Each lobe consists of impulse functions at intervals of the fundamental frequency, f_0 , which equals $1/T_0$, where T_0 is the period of the

pulse train. In this case, the upper ground plane causes a reflection of the original structure, but with opposite polarity, at a distance of $2l$ from the lower ground plane. Therefore the number of impulses in each lobe of the sinc function equals $2l/d$. This can be investigated graphically as well. Figures 14 to 19 (pages 48 to 50) illustrate the field computed for a structure with a gap distance (d) of 0.06 meters and upper plate height of 9.54 meters and fed by a constant one volt source for various numbers of terms in the series. As can be expected, when the number of terms are not an integral multiple of l/d , excess oscillations occur. It is also important to note that as the number of terms increase, the calculated curve approaches the ideal value at the discontinuities, while the pointwise error along the rest of the curve increases. However, the error in the least square sense decreases. This is known as the Gibbs phenomenon. Near a discontinuity for a large number of terms, the overshoot is approximately 8.95 percent of the desired value, or -18.17 volts [Ref. 5 p. 557]. This value is reached when the number of terms equals $3l/d$ as seen in Figure 19, therefore additional terms will not reduce the error at the discontinuities. From these graphs, one can see that the number of terms used to represent the electric field in the gap region should be an integer multiple, less than or equal to three, of the ratio of upper plate height to gap distance. An upper plate height

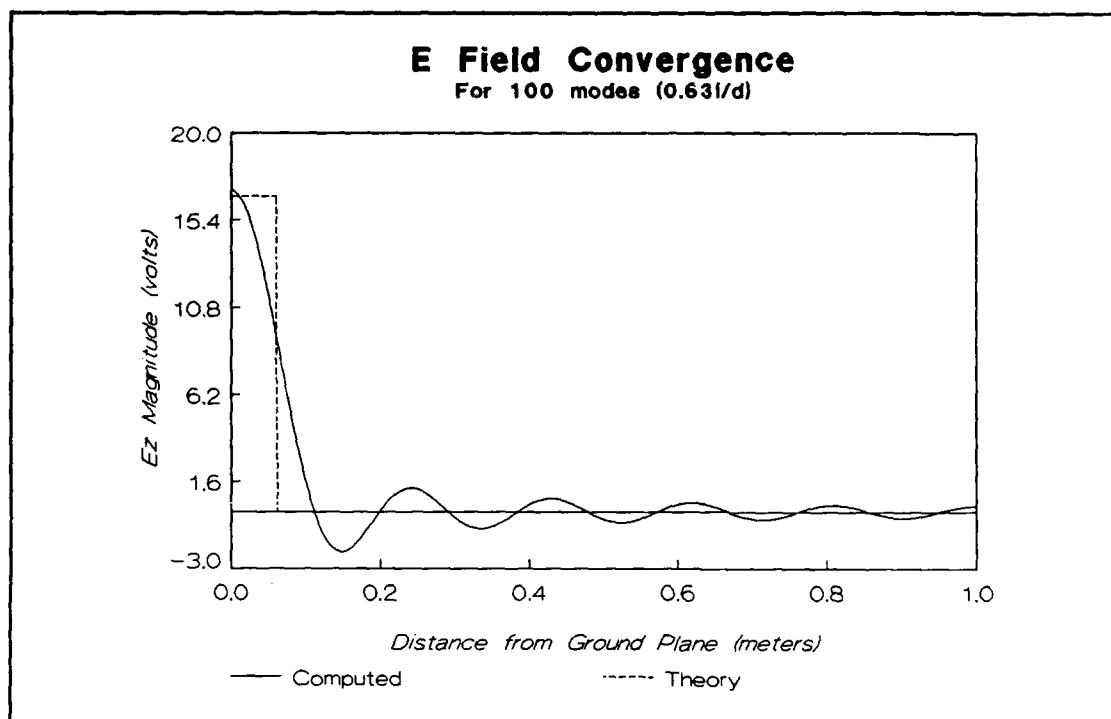


Figure 14 Gap Field Representation for 100 Terms

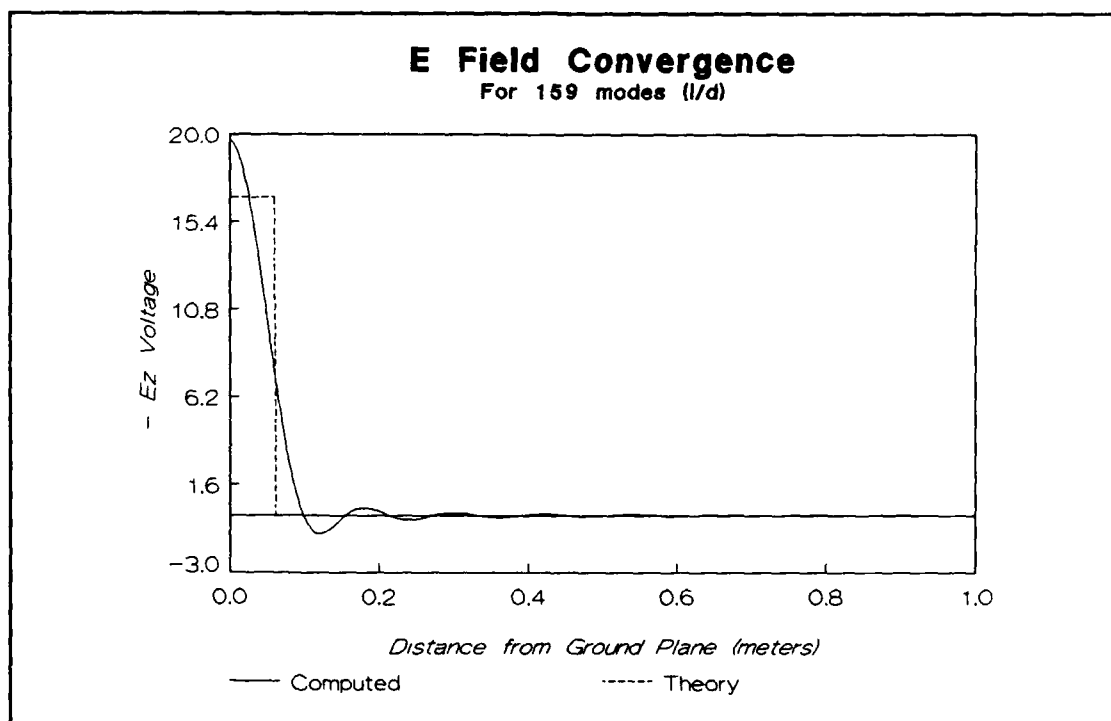


Figure 15 Gap Field Representation for 159 Terms

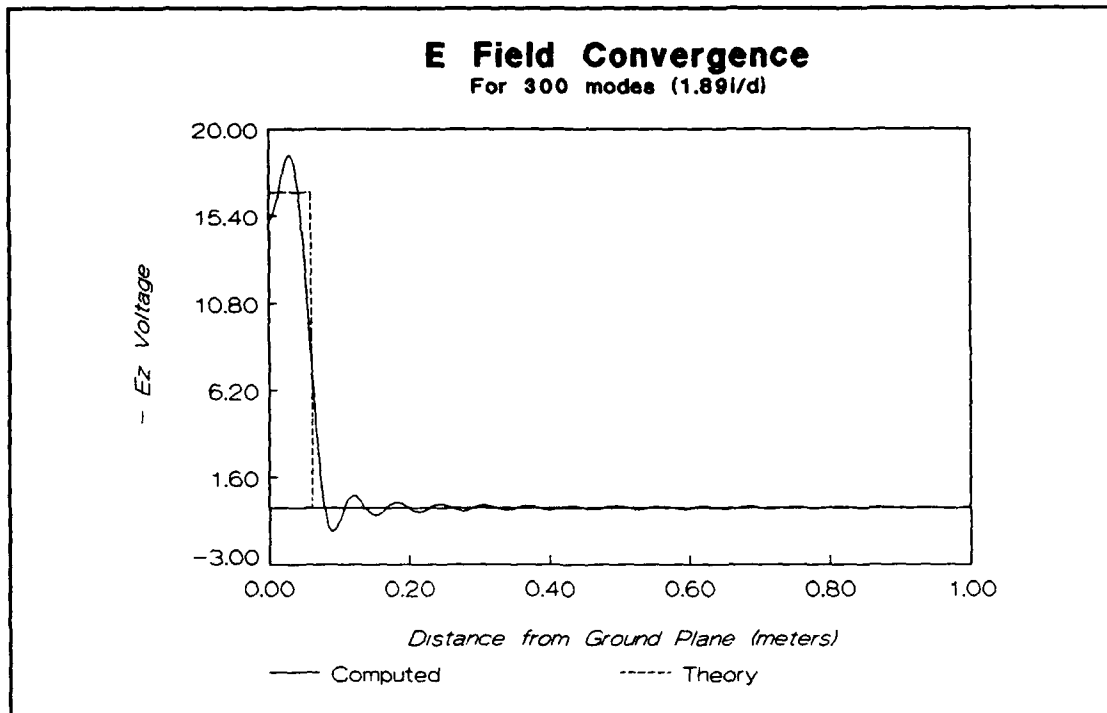


Figure 16 Gap Field Representation for 300 Terms

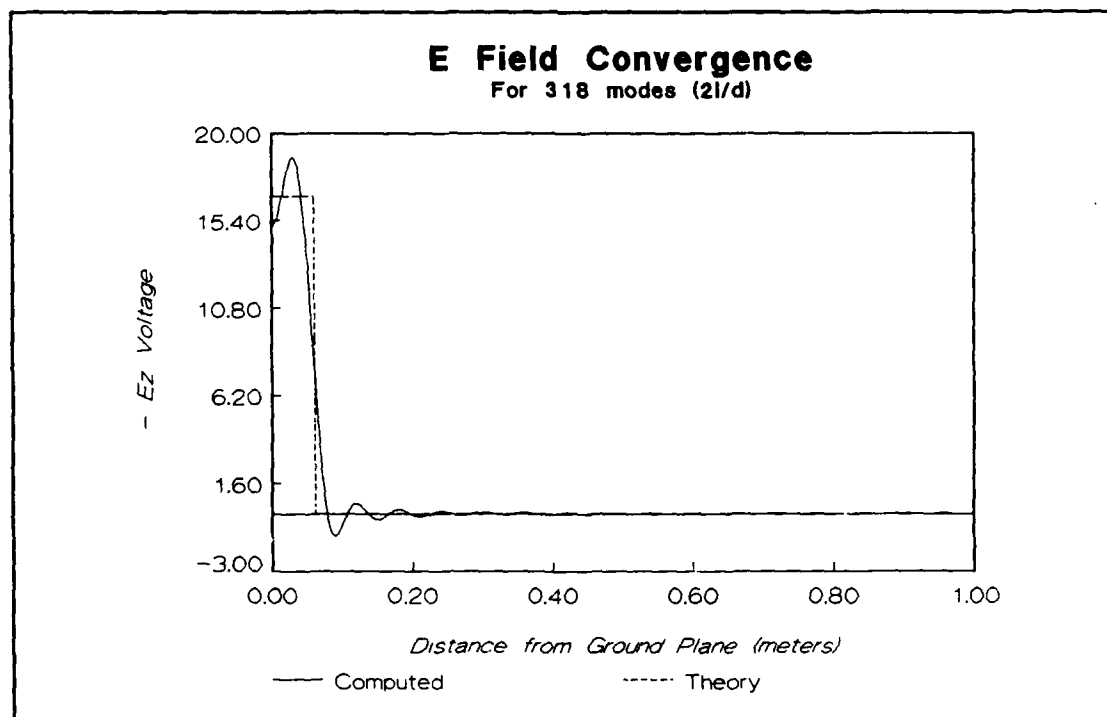


Figure 17 Gap Field Representation for 318 Terms

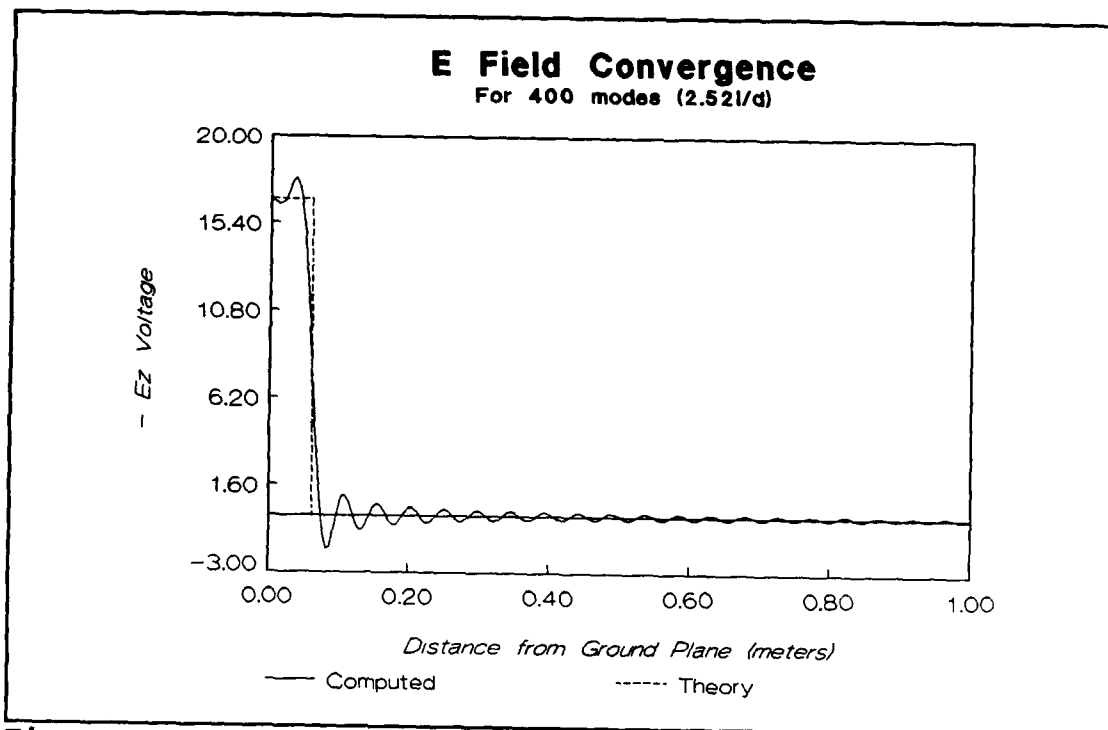


Figure 18 Gap Field Representation for 400 Terms

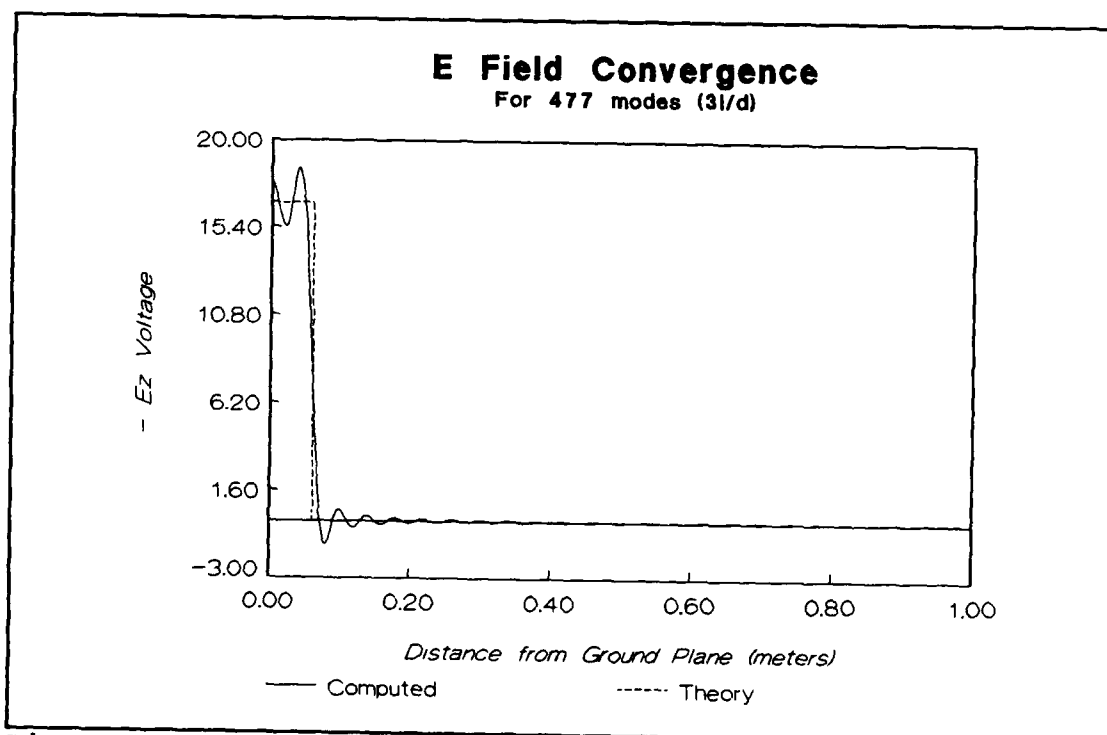


Figure 19 Gap Field Representation for 477 Terms

to gap distance ratio of 250 was considered to be the maximum desired. Therefore to insure the code would fit easily into the 640 kilobyte limit, the number of terms used for this expansion was set at $2l/d$. This was the value used for all the validation calculations completed in Chapter 3.

C. EFFECT OF REDUCING N_1 AND N_2

If the number of terms can be reduced and still provide consistent results, one can then decrease the size of the internal arrays and reduce the computation time. For example, by reducing N_1 by 50%, the computation time is reduced by almost 48%, and when both N_1 and N_2 are reduced by 50%, the computation time is reduced by 71.5%! However, the current distribution along the antenna is unknown, making it difficult to calculate the number of coefficients required for consistent results based on the input parameters. The results obtained by independently varying N_1 and N_2 are shown in Table IV and are compared to the results obtained in Chapter 3 for an antenna with the following physical parameters:

Antenna Height (h)	0.24 λ
Antenna Radius (a)	0.01 λ
Gap Distance (d)	0.02 λ
Plate Spacing (l)	2.17 λ
Number of terms for Gap Region (M_1)	217

Table IV COMPARISON OF RESULTS AS N_1 AND N_2 VARY

N1	N2	Rin	Xin	% Diff	
				Rin	Xin
60	60	43.08	13.98	N/A	N/A
50	50	42.70	13.50	0.88	3.43
40	40	42.80	13.10	0.65	6.29
30	30	41.60	12.40	3.44	11.30
20	20	41.20	9.80	4.36	29.90
50	60	42.20	12.50	2.04	10.59
40	50	41.80	11.30	2.97	19.17
30	40	39.90	8.60	7.38	38.48
20	30	35.60	-0.80	17.36	105.72
60	50	44.60	16.70	3.53	19.46
50	40	44.90	17.47	4.22	24.96
40	30	45.70	18.99	6.08	35.84
30	20	47.40	22.60	10.03	61.66

As expected, the difference in the input impedance increases as the number of terms is reduced. However, the interesting point is the effect that the apparent relationship between N_1 and N_2 has on the result. If N_1 and N_2 are equal, acceptable results are obtained for as low as 30 terms, while one must use at least 50 terms if the values are not equal, to get comparable results. A mathematical explanation for this relationship is not yet understood and will be investigated in future thesis efforts. Figure 20 represents the current distribution as N_1 and N_2 vary independently compared with the result when N_1 and N_2 equal 60.

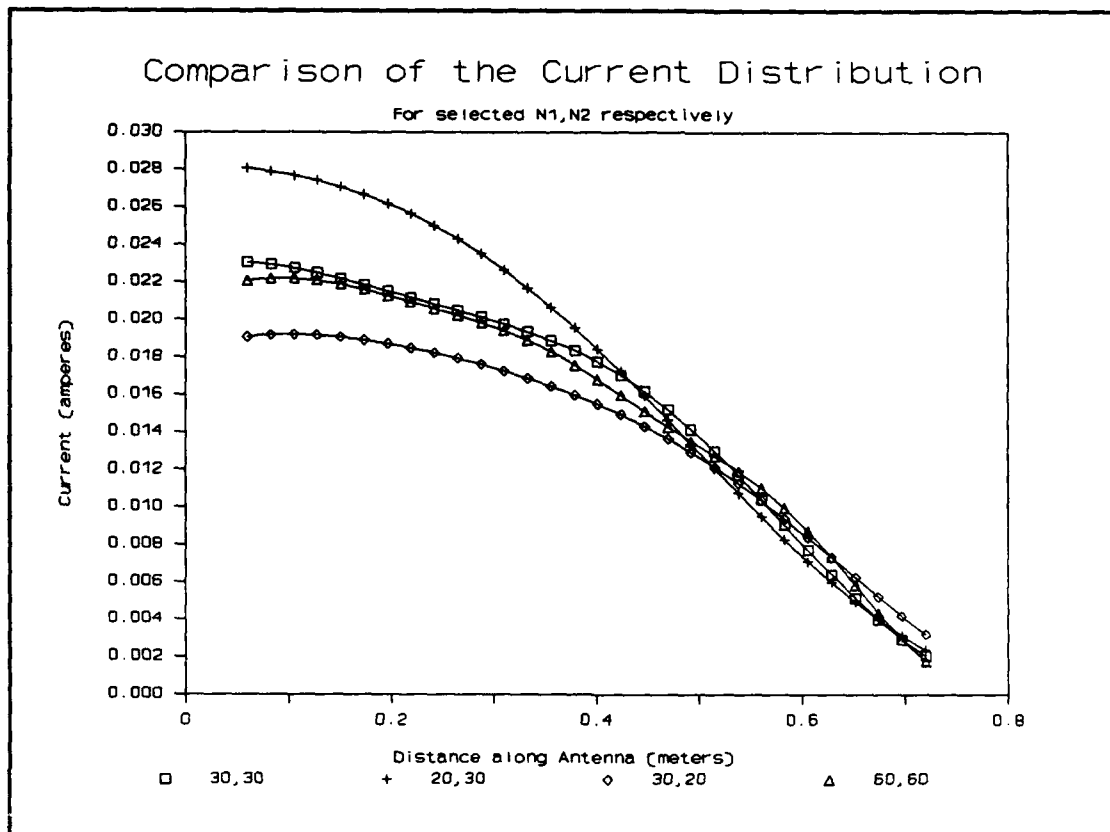


Figure 20 Current Distribution as N_1 and N_2 Vary

D. EFFECT ON ACCURACY AS M_1 VARIES

As seen in the previous section, one can reduce the memory requirements and computation time by reducing the number of coefficients used in Regions I and II. Using Fourier analysis, the user can calculate a value for the number of terms required to accurately represent the electric field along the gap (M_1). Since this value is much larger than N_1 and N_2 , one could dramatically reduce the required

storage and speed up the computations by reducing M_1 to the same order as N_1 and N_2 .

To demonstrate the sensitivity of the input impedance to the number of terms used for the electric field along the gap, one can compare the results against those found when N_1 and N_2 are 60 terms and M_1 is computed as $2l/d$. Table V lists the results for same antenna structure described on page 51. As expected, the errors in the calculated input impedance begin to increase as the number of terms are reduced. However, this difference is not linear for all values of N_1 and N_2 . In fact, Figure 21 suggests an optimal number of M_1 terms, for given N_1 and N_2 , exists which results in smaller differences between the two cases. Since M_1 is a function of the gap distance,

Table V MONO SENSITIVITY TO (M_1) FOR GIVEN N_1 AND N_2

N1	N2	M1	R	X	% Dif	
					R	X
60	60	217	43.08	13.98	N/A	N/A
60	60	60	43.31	13.87	0.53	0.77
60	60	50	43.02	13.85	0.14	0.92
60	60	40	43.39	13.95	0.72	0.20
60	60	30	42.44	14.14	1.49	1.16
50	50	60	42.81	13.44	0.63	3.85
50	50	50	42.59	13.42	1.14	3.99
50	50	40	43.12	13.53	0.09	3.21
50	50	30	42.13	13.72	2.21	1.85
30	30	40	41.72	12.39	3.16	11.36
30	30	30	40.70	12.64	5.52	9.57
30	30	20	42.02	13.26	2.46	5.14
30	30	15	39.41	13.61	8.52	2.63
30	30	10	38.29	14.73	11.12	5.38

the input impedances were recalculated when the gap distance is reduced to 0.01λ for selected values of N_1 and N_2 as shown in Figure 22. While this clearly demonstrates that an optimal number of terms may exist that produces results which approach those for large values of M_1 , N_1 and N_2 , a clear relationship between the physical structure and these values are not yet fully understood.

But how can the number of terms be reduced by almost 91 percent, and yet the difference is no greater than 5.13 percent? First, the basis for selecting the number of terms used was based on obtaining accurate representation for the electric field along the antenna. However, since the far field patterns are derived directly from the currents, it is the current that must remain consistent and not necessarily the electric field along the surface of the antenna. From Equation 1-31, we see that the current is derived from the H_ϕ , or the first derivative of the potential field with respect to ρ . However, the electric field along the z direction is a function of the second derivative of the potential with respect to z . Since the derivative process increases the noise, or errors, it is evident that small differences in the potential field may yield wide variations in the electric field while the magnetic field, and therefore the current distribution, may remain within accepted accuracy limits. To prove this point, Equation 4-2 shows an expression that

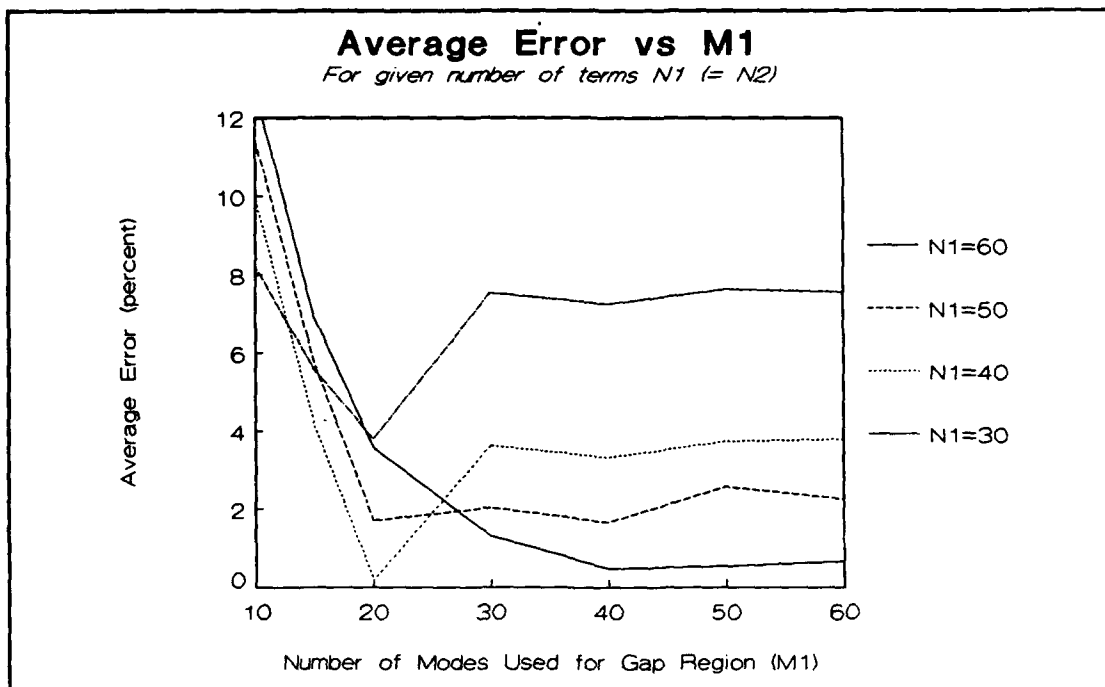


Figure 21 Average Differences for Reduced Values of M_1 for Given N_1 and N_2 Values. (Gap = 0.02λ)

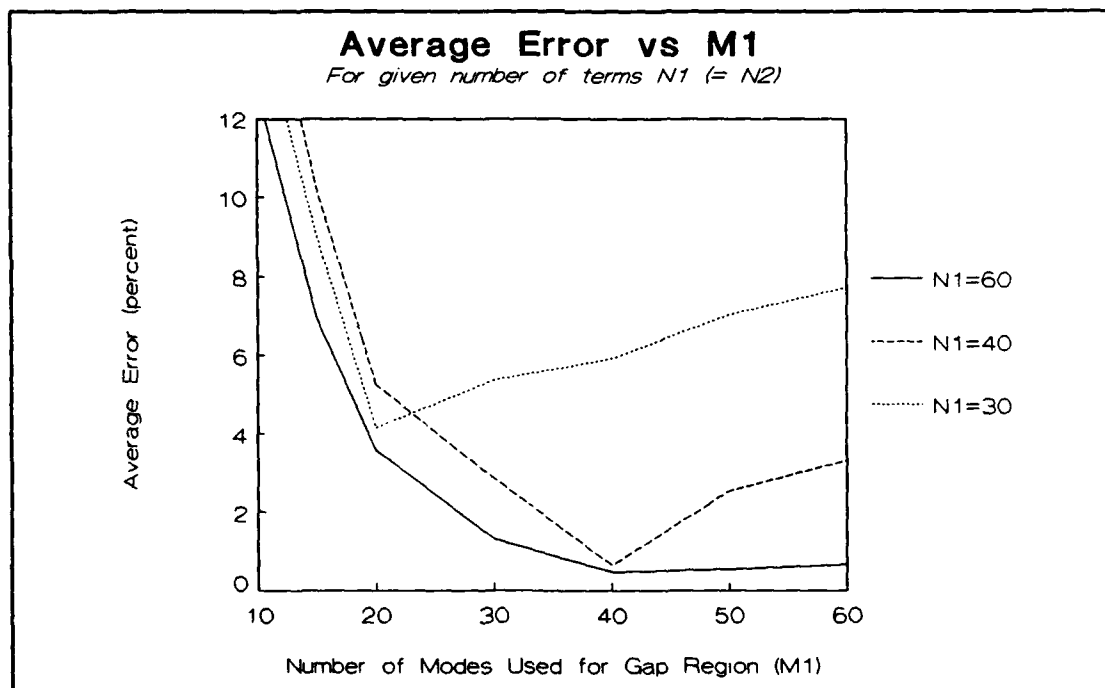


Figure 22 Average Differences for Reduced Values of M_1 for Given N_1 and N_2 . (Gap = 0.01λ)

approximates the electric field along the surface of the antenna by taking the second derivative of Equation 1-31 with respect to z .

$$\frac{d^2}{dz^2} I(z) = \left(\frac{\pi}{2} \right)^2 \left\{ 2\pi a \sum_{n=0}^{N_1} \left[n^2 v_n a_n H_1^{(2)}(v_n a) \cos \left(\frac{n\pi z}{l} \right) \right] \right. \\ \left. + j\omega \epsilon_0 \frac{V_0}{d} \sum_{m=0}^{M_1} \left[m^2 \frac{I_m^{(3)} H_1^{(2)}(v_m a)}{v_m I_m^{(1)} H_0^{(2)}(v_m a)} \cos \left(\frac{m\pi z}{l} \right) \right] \right\} \quad \text{(Eq. 4-2)}$$

This equation can now be used to visualize the approximate change in the electric field along the antenna for a given number of modes M_1 . As shown in Figure 23, the change in the magnitude of the current distribution when M_1 is changed from 217 (which equals $2l/d$) to 30 is negligible. However, Figure 24 shows the curves obtained from Equation 4-2 for the same parameters as used in Figure 23. As one can see, the field is accurately represented near the end of the wire, however near the gap region, there are an insufficient number of coefficients to accurately compute the fields in this region. This refutes the original assumption that the electric fields must be accurately represented to guarantee an accurate current solution. Additionally, since M_1 can be on the same order as the values used for N_1 and N_2 , then the coefficients used to describe the gap field and the field along the structure can be combined into one coefficient. The next

chapter will explore the theory and the differences this new approach has over calculating a separate set of expansion coefficients for the gap region.

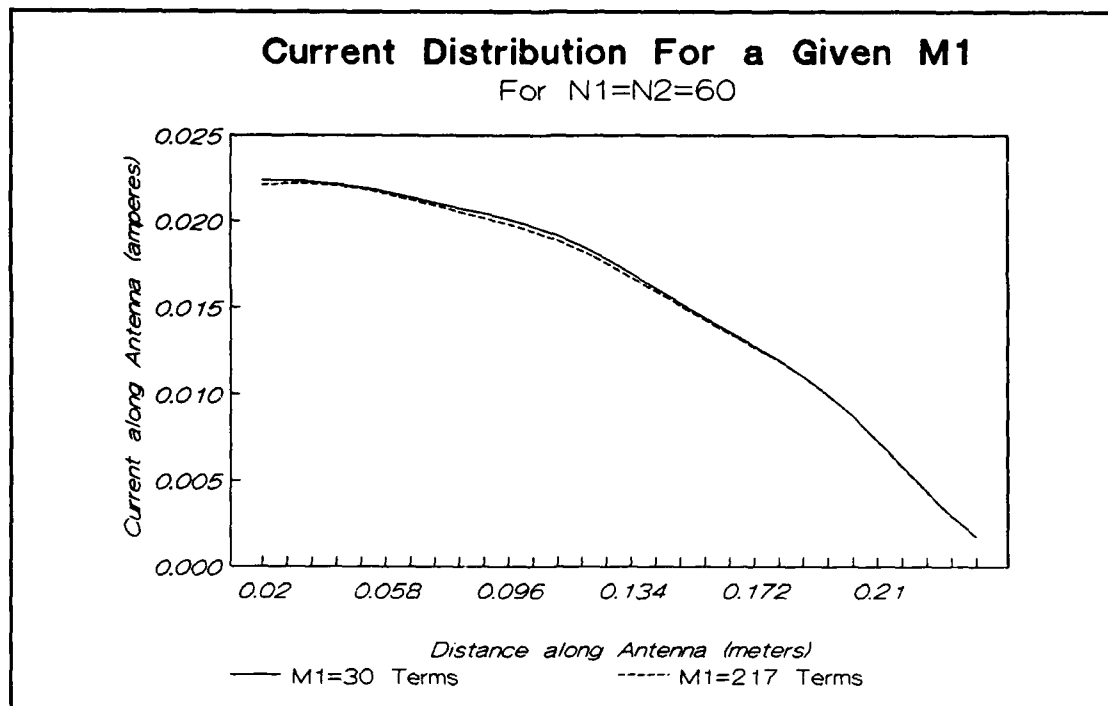


Figure 23 Current Distribution as M1 Varies ($h=0.24\lambda$)

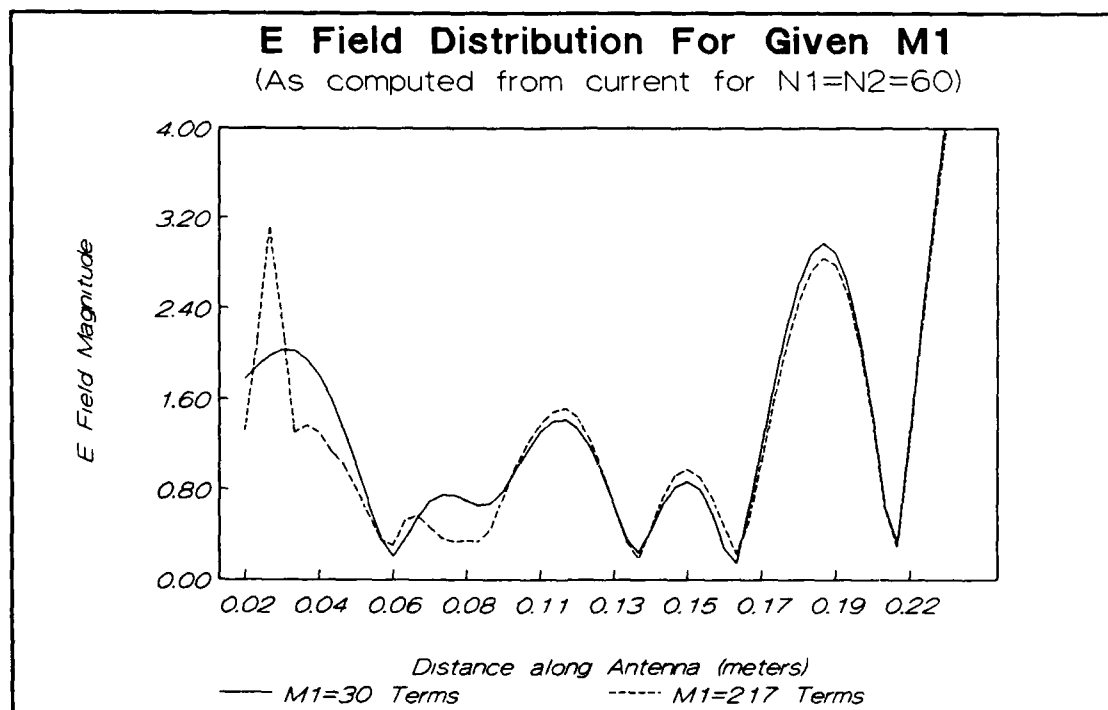


Figure 24 Approximated Electric Field Distribution
(Calculated using Equation 4-2)

V. A SIMPLER APPROACH

During the early stages of the software development, it was decided that a separate expansion for the constant electric field in the gap region was required to obtain consistent results for the input impedance and current distribution along the structure. This decision was based on the belief that large errors in the total electric field along the structure would result in large errors in the current distribution. However since the current distribution is derived directly from the magnetic field, and is relatively insensitive to the electric field, the number of terms used for the gap region expansion was reduced to the same order as those used for N_1 and N_2 without introducing appreciable errors. Noting this, the original method of describing the system was reevaluated such that one could reduce the required memory and speed up the calculations even further by combining the a_n and b_n coefficients used in Equation 1-10 (page 11) into one set of terms and by deleting the separate expansion along the gap region entirely. This chapter will work backwards from the technique presented in Chapter 2 and will note the changes in the system equations resulting from this approach. The resulting code, which will be referred to as MONO8, will then be compared to the results obtained for the cases with

the largest differences between NEC and the code using the separate expansion (called MONO7).

A. MODIFYING THE TECHNIQUE

As was discussed in Chapter 2, the previous approach used two expansions in Region I where $\rho \geq a$. The first expansion sets the tangential electric field to zero from the lower ground plane to the top of the antenna. A second expansion sets the tangential electric field to $-V_0/d$ between the lower ground plane and the feed point of the antenna and sets E_z to zero from this point to the upper ground plane. Since the Fourier transform of a sum is the sum of the transforms [Ref. 7], we can combine the expansions for the potential field in Region I as shown below

$$\psi(\rho, z) = \sum_{n=0}^{N_1} a_n H_0^{(2)}(v_n \rho) \cos\left(\frac{n\pi z}{l}\right) \quad \text{(Eq. 5-1)}$$

where a_n equals the sum of the a_n and b_n coefficients used in Chapter 2. Again we match the magnetic fields across the boundary between Region I and II such that

$$\begin{aligned} H_\phi(a, z) &\approx \sum_{n=0}^{N_1} v_n a_n H_1^{(2)}(v_n a) \cos\left(\frac{n\pi z}{l}\right) \\ &\approx \sum_{n=0}^{N_2} u_n c_n J_1(u_n a) \cos\left[\frac{n\pi(z-h)}{q}\right] \end{aligned} \quad \text{(Eq. 5-2)}$$

By utilizing the orthogonality property of the Fourier moment integrations used in Equation 1-15, the system equation can be expressed as

$$\sum_{k=0}^{N_1} v_k a_k H_1^{(2)}(v_k a) \left\{ \sum_{n=0}^{N_2} \frac{u_n J_0(u_n a) T_{m,n} T_{k,n}}{I_n^{(2)} J_1(u_n a)} \right\} - v_m^2 a_m H_0^{(2)}(v_m a) I_m^{(1)} = \hat{y} \frac{V_0}{d} I_m^{(3)} \quad \text{(Eq. 5-3)}$$

for $m = 0$ to N_1 . This can be expressed in matrix form as

$$\sum_{k=0}^{N_1} A_{m,k} a_k = B_m \quad \text{for } m = 0, N_1 \quad \text{(Eq. 5-4)}$$

where $A_{m,k}$ is given in Equation 1-29. As the b_m coefficients are now included in the a_n terms, the driving vector, B_m , is reduced to

$$B_m = \hat{y} I_m^{(3)} \frac{V_0}{d} \quad \text{(Eq. 5-5)}$$

Once the unknown a_n coefficients are found, the current along the antenna, as a function of z , is now given by

$$I(z) = 2\pi a \sum_{n=0}^{N_1} v_n a_n H_1^{(2)}(v_n a) \cos\left(\frac{n\pi z}{l}\right) \quad \text{(Eq. 5-6)}$$

B. SOFTWARE MODIFICATIONS

As seen in Equations 5-3 to 5-6 above, removing the separate expansion for the electric field along the gap region

requires changing the software code for only the driving vector B_m and the expression for the current as a function of position along the antenna structure. The first advantage realized was the reduction in the amount of memory storage required to run the program. Since it was shown in the previous chapter that the system had converged when the number of modes in Regions I and II were set at 60, independent of the number of modes in the gap region, it was not necessary to dimension any array greater than 60. However, we can now reduce the size of the I , T , J_a , and $P_{m,k}$ matrices by almost an order of magnitude, such that the amount of memory required to run the program has decreased by 75 percent to less than 104 kilobytes. Additionally, the execution time of the program has decreased by an average of 35 percent for the runs presented here.

But does this method yield results that are comparable to the results when the separate expansion is used? We will examine the differences between MONO7 and MONO8 for various plate spacings, antenna heights, as well as the effect that independently varying N_1 and N_2 has on the results obtained earlier.

C. RESULTS

As a first test of the accuracy for MONO8, we will examine the differences in the calculated input impedance

between MONO7 and MONO8 as the ground plane spacing is varied. The three structures used in Chapter 3 for Table II were rerun where N_1 and N_2 were set to 60. Table VI indicates that the

Table VI COMPARISON OF MONO7, MONO8 FOR VARIOUS l

Plate Spacing	MONO7		MONO8		% Diff	
	Rin	Xin	Rin	Xin	R	X
3.10λ	42.65	13.14	43.09	13.12	1.03	0.15
1.40λ	43.14	13.95	43.15	13.96	0.02	0.07
0.81λ	44.67	13.84	44.68	13.82	0.02	0.14

results obtained from the new method differ only slightly from the results obtained when the gap expansion is used.

The next test of the accuracy considered different antenna heights. In this case, the comparison is made between the structures that resulted in the highest difference between MONO7 and NEC, or when the antenna radius was 0.02λ . Table VII shows the results of this comparison for a plate spacing of 1.4λ . Once again, the calculated input impedances differ very little from those obtained using the separate gap expansion.

Table VII COMPARISON OF MONO7, MONO8 FOR SELECTED h

Antenna Length	MONO7		MONO8		% Diff	
	Rin	Xin	Rin	Xin	R	X
0.12λ	13.35	-92.19	13.32	-92.13	0.22	0.06
0.24λ	46.08	15.90	46.08	15.87	0.00	0.18
0.48λ	220.12	-120.91	219.44	-121.34	0.31	0.35

As noted in Chapter 4, the results are more consistent with the solutions obtained from NEC when N_1 equals N_2 . Figure 25 illustrates that this same phenomenon occurs for MON08. Further investigation and study is required to understand the relationship that the number of modes in Regions I and II have on each other. Once this is understood, it may be possible

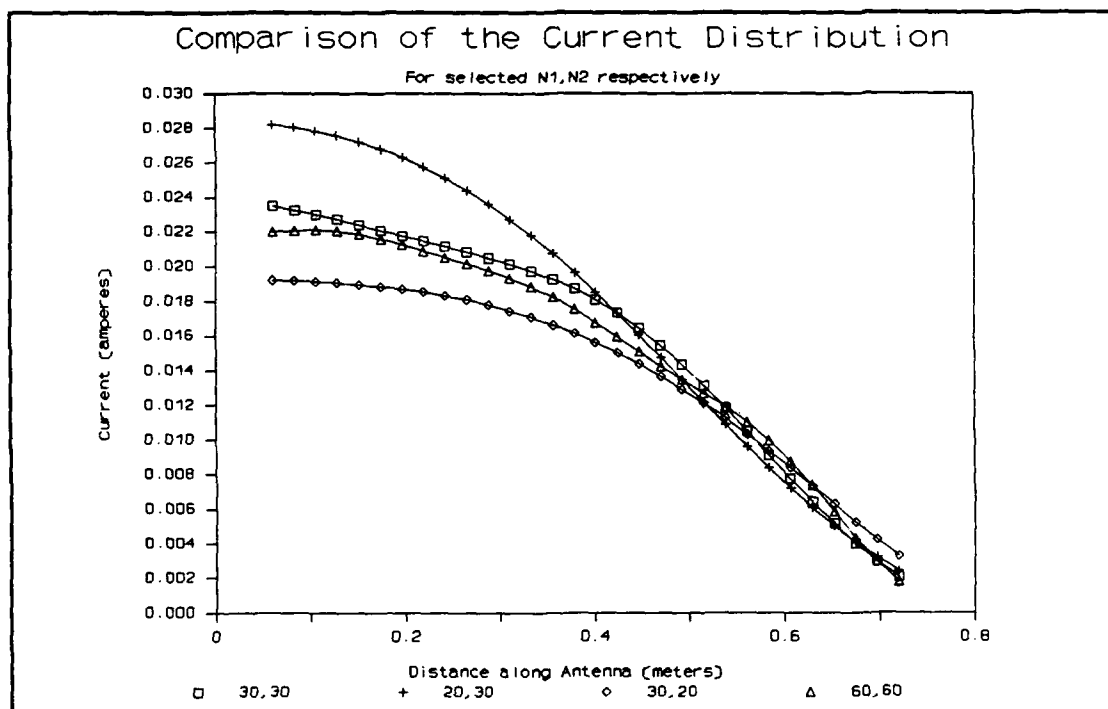


Figure 25 Current Distribution using MON08 as N_1 and N_2 Vary

to derive an expression for the minimum number of modes required to obtain results within a specified accuracy range. This expression could then be used to allow the software to dynamically adjust the number of modes required to obtain accurate results at run time.

In all the above cases, the results were compared to the solution using MONO7 where M_1 was chosen as $2l/d$. However, Figures 21 and 22 (page 56) indicates that there is an optimum number of modes for the gap region to reduce the differences between the solutions of MONO and NEC. Table VIII shows that MONO8 returns the same result for the input impedance as MONO7 did where M_1 , N_1 and N_2 were equal. While this result may not be the closest to NEC's results, the differences are consis-

Table VIII COMPARISON OF MONO8 AND MONO7 AS M_1 VARIES

N1=N2	MONO8 R/X	MONO7 R/X			
		M1=60	M1=50	M1=40	M1=30
60	43.31	43.31	43.02	43.39	42.44
	13.87	13.87	13.85	13.95	14.14
50	42.59	42.81	42.59	43.12	42.13
	13.42	13.44	13.42	13.53	13.72
30	40.70	41.61	41.66	41.72	40.70
	12.64	12.32	12.32	12.39	12.64

tently less than ten percent.

In conclusion, consistent results are obtained without the separate expansion for the gap region. While these results may not offer the closest possible solution to that available by NEC, the small difference in the solution obtained without the extra terms is more than offset by the significant reduction in required memory and calculation time.

When the relationship between the physical structure and the minimum number of modes that are required to obtain the best possible solution is understood, then the software can be modified so as to select the number of terms required at run time. Until then, MONO8 should be the method of choice as its results are more predictable and is capable of returning the result within acceptable accuracy limits without "trial and error".

VI. CONCLUSIONS AND RECOMMENDATIONS

A. CONCLUSIONS

We have shown that one can calculate the current distribution along a monopole using multiregional cylindrical harmonic expansions that are consistent with the results obtained from the Numerical Electromagnetics Code (NEC). While this software package is not intended as a replacement for NEC, it is the beginning step in the development of software directed towards solid antenna structures that are rotated about a symmetrical axis with a simple and flexible input structure. The particular software that has been developed has the following characteristics:

- Simple input data structure. All inputs entered directly, via unformatted ASCII file, or redirected using standard DOS redirection codes allowing batch processing of multiple runs.
- Very flexible for a given monopole antenna structure.
- Can be readily modified to allow for a homogeneous dielectric coating on the surface of the antenna. This coating could be used to modify the surface currents and the far field radiation pattern.

As currently written for the simple monopole, the user is able to modify all the physical parameters of the structure including driving source frequency. With some modifications, including the incorporation of a finite element algorithm in

one sub-region, the user may also include the effect of a nonhomogeneous dielectric coating so that the far field radiation pattern may be tailored as desired.

One difference that should be noted between the techniques used by NEC and MONO is the location used to calculate the input impedance. Due to the NEC's segmentation of the entire structure, the input impedance is actually calculated in the center of the gap region. However, MONO calculates the input impedance based on the value of the current at the base of the antenna. This difference may lead to large discrepancies in the calculated input impedances if the value of the current is changing rapidly at the end of the gap region, as was observed for monopoles whose height approaches a half wavelength. Other differences include:

- MONO requires longer computation time for larger structures than does NEC.
- MONO Requires larger available memory.
- MONO currently has limited error detection and correction within the subroutines.
- The current inability to calculate a number of internal parameters requires a "trial and error" approach to determining the minimum number of modes required for proper convergence.
- User is required to make extensive modifications to MONO's code for various types of antenna structures.
- MONO is a highly specific, concept validation platform vice a generally applicable software package.

B. RECOMMENDATIONS

Continued research is required in order to understand the effect that the apparent relationship between N_1 and N_2 has on the accuracy of the result. Additionally, there appears to be an optimal number of terms required for the gap region that results in an apparent improvement of the result when compared to those obtained using NEC. These unanswered questions point out the need for additional analysis of the relationship between the number of terms required to represent the electric field in a specific region and the overall accuracy of the final result. When this is accomplished, modifications should be made to allow the software to calculate the optimal number of terms required for each expansion that would yield results in the shortest time possible for a specified accuracy range.

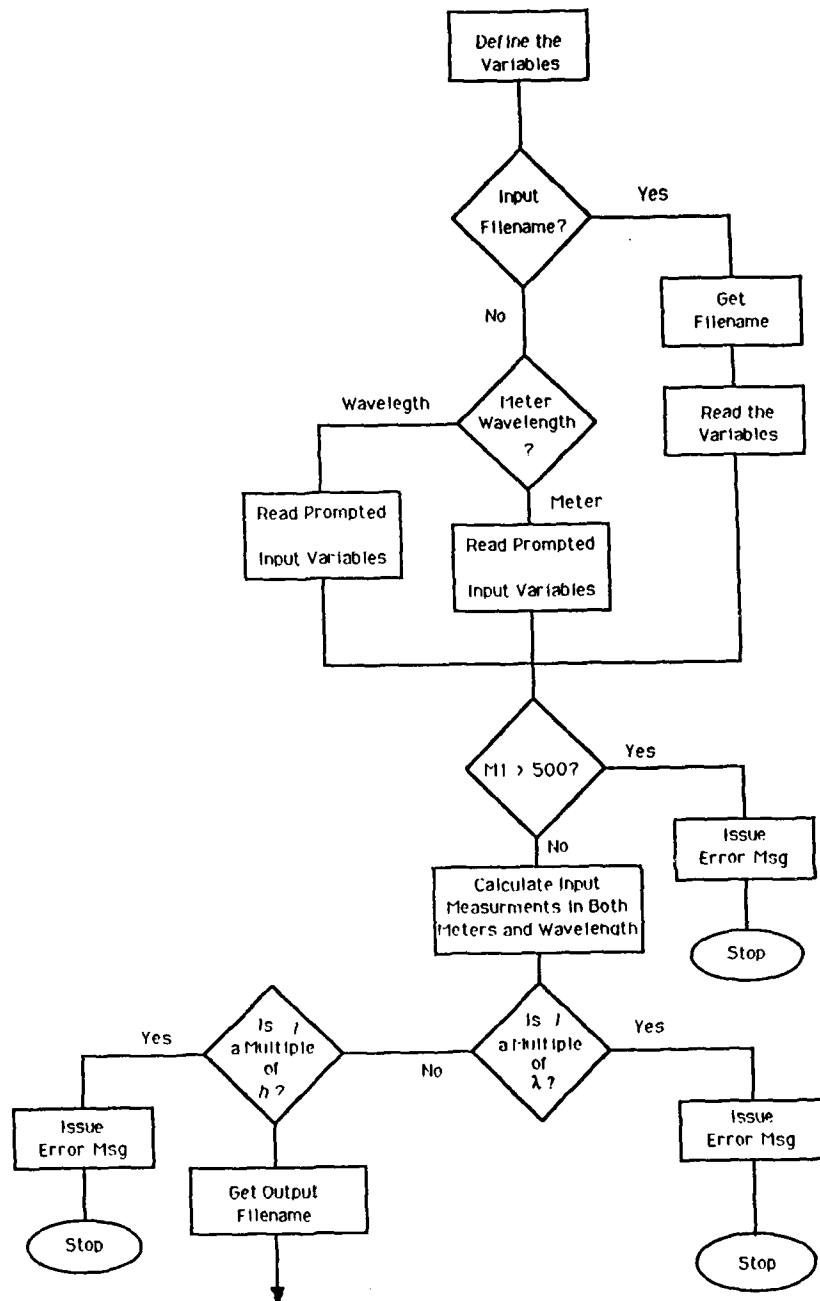
Another modification could be made to the code that would reduce the amount of memory required to run the program. This can be accomplished by temporarily storing only one row of the $P_{m,k}$ matrix at a time, vice storing the entire matrix. This approach could reduce the amount of required memory by as much as 50 percent.

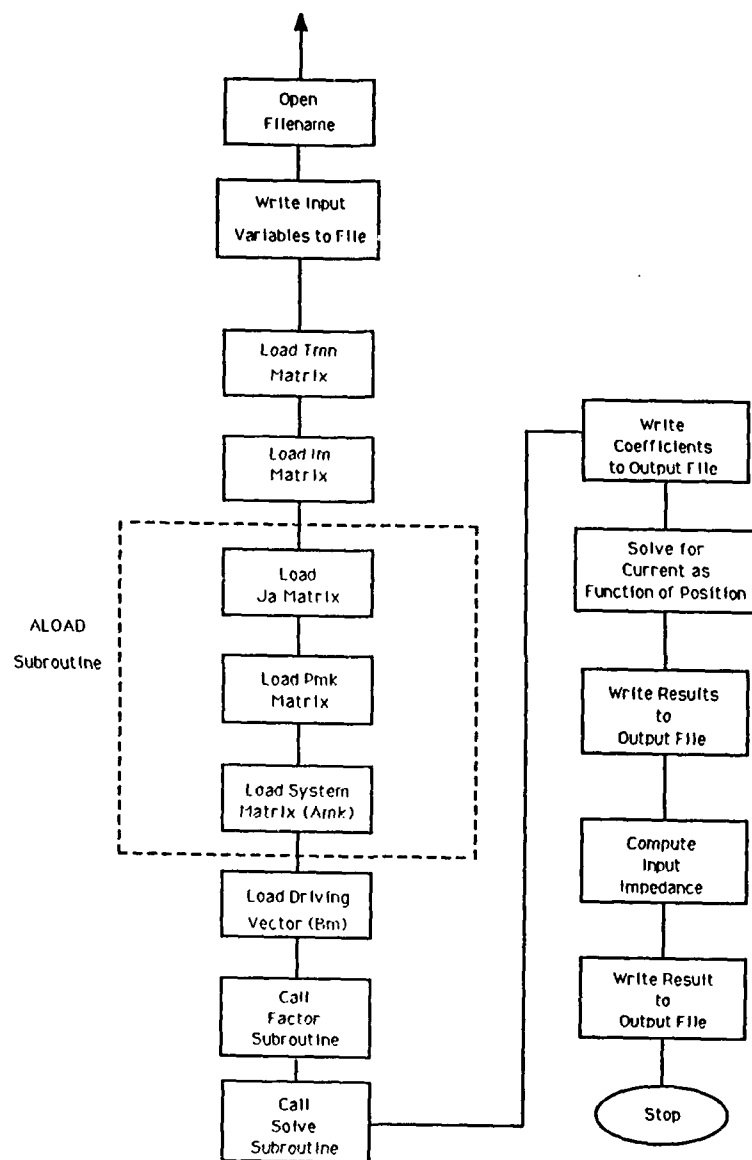
To better assess the benefits of this method over the one used in other computational schemes, experimental data should be compared to the computed results for a variety of structures. In this way, a basic understanding of when this method

best approximates the actual performance characteristics of an operational antenna can be obtained. Once these areas are better understood, a collection of routines for various physical structures should be developed using the basic technique developed in Chapter 2. This collection could include top loaded monopoles, and conical and other structures that feature symmetry about a axis of rotation.

APPENDIX A

SOFTWARE FLOW CHART FOR MONO WITH GAP FIELD EXPANSION





APPENDIX B

SOURCE CODE FOR MONO WITH GAP FIELD EXPANSION

```

C      PROGRAM MONO
C      (Revision 7.3)
C
C      Computing Currents on a Monopole Between Parallel
C      Plates using Cylindrical Harmonic Expansions in 2 Regions.
C      Links with SUBS4.OBJ.      Created 05/87 LT. R.C. Hurley
C
C      ----- Variables -----
C      FMHZ      = Frequency in MHz
C      h         = Monopole height in Meters
C      a         = Monopole radius in Meters
C      d         = Distance between lower ground plane and feed point
C                in Meters
C      l         = Distance between ground planes in Meters
C      q         = height from top of monopole to upper ground plane
C                in Meters
C      j         = Imaginary One
C      pi        = Value of pi (3.1415927)
C      K0        = 2*pi*F/c
C      where F   = frequency of operation in Hz
C                c = Speed of Light
C      K2        = K0**2
C      N1,N2     = Number of Coefficients in each of the two regions
C      NBIG      = Size of the arrays used in FACTOR and SOLVE
C
C      Unit 6     = Screen Output
C      Unit 7     = Main Output File to Disk (Name selected by User.)
C      ***** Variable Definitions *****
C
C      INTEGER k,m,M1,Mmax,mpn,n,ns,N1,N2,Nbig,Nl,Nmax,P(61)
C      REAL a,ai,Am,An,Bl,c,C1,CM,CP,CR,d,di,DeltaZ,Denom,eps,FMHZ,h,hi
C      REAL I(0:500,1:3),K0,K2,l,li,Lambda,Pi,q,Rin,S
C      REAL T(0:500,0:60),w,Xin,y,yhat
C      COMPLEX Amk(61,61),B(61),C1,C2,IZ(61),j,J0,J1,Ja(0:500,1:4)
C      COMPLEX Pmk(0:60,0:500),Sum,Sum1,Y0,Y1,Zin
C      CHARACTER*25 Fname
C      CHARACTER*1 Bell
C      CHARACTER*1 HOW
C      CHARACTER*1 INPUT
C      CHARACTER*12 INname
C      COMMON/Plk1/I,j,N1,Pi,d,Nbig
C      COMMON/Blk2/K2,l,Mmax,N2,q,a,T
C
C      *****
C      *      Main Program Code      *
C      *****
C
C      *****
C      *      Input Section      *
C      *****
C
C      Bell=CHAR(7)

```

```

Nbig=61
c=3.0E+08
WRITE(6,*) 'Do you wish to use an input data file [Y/N]?'
READ(0,100) HOW
IF (HOW.EQ.'Y'.OR.HOW.EQ.'Y') THEN
    WRITE(6,*) 'Enter input data file name with extension : '
    READ(0,100) INname
    OPEN(Unit=4,File=INname)
    READ(4,100) INPUT
    IF ((INPUT.EQ.'W') .OR. (INPUT.EQ.'W') .OR. (INPUT.EQ.
+ 'm') .OR. (INPUT.EQ.'M')) THEN
        READ(4,*) FMHZ,hi,ai,di,li,N1,N2,M1,N1
    ELSE
        WRITE(*,*) Bell
        WRITE(6,*) 'Error detected in first line of data file '
+ INname
        WRITE(6,*) 'First line must be either M or W for meter
+ values or wavelength values.'
        STOP
    ENDIF
ELSE
    2 WRITE(6,*) 'Enter data in either [M]eters or [W]avelength [M
+ /W]?'
    READ(0,100) INPUT
    IF (INPUT.EQ.'m'.OR.INPUT.EQ.'M') THEN
        WRITE(6,*) 'Enter Frequency in MHz: '
        READ(0,*) FMHZ
        WRITE(6,*) 'Enter Monopole Height, h, in meters: '
        READ(0,*) hi
        WRITE(6,*) 'Enter Monopole Radius, in meters: '
        READ(0,*) ai
        WRITE(6,*) 'Enter Feed Gap, d, in meters: '
        READ(0,*) di
        WRITE(6,*) 'Enter Upper Plane Height, l (meters): '
        READ(0,*) li
    ELSEIF (INPUT.EQ.'w'.OR.INPUT.EQ.'W') THEN
        WRITE(6,*) 'Enter Frequency in MHz: '
        READ(0,*) FMHZ
        WRITE(6,*) 'Enter Monopole Height, h, as factor of wav
+ elength : '
        READ(0,*) hi
        WRITE(6,*) 'Enter Monopole Radius, as factor of wavele
+ ngth : '
        READ(0,*) ai
        WRITE(6,*) 'Enter Feed Gap, d, as factor of wavelength
+ : '
        READ(0,*) di
        WRITE(6,*) 'Enter Upper Plane Height, l, as factor of
+ wavelength : '
        READ(0,*) li
    ELSE
        WRITE(*,*) Bell
        WRITE(6,*) 'You must enter either an M or W.
+ Reenter.. '
        GOTO 2
    ENDIF
    WRITE(6,*) 'Enter # Region 1 Coeffs. (N1 .LE. 60): '
    READ(0,*) N1
    WRITE(6,*) 'Enter # Region 2 Coeffs. (N2 .LE. 60): '
    READ(0,*) N2
    WRITE(6,*) 'Enter # Gap Region Coeffs.(M1 .LE. 500): '
    READ(0,*) M1
    WRITE(6,*) 'Enter No. Points for I(z) including ends: '
    READ(0,*) N1

```

```

ENDIF
IF (M1.GT.500) Then
  WRITE(*,*) Bell
  WRITE(6,*) 'Ratio l/d too large. Adjust either:'
  WRITE(6,*) '      a) l or d such that 2l/d < 500'
  WRITE(6,*) '      b) Array sizes of lm,T,Ja'
  STOP
ENDIF

C      *****
C      *
C      *      Calculate the Physical Parameters      *
C      *      in both Wavelength and Meters          *
C      *
C      *****

Lambda=c/(FMHZ*10**(6))
IF (INPUT.EQ.'w'.OR.INPUT.EQ.'W') THEN
  h=hi*Lambda
  a=ai*Lambda
  d=di*Lambda
  l=li*Lambda
ELSE
  h=hi
  hi=h/Lambda
  a=ai
  ai=a/Lambda
  d=di
  di=d/Lam...
  l=li
  li=l/Lambda
ENDIF

C      *****
C      *
C      *      Is Upper Plate Height an              *
C      *      Even Multiple of Wavelength?          *
C      *
C      *****

IF (MOD((l*2),Lambda).LT. 1E-05) THEN
  WRITE(*,*) Bell
  WRITE(6,*) ' '
  WRITE(6,*) 'ERROR! Upper Plate Height is almost an even mul
+title of half the wavelength.'
  WRITE(6,*) 'Ensure l is NOT within 0.00001 of an integer mul
+title of half the wavelength.'
  STOP
ENDIF

C      *****
C      *
C      *      Is Upper Plate Height an              *
C      *      Even Multiple of Antenna Height?      *
C      *
C      *****

E=(10*h)-(ANINT((10*h)/l)*l)
IF ((MOD(l,h)).LT.1E-05) THEN
  WRITE(*,*) Bell
  WRITE(6,*) ' '
  WRITE(6,*) 'ERROR! Upper Plate Height is almost an even mul
+title of the antenna height.'
  WRITE(6,*) 'Ensure l is NOT within 0.00001 of an integer mul
+title of h (in wavelength).'

```

```

      STOP
ENDIF
WRITE(6,*) 'Enter output file name and extension: '
READ(0,100) Fname
OPEN (Unit=7,File=Fname)
WRITE(7,210) FMHZ
WRITE(7,220) h,hi
WRITE(7,230) a,ai
WRITE(7,240) d,di
WRITE(7,250) l,li
WRITE(7,*) 'Region I Coeffs. (M1): ',M1
WRITE(7,*) 'Region II Coeffs. (M2): ',M2
WRITE(7,*) 'No. Gap Coeffs. (M1): ',M1
WRITE(7,*) 'No. Points for I(z): ',N1
j=(0.0,1.0)
Pi=3.1415927
K0=Pi*FMHZ/150.0
K2=K0*K0
q=l-h
Nmax=MAX0(N1,N2)
Mmax=MAX0(Nmax,M1)
WRITE(6,*) 'Loading the Moment Matrices ..... '
WRITE(6,*) ' '

C      *****
C      *
C      *      Evaluating Moment Integrations      *
C      *      Over Region h < z < l.              *
C      *
C      *****

      T(0,0)=q
      DO 11 k=1,N2
        T(0,k)=0.0
11    CONTINUE
      DO 22 m=1,Mmax
        Am=m*Pi/l
        DO 22 n=0,N2
          An=n*Pi/q
          IF((ABS(Am-An)).GT.1.0E-3) THEN
            Denom=Am*Am-An*An
            S=SIN(Am*h)
            T(m,n)=-Am*S/Denom
          ELSE
            mpn=m+n
            T(m,n)=0.5*q*((-1)**mpn)
          ENDIF
        CONTINUE
22    WRITE(6,*) '      Moment Mat ix T Loaded.'
      WRITE(6,*) ' '

C      *****
C      *
C      *      Loading the Im Matrix for the      *
C      *      Largest Number of Coefficients      *
C      *
C      *****

      DO 33 m=0,Mmax
        IF(m.EQ.0) Then
          I(m,1)=l
          I(m,2)=q
          I(m,3)=d
        ELSE

```

```

        I(m,1)=l/2.0
        I(m,2)=q/2.0
        Am=m*Pi/l
        I(m,3)=SIN(Am*d)/Am
    ENDIF
33  CONTINUE
    WRITE(6,*) '          Moment Matrix I Loaded.'
    WRITE(6,*) ' '
    WRITE(6,*) 'Loading System Matrix .....'
    CALL ALOAD(Ja,Pmk,Amk)
    WRITE(6,*) 'System Matrix Amk Loaded.'
    WRITE(6,*) ' '
    WRITE(6,*) 'Loading Driving Vector .....'
    CALL BLOAD(FMHZ,N1,Pmk,Ja,B)
    WRITE(6,*) 'Driving Vector B Loaded.'
    WRITE(6,*) ' '
    WRITE(6,*) 'Solving the Linear System .. Please Wait .... '
    Ns=N1+1
    CALL FACTOR(Amk,P,Ns,Nbig)
    CALL SOLVE(Amk,B,P,Ns,Nbig)
    WRITE(7,*) 'Listing the Expansion Coefficients'
    WRITE(6,*) '      Listing the Expansion Coefficients .....'
    WRITE(7,*) 'N and B(N): '
    DO 44 N=0,N1
        WRITE(7,*) N,B(N+1)
44  CONTINUE

C          *****
C          *
C          *      Computing Current from the      *
C          *      Expansion Coefficients          *
C          *
C          *****

    WRITE(6,*) ' '
    WRITE(6,*) 'Computing current on the monopole.....'
    WRITE(7,*) 'Listing the Current on the Monopole'
    DeltaZ=(h-d)/(N1-1)
    WRITE(7,*) 'Position      Distance      I(z) (A)'
    WRITE(7,*) '      Number      (Meters)      Mag      Phase'
    eps=8.854E-12
    w=2.0E6*Pi*FMHZ
    yhat=w*eps
    y=d
    k=1
55  Sum=(0.,0.)
    DO 66 n=0,N1
        Sum=Sum+(B(n+1)*Ja(n,3)*cos(n*Pi*y/l))
66  CONTINUE
    Sum1=(0.0,0.0)
    DO 77 m=0,N1
        Sum1=Sum1+((I(m,3)*Ja(m,3)*COS(m*Pi*y/l))/(Ja(m,4)*I(m,1)))
77  CONTINUE
    IZ(k)=2.0*Pi*a*(Sum-j*yhat*Sum1/d)
    CM=CABS(IZ(k))
    CR=REAL(IZ(k))
    CI=AIMAG(IZ(k))
    CP=180.*ATAN2(CI,CR)/pi
    WRITE(7,200) k,y,CM,CP
    y=y+DeltaZ
    k=k+1
    IF(y.LE.(h+1.E-6)) GO TO 55
    WRITE(6,*) 'Complete.'

```

```

C          *****
C          *
C          *      Computing Input Impedance      *
C          *
C          *****

Zin=(1.0,0.0)/12(1)
Rin=REAL(Zin)
Xin=AIMAG(Zin)
WRITE(7,*) 'Input Resistance = ',Rin
WRITE(7,*) 'Input Reactance = ',Xin

C          *****
C          *
C          *      I/O Format Statements          *
C          *
C          *****

100  FORMAT(A)
102  FORMAT(I5)
103  FORMAT(E12.3)
200  FORMAT(2X,I3,5X,F8.3,5X,1PE12.3,5X,0PF8.2,1PE12.3,5X,0PF8.2,
+1PE12.3,5X,0PF8.2)
210  FORMAT(' Driving Frequency, ',9X,F7.3,' MHz')
220  FORMAT(' Monopole Height, ',9X,F7.3,' meters (' ,F5.3,' Lambda)')
230  FORMAT(' Monopole Radius, ',9X,F7.3,' meters (' ,F5.3,' Lambda)')
240  FORMAT(' Feed Gap Distance, ',9X,F7.3,' meters (' ,F5.3,' Lambda)')
250  FORMAT(' Upper Plane Height, ',9X,F7.3,' meters (' ,F5.3,' Lambda)')
STOP
END

```

SUBROUTINE ALOAD(Ja,Pmk,Amk)
Revision 7.3)

80

```

DO 11 n=0,Mmax
  R1=K2-((n*Pi/q)*(n*Pi/q))
  R2=K2-((n*Pi/L)*(n*Pi/L))
  un=CSR(R1)
  vn=CSR(R2)
  zu=un*a
  zv=vn*a
  Call BES1(zu,J0n,J1n)
  Call HAN1(zv,H0n,H1n)
  Ja(n,1) = Un*J0n
  Ja(n,2) = J1n
  Ja(n,3) = Vn*H1n
  Ja(n,4) = Vn*Vn*H0n
  write(7,*) 'n=',n,'ja(n,4)=',ja(n,4)
C
11 Continue
  WRITE(6,*) '      Completed.'
  WRITE(6,*) ' '
  WRITE(6,200) n1,Mmax
C
C Loading the Pmk Matrix (size N1 x Mmax)
C
DO 22 m=0,N1
  WRITE(6,300) m,cr
  DO 22 k=0,Mmax
    Pmk(m,k)=(0.0,0.0)
    DO 33 n=0,N2
      S1=(Ja(n,1)*T(m,n)*T(k,n))/(l(n,2)*Ja(n,2))
      Pmk(m,k)=Pmk(m,k)+S1
33 CONTINUE
22 CONTINUE
  WRITE(6,*) '      Completed.'
DO 44 m=0,N1
  DO 44 k=0,N1
    If(m.EQ.k) Then
      Amk(m+1,k+1)=Ja(k,3)*Pmk(m,m)-Ja(k,4)*I(m,1)
    ELSE
      Amk(m+1,k+1)=Ja(k,3)*Pmk(m,k)
    ENDIF
44 CONTINUE
100 FORMAT('      Loading Ja matrix of size',I3,' x 4.....')
200 FORMAT('      Loading Pmk Matrix of size',I3,' x ',I3,'.....')
300 FORMAT('      Calculating row',i3,a,\)
RETURN
END
C
C *****
C
C SUBROUTINE BLOAD(FMHZ,M1,Pmk,Ja,B)
C
C *****
C *
C * Variable Definitions
C *
C *****
C B(m) = Driving Matrix
C N1 = Number of Coefficient Expansions in Region 1
C I3(m) = Trig. Moment Integrations
C FMHZ = Driving voltage frequency in megahertz
C eps = 8.854E-12
C j = Imaginary One
C
Real d,I(0:500,'.3),Pi,eps,w
Integer k,M,M1,N1,Nbig
Complex B(Nbig),j,Ja(0:500,1:4),Pmk(0:60,0:500),Sum

```



```

COMMON/Blk1/I,J,N1,Pi,d,Nbig
eps=8.854E-12
w=2.0E6*Pi*FMHZ
DO 22 m=0,N1
    Sum=(0.0,0.0)
    DO 33 k=0,M1
        Sum=Sum+((I(k,3)*Ja(k,3)*Pmk(m,k))/(I(k,1)*Ja(k,4)))
33    CONTINUE
    B(m+1)=j*w*eps*Sum/d
22    CONTINUE
    RETURN
    END

C
C *****
C

FUNCTION CSR(R)
REAL R
COMPLEX CSR
C Evaluating SQRT(R) with special consideration to neg. reals
IF(R.GE.0.0) then
    CSR=SQRT(R)
else
    CSR=(0.,-1.)*SQRT(-R)
end if
RETURN
END

C
C *****
C

SUBROUTINE BES1(Z,J0,J1)
C
C Computing Bessel Functions for n=0,1 with
C Complex Argument, Z. Direct Power Series Method for
C CABS(Z) .LE. 6 and Hankel's Asymptotic Formula for
C CABS(Z) .GT. 6. Written 11/5/87 by M.A. Morgan
C
INTEGER M,M2
REAL C(34),DM,F(34),G0,P(34),Pi,P2
COMPLEX Z,Z2,Z3,Z4,J0,J1,AM,CL,P0,P1,Q0,Q1,C0,C1,S0,S1
Pi=3.1415927
P2=2.0/Pi
IF(CABS(Z).LE.6.0) THEN
C
C Utilizing the Direct Power Series Method
C
    G0= 1.781072
    Z2=0.5*Z
    CL=CLOG(G0*Z2)
C
C Computing F(m) = m ! and P(m) = 1 + 1/2 + 1/3 + ....+ 1/m
C
    F(1)=1.0
    P(1)=1.0
    DO 11 M=2,34
        F(M)=M*F(M-1)
        P(M)=P(M-1)+1.0/M
11    CONTINUE
C
C Computing Power Series Coefficients
C
    DM=-1.0

```

```

      DO 22 M=1,34
        C(M)=DM/(F(M)*F(M))
        DM=-DM
22     CONTINUE
C
C     Computing J0 and J1
C
      J0=(1.,0.)
      J1=(0.,0.)
      M=0
33     M=M+1
      M2=2*M
      AM=C(M)*(Z2**M2)
      J0=J0+AM
      J1=J1-M*AM
      IF((CABS(AM).GT.1.0E-10).AND.(M.LT.34)) GO TO 33
      J1=J1/Z2
      return
    ELSE
C
C     Hankel' Asymptotic Formula (Abram. & Stegun p. 364)
C
      Z2=Z*Z
      Z3=Z*Z2
      Z4=Z*Z3
      P0=1.0-.0703125/Z2+.1121521/Z4
      Q0=-.125/Z+.0732422/Z3
      P1=1.0+.1171875/Z2-.1441956/Z4
      Q1=.375/Z-.10253906/Z3
      C0=CCOS(Z-.25*PI)
      S0=CSIN(Z-.25*PI)
      C1=CCOS(Z-.75*PI)
      S1=CSIN(Z-.75*PI)
      AM=CSQRT(P2/Z)
      J0=AM*(P0*C0-Q0*S0)
      J1=AM*(P1*C1-Q1*S1)
    ENDIF
  RETURN
  END

C
C *****
C

      SUBROUTINE HAN1(Z,H0,H1)
C
C     Computing Hankel Functions for n=0,1 with
C     Complex Argument, Z. Direct Power Series Method for
C     CABS(Z) .LE. 5 and Hankel's Asymptotic Formula for
C     CABS(Z) .GT. 5. Written 11/6/87 by M.A. Morgan
C
      INTEGER M,M2
      REAL C(34),DM,F(34),G0,P(34),PI,P2
      COMPLEX Z,Z2,Z3,Z4,J0,J1,Y0,Y1,AM,CL,P0,P1,Q0,Q1
      COMPLEX E0,E1,X0,X1,H0,H1,j
      PI=3.1415927
      P2=2.0/PI
      j=(0.,1.)
      IF(CABS(Z).LE.5.0) THEN
C
C     Direct Power Series Method
C
      G0= 1.78072
      Z2=0.5*Z

```

```

      CL=CLOG(G0*Z2)
C
C   Computing F(m) = m! and P(m) = 1 + 1/2 + 1/3 + ....+ 1/m
C
      F(1)=1.0
      P(1)=1.0
      DO 11 M=2,34
          F(M)=M*F(M-1)
          P(M)=P(M-1)+1.0/M
11      CONTINUE
C
C   Computing Power Series Coefficients
C
      DM=-1.0
      DO 22 M=1,34
          C(M)=DM/(F(M)*F(M))
          DM=-DM
22      CONTINUE
C
C   Computing J0 and J1
C
      J0=(1.,0.)
      J1=(0.,0.)
      M=0
33      M=M+1
          M2=2*M
          AM=C(M)*(Z2**M2)
          J0=J0+AM
          J1=J1-M*AM
          IF((CABS(AM).GT.1.0E-10).AND.(M.LT.34)) GO TO 33
      J1=J1/Z2
C
C   Computing Y0 and Y1
C
      M=0
      Y0=CL*J0
      Y1=Z2*CL*J1-0.5*J0
44      M=M+1
          M2=2*M
          AM=C(M)*P(M)*(Z2**M2)
          Y0=Y0-AM
          Y1=Y1+M*AM
          IF((CABS(AM).GT.1.0E-10).AND.(M.LT.34)) GO TO 44
      Y0=P2*Y0
      Y1=P2*Y1/Z2
      H0=J0-j*Y0
      H1=J1-j*Y1
      RETURN
  ELSE
C
C   Hankel' Asymptotic Formula (Abram. & Stegun p. 364)
C
      Z2=Z*Z
      Z3=Z*Z2
      Z4=Z*Z3
      P0=1.0-.0703125/Z2+.1121521/Z4
      Q0=-.125/Z+.0732422/Z3
      P1=1.0+.1171875/Z2-.1441956/Z4
      Q1=.375/Z-.10253906/Z3
      X0=(Z-.25*P1)
      X1=(Z-.75*P1)
      E0=CEXP(-j*X0)
      E1=CEXP(-j*X1)
      AM=CSQRT(P2/Z)

```

```

      H0=AM*(P0-J*Q0)*E0
      H1=AM*(P1-J*Q1)*E1
ENDIF
RETURN
END

```

```

C
C *****
C

```

```

C      SUBROUTINE FACTOR (A,P,N,NMX)
C      PERFORMING LU-DECOMPOSITION WITH PIVOTING ON THE A-MATRIX
C      WRITTEN BY M.A. MORGAN
C

```

```

      INTEGER I,J,JP1,K,P(NMX),PJ,PR,R,RM1,RP1
      REAL DMAX,ELMAG
      COMPLEX A(NMX,NMX),D(120)
      DO 60 R=1,N
10         DO 10 K=1,N
            D(K)=A(K,R)
            RM1=R-1
            IF(RM1.LT.1) GO TO 31
            DO 30 J=1,RM1
                PJ=P(J)
                A(J,R)=D(PJ)
                D(PJ)=D(J)
                JP1=J+1
                DO 20 I=JP1,N
20                 D(I)=D(I)-A(I,J)*A(J,R)
30                 CONTINUE
31                 CONTINUE
                DMAX=CABS(D(R))
                P(R)=R
                RP1=R+1
                IF(RP1.GT.N) GO TO 41
                DO 40 I=RP1,N
                    ELMAG=CABS(D(I))
                    IF(ELMAG.LT.DMAX) GO TO 40
                    DMAX=ELMAG
40                 P(R)=I
41                 CONTINUE
                    PR=P(R)
                    A(R,R)=D(PR)
                    D(PR)=D(R)
                    IF(RP1.GT.N) GO TO 51
                    DO 50 I=RP1,N
50                     A(I,R)=D(I)/A(R,R)
51                 CONTINUE
60                 CONTINUE
            RETURN
            END

```

```

C
C *****
C

```

```

C      SUBROUTINE SOLVE (A,B,P,N,NMX)
C      BACK SUBSTITUTION TO INVERT THE LINEAR SYSTEM
C      WRITTEN BY M.A. MORGAN
C
      COMPLEX A(NMX,NMX),B(NMX),Y(120),SUM
      INTEGER I,IP1,J,K,P(NMX),PP1
      DO 20 I=1,N

```

```

      PPI=P(I)
      Y(I)=B(PPI)
      B(PPI)=B(I)
      IP1=I+1
      IF(IP1.GT.N) GO TO 11
      DO 10 J=IP1,N
        B(J)=B(J)-A(J,I)*Y(I)
10    CONTINUE
11    CONTINUE
20    CONTINUE
      DO 40 K=1,N
        I=N-K+1
        SUM=(0.,0.)
        IP1=I+1
        IF(IP1.GT.N) GO TO 31
        DO 30 J=IP1,N
          SUM=SUM+A(I,J)*B(J)
30    CONTINUE
31    CONTINUE
      B(I)=(Y(I)-SUM)/A(I,I)
40    CONTINUE
      RETURN
      END

C
C *****
C
C      PROGRAM PLOT

C      Program to Plot a Solid Line Plot with Option to Overlay a
C      ++++ Line Plot for Comparison.  Uses PLOT2 Data File Format.
C
C      Original MS-FORTRAN Version of PLOT2 4/24/87 by M.A. Morgan.
C      Mods: 5/30/87 XMIN; 11/3/87 RM-FORTRAN 2nd Plot Option.
C
C      INPUT DATA FORMAT
C
C      Unit #3: Solid Line Plot
C
C      TITLE1- 64 Space Header
C      N      - # Data Points 15 (Integer*2)
C      XMIN   - Real Min X value  E12.3
C      XMAX   - Real Max X value  E12.3
C      F1(N)  - Input Data Array  E12.3
C
C      Unit #4: + Symbol Plot
C
C      TITLE2- 64 Space Header
C      N      - # Data Points 15 (Integer*2)
C      XMIN   - Real Min X value  E12.3
C      XMAX   - Real Max X value  E12.3
C      F2(N)  - Input Data Array  E12.3
C
C      CHARACTER*1 YN,YN1,DUM,YN2,SYMBOL
C      CHARACTER*4 LINE
C      CHARACTER*7 CROSS
C      CHARACTER*16 LTIT,CTIT
C      CHARACTER*32 SCALE
C      CHARACTER*64 TITLE,FNAME
C      REAL X(1025),F1(1025),F2(1025)
C      INTEGER*2 N,JROW,JCOL,ISYMBL,ITYPE
C      SCALE='is the Vertical Scale Multiplier'
C      LINE='--- '
C      CROSS=' +++ '

```

```

CALL QBEEP
WRITE(*,*) 'Press RET to Exit from Screen Plot'
WRITE(*,*) 'Printer Hardcopy ? (Y/N): '
READ(*,100) YN
WRITE(*,*) 'Enter Data File Name for ---- Plot: '
READ(*,100) FNAME
C Reading from Unit # 3
OPEN(3,FILE=FNAME)
READ(3,100) TITLE
READ(3,120) N
READ(3,130) XMIN
READ(3,130) XMAX
WRITE(*,*) '---- Plot TITLE, N, XMIN, XMAX: '
WRITE(*,*) TITLE
WRITE(*,*) N,XMIN,XMAX
WRITE(*,*) 'Enter ---- Plot Caption (16 char max): '
READ(*,100) LTIT
DX=(XMAX-XMIN)/(N-1.0)
FMIN=0.0
FMAX=0.0
DO 22 K=1,N
X(K)=XMIN+(K-1.0)*DX
READ(3,130) F1(K)
IF(F1(K).LT.FMIN) FMIN=F1(K)
IF(F1(K).GT.FMAX) FMAX=F1(K)
22 F2(K)=0.0
WRITE(*,*) 'Comparison Plot (++++) on Same Graph ??? (Y/N): '
READ(*,100) YN1
IF((YN1.EQ.'N').OR.(YN1.EQ.'n')) GO TO 11
WRITE(*,*) 'Enter Data File Name for ++++ Plot: '
READ(*,100) FNAME
C Reading from Unit # 4
OPEN(4,FILE=FNAME)
READ(4,100) TITLE
READ(4,120) N
READ(4,130) XMIN
READ(4,130) XMAX
WRITE(*,*) '++++ Plot TITLE, N, XMIN, XMAX:'
WRITE(*,*) TITLE
WRITE(*,*) N,XMIN,XMAX
WRITE(*,*) 'Enter ++++ Plot Caption (16 char max): '
READ(*,100) CTIT
DO 27 K=1,N
READ(4,130) F2(K)
IF(F2(K).LT.FMIN) FMIN=F2(K)
IF(F2(K).GT.FMAX) FMAX=F2(K)
27 CONTINUE
CLOSE (4)
11 CONTINUE
CALL QBEEP
WRITE(*,*) 'Enter TITLE for Plot (64 Char. Max):'
WRITE(*,*) ' '
READ (*,100) TITLE
CLOSE (3)
IF(FMIN.GT.0.0) FMIN=0.0
IF(FMAX.LT.0.0) FMAX=0.0
C Computing Sca' Factors for Vertical Axis
ABSMIN=ABS(FMIN)
ABSMAX=ABS(FMAX)
YMAX=AMAX1(ABSMIN,ABSMAX)
NSCL=INT(LOG10(YMAX))
IF (YMAX.LT.1.0) NSCL=NSCL-1
YSCL=10.**NSCL
FMIN=FMIN/YSCL

```

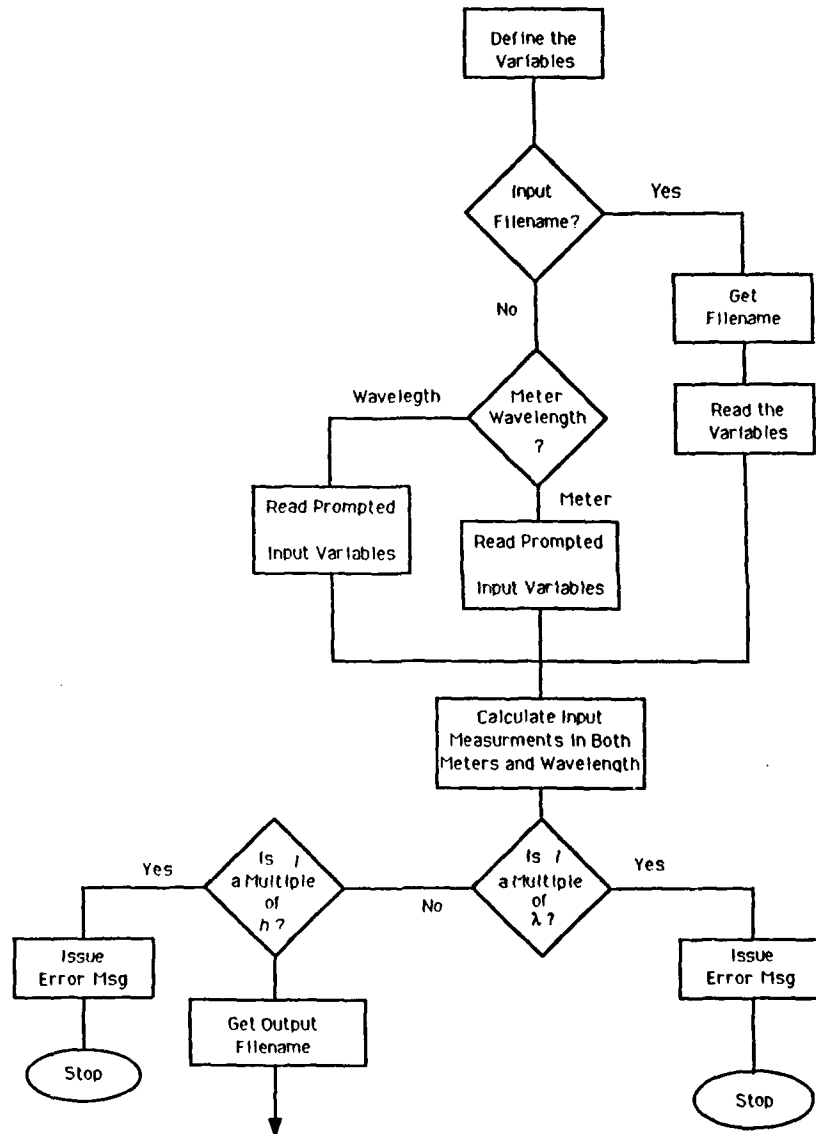
```

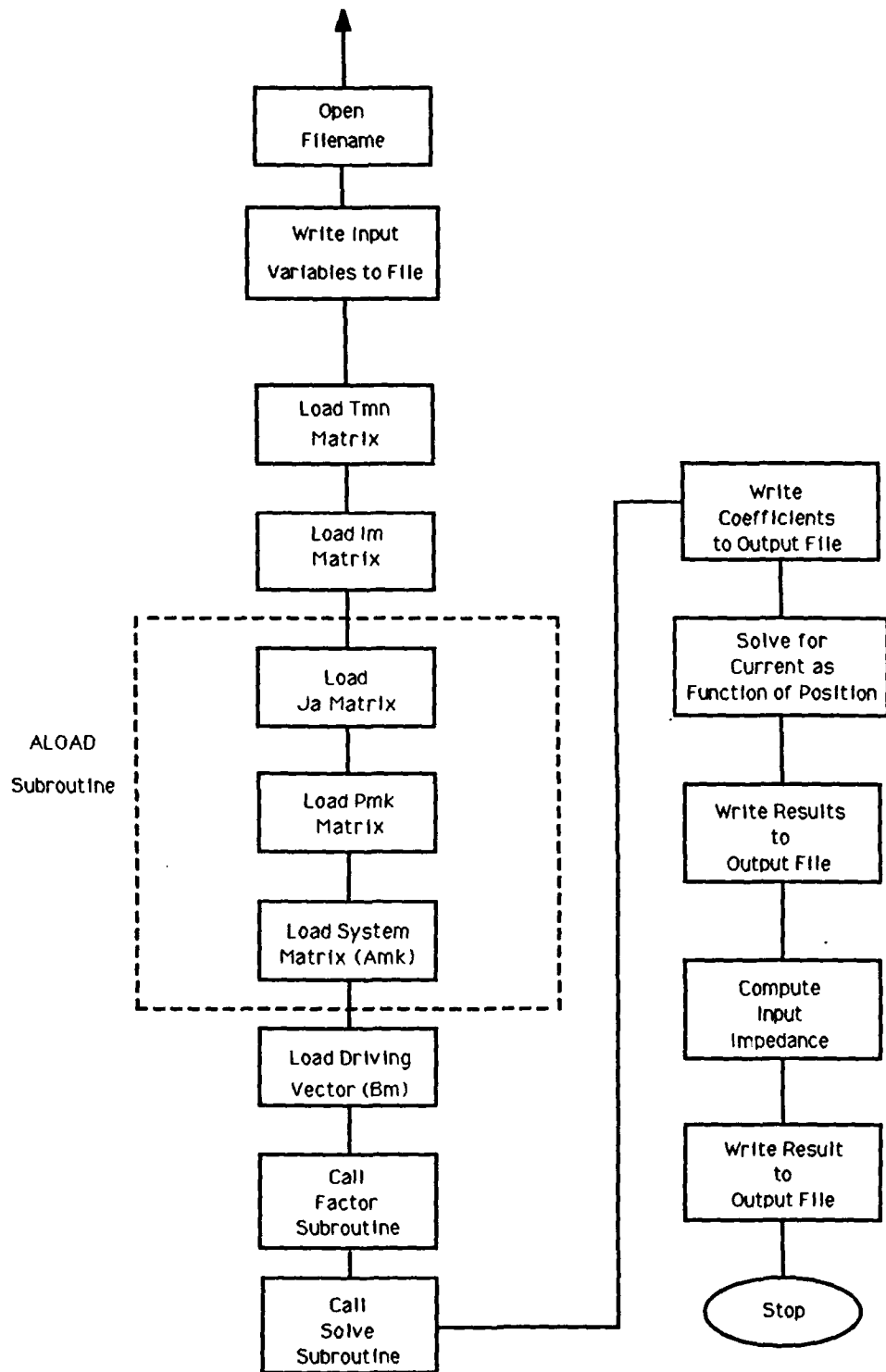
      FMAX=FMAX/YSCL
      ABSMIN=ABSMIN/YSCL
      ABSMAX=ABSMAX/YSCL
      DO 33 K=1,N
      F1(K)=F1(K)/YSCL
33    F2(K)=F2(K)/YSCL
      YMIN=0.0
      IF(FMIN.EQ.0.0) GO TO 37
35    YMIN=YMIN+1.0
      IF(ABSMIN.GT.YMIN) GO TO 35
      YMIN=YMIN*FMIN/ABSMIN
37    CONTINUE
      YMAX=0.0
      IF(FMAX.EQ.0.0) GO TO 41
39    YMAX=YMAX+1.0
      IF(ABSMAX.GT.YMAX) GO TO 39
      YMAX=YMAX*FMAX/ABSMAX
41    CONTINUE
C    Calling GRAFMATIC Routines and Plotting F1 Solid Line Graph
      ITYPE=1
      ISYMBL=-2
      CALL QSMODE(6)
      CALL QCMOV(0,21)
      WRITE(*,150) YSCL
      CALL QPTXT(32,SCALE,3,25,20)
      CALL QPLOT(100,530,12,147,XMIN,XMAX,YMIN,YMAX,0.,0.,0,1.,1.5)
      CALL QSETUP(0,3,ISYMBL,3)
      XMAJOR=XMAX/5.0
      CALL QXAXIS(XMIN,XMAX,XMAJOR,1,1,2)
      YMAJOR=1.0
      CALL QYAXIS(YMIN,YMAX,YMAJOR,1,1,2)
      CALL QPTXT(64,TITLE,3,14,24)
      CALL QPTXT(4,LINE,3,14,22)
      CALL QPTXT(16,LTIT,3,18,22)
      JROW=(ABS(YMIN)/(ABS(YMAX)+ABS(YMIN)))*135
      JCOL=70-430*XMIN/(XMAX-XMIN)
      CALL QGTXT(3,'0.0',3,JCOL,JROW,0)
      CALL QTABL(ITYPE,N,X,F1)
      IF((YN1.EQ.'N').OR.(YN1.EQ.'n')) GO TO 43
C    Plotting F2 Graph using + Symbol
      CALL QPTXT(7,CROSS,3,34,22)
      CALL QPTXT(16,CTIT,3,41,22)
      ISYMBL=43
      ITYPE=0
      CALL QSETUP(0,3,ISYMBL,3)
      CALL QTABL(ITYPE,N,X,F2)
43    CONTINUE
      READ(*,100) DUM
      IF((YN.EQ.'N').OR.(YN.EQ.'n')) GO TO 44
      CALL QPSCRN
44    CONTINUE
      CALL QSMODE(2)
      WRITE(*,*) 'End of PLOT Program'
100   FORMAT(A)
120   FORMAT(15)
130   FORMAT(E12.3)
150   FORMAT(13X,1PE11.3)
      STOP
      END

```

APPENDIX C

SOFTWARE FLOW CHART FOR MONO WITHOUT GAP FIELD EXPANSION





APPENDIX D

SOURCE CODE FOR MONO WITHOUT GAP FIELD EXPANSION

```

C      PROGRAM MONO
C      (Revision 8.1)
C
C      Mod of Mono 7.2, not using the expansion for the Gap Region
C      Computing Currents on a Monopole Between Parallel
C      Plates using Cylindrical Harmonic Expansions in 2 Regions.
C      Links with SUBS4.08J.      Created 05/88  LT. R.C. Hurley
C                                  Modified 10/88 M. A. Morgan
C
C      ----- Variables -----
C      FMHZ      = Frequency in MHz
C      h          = Monopole height in Meters
C      a          = Monopole radius in Meters
C      d          = Distance between lower ground plane and feed point
C                  in Meters
C      l          = Distance between ground planes in Meters
C      q          = height from top of monopole to upper ground plane
C                  in Meters
C      j          = Imaginary One
C      Pi         = Value of pi (3.1415927)
C      K0         =  $2\pi F/c$ 
C      where F = frequency of operation in Hz
C      c         = Speed of Light
C      K2         =  $K0^2$ 
C      N1,N2      = Number of Coefficients in each of the two regions
C      NBIG       = Size of the arrays used in FACTOR and SOLVE
C      Unit 0     = Standard Input Device
C      Unit 6     = Screen Output
C      Unit 7     = Main Output File to Disk (Name selected by User.)
C      ***** Variable Definitions *****
C
C      $Large:Amk
C      INTEGER k,m,mpn,n,N1,N2,Nbig,Nl,Nmax,Ns,NZ,P(61)
C      REAL a,ai,Am,An,c,C1,CM,CP,CR,d,di,DeltaZ,Denom,Dz,EzM,eps,FMHZ
C      REAL h,hi,I(0:60,1:3),K0,K2,l,li,Lambda,Pi,q,Rin,S
C      REAL T(0:60,0:60),w,Xin,y,yhat,Z,Zmin,Zmax
C      COMPLEX Amk(61,61),B(61),C1,C2,I2(61),j,J0,J1,Ja(0:60,1:4)
C      COMPLEX Pmk(0:60,0:60),Sum,Y0,Y1,Zin
C      CHARACTER*25 Fname
C      CHARACTER*1 Bell
C      CHARACTER*1 HOW
C      CHARACTER*1 INPUT
C      CHARACTER*1 Eok
C      CHARACTER*12 INname
C      COMMON/Blk1/I,j,N1,Pi,d,Nbig
C      COMMON/Blk2/K2,l,Nmax,N2,q,a,T
C
C      *****
C      *      Main Program Code      *
C      *****

```

C
C
C
C

* Input Section *

```

Bell=CHAR(7)
Nbig=61
c=3.0E+08
WRITE(6,*) 'Do you wish to use an input data file [Y/N]?'
READ(0,100) NOW
IF (NOW.EQ.'Y'.OR.NOW.EQ.'Y') THEN
    WRITE(6,*) 'Enter input data file name with extension : '
    READ(0,100) INname
    OPEN(Unit=4,File=INname)
    READ(4,100) INPUT
    IF ((INPUT.EQ.'M') .OR. (INPUT.EQ.'W') .OR. (INPUT.EQ.
+ 'm') .OR. (INPUT.EQ.'M')) THEN
        READ(4,*) FMHZ,hi,ai,di,li,N1,N2,N1
    ELSE
        WRITE(*,*) Bell
        WRITE(6,*) 'Error detected in first line of data file '
+ INname
        WRITE(6,*) 'First line must be either M or W for meter
+ values or wavelength values.'
        STOP
    ENDIF
ELSE
2   WRITE(6,*) 'Enter data in either [M]eters or [W]avelength [M
+ /W]?'
    READ(0,100) INPUT
    IF (INPUT.EQ.'M'.OR.INPUT.EQ.'M') THEN
        WRITE(6,*) 'Enter Frequency in MHz: '
        READ(0,*) FMHZ
        WRITE(6,*) 'Enter Monopole Height, h, in meters: '
        READ(0,*) hi
        WRITE(6,*) 'Enter Monopole Radius, in meters: '
        READ(0,*) ai
        WRITE(6,*) 'Enter Feed Gap, d, in meters: '
        READ(0,*) di
        WRITE(6,*) 'Enter Upper Plane Height, l (meters): '
        READ(0,*) li
    ELSEIF (INPUT.EQ.'W'.OR.INPUT.EQ.'W') THEN
        WRITE(6,*) 'Enter Frequency in MHz: '
        READ(0,*) FMHZ
        WRITE(6,*) 'Enter Monopole Height, h, as factor of wav
+ elength : '
        READ(0,*) hi
        WRITE(6,*) 'Enter Monopole Radius, as factor of wavele
+ ngth : '
        READ(0,*) ai
        WRITE(6,*) 'Enter Feed Gap, d, as factor of wavelength
+ : '
        READ(0,*) di
        WRITE(6,*) 'Enter Upper Plane Height, l, as factor of
+ wavelength : '
        READ(0,*) li
    ELSE
        WRITE(*,*) Bell
        WRITE(6,*) 'You must enter either an M or W.
+ Reenter.. '
        GOTO 2
    ENDIF
    WRITE(6,*) 'Enter # Region 1 Coeffs. (N1 .LE. 60): '
    READ(0,*) N1

```

```

WRITE(6,*) 'Enter # Region 2 Coeffs. (N2 .LE. 60): '
READ(0,*) N2
WRITE(6,*) 'Enter No. Points for I(z) including ends: '
READ(0,*) N1
ENDIF

C          *****
C          *
C          *          Calculate the Physical Parameters          *
C          *          in both Wavelength and Meters            *
C          *
C          *****

Lambda=c/(FMHZ*10**(6))
IF (INPUT.EQ.'W'.OR.INPUT.EQ.'W') THEN
    h=hi*Lambda
    a=ai*Lambda
    d=di*Lambda
    l=li*Lambda
ELSE
    h=hi
    hi=h/Lambda
    a=ai
    ai=a/Lambda
    d=di
    di=d/Lambda
    l=li
    li=l/Lambda
ENDIF

C          *****
C          *
C          *          Is Upper Plate Height an                  *
C          *          Even Multiple of Wavelength?              *
C          *
C          *****

IF (MOD((l*2),Lambda).LT. 1E-05) THEN
    WRITE(*,*) Bell
    WRITE(6,*) ' '
    WRITE(6,*) 'ERROR! Upper Plate Height is almost an even mul
+title of half the wavelength.'
    WRITE(6,*) 'Ensure l is NOT within 0.00001 of an integer mul
+title of half the wavelength.'
    STOP
ENDIF

C          *****
C          *
C          *          Is Upper Plate Height an                  *
C          *          Even Multiple of Antenna Height?          *
C          *
C          *****

IF ((MOD(l,h)).LT.1E-05) THEN
    WRITE(*,*) Bell
    WRITE(6,*) ' '
    WRITE(6,*) 'ERROR! Upper Plate Height is almost an even mul
+title of the antenna height.'
    WRITE(6,*) 'Ensure l is NOT within 0.00001 of an integer mul
+title of h (in wavelength).'
    STOP
ENDIF
WRITE(6,*) 'Enter output file name and extension: '

```

```

READ(0,100) Fname
OPEN (Unit=7,File=Fname)
WRITE(7,210) FMHZ
WRITE(7,220) h,hi
WRITE(7,230) a,ai
WRITE(7,240) d,di
WRITE(7,250) l,li
WRITE(7,*) 'Region I Coeffs. (N1): ',N1
WRITE(7,*) 'Region II Coeffs. (N2): ',N2
WRITE(7,*) 'No. Points for I(z): ',N1
j=(0.0,1.0)
Pi=3.1415927
K0=Pi*FMHZ/150.0
K2=K0*K0
eps=8.854E-12
w=2.0E6*Pi*FMHZ
yhat=w*eps
q=l-h
Nmax=MAX0(N1,N2)
WRITE(6,*) 'Loading the Moment Matrices ..... '
WRITE(6,*) ' '

C          *****
C          *
C          *      Evaluating Moment Integrations      *
C          *      Over Region h < z < l.              *
C          *
C          *****

T(0,0)=q
DO 11 k=1,N2
  T(0,k)=0.0
11 CONTINUE
DO 22 m=1,Nmax
  Am=m*Pi/l
  DO 22 n=0,N2
    An=n*Pi/q
    IF((ABS(Am-An)).GT.1.0E-3) THEN
      Denom=Am*Am-An*An
      S=SIN(Am*h)
      T(m,n)=-Am*S/Denom
    ELSE
      mpn=m+n
      T(m,n)=0.5*q*((-1)**mpn)
    ENDIF
  22 CONTINUE
  WRITE(6,*) '      Moment Matrix T Loaded.'
  WRITE(6,*) ' '

C          *****
C          *
C          *      Loading the Im Matrix for the
C          *      Largest Number of Coefficients
C          *
C          *****

DO 33 m=0,Nmax
  IF(m.EQ.0) Then
    I(m,1)=l
    I(m,2)=q
    I(m,3)=d
  ELSE
    I(m,1)=l/2.0
    I(m,2)=q/2.0
  33 CONTINUE

```

```

      Am=n*Pi/l
      I(m,3)=SIN(Am*d)/Am
    ENDIF
33  CONTINUE
    WRITE(6,*) '          Moment Matrix I Loaded.'
    WRITE(6,*) ' '
    WRITE(6,*) 'Loading System Matrix .....'
    CALL ALOAD(Ja,Pmk,Amk)
    WRITE(6,*) 'System Matrix Amk Loaded.'
    WRITE(6,*) ' '
    WRITE(6,*) 'Loading Driving Vector .....'
    DO 40 m=0,N1
      B(m+1)=j*yhat*I(m,3)/d
40  CONTINUE
    WRITE(6,*) 'Driving Vector B Loaded.'
    WRITE(6,*) ' '
    WRITE(6,*) 'Solving the Linear System .. Please Wait .... '
    Ns=N1+1
    CALL FACTOR(Amk,P,Ns,Nbig)
    CALL SOLVE(Amk,B,P,Ns,Nbig)
    WRITE(7,*) 'Listing the Expansion Coefficients'
    WRITE(6,*) '      Listing the Expansion Coefficients .....'
    WRITE(7,*) 'N and B(N): '
    DO 44 N=0,N1
      WRITE(7,*) N,B(N+1)
44  CONTINUE

C      *****
C      *
C      *      Computing Current from the      *
C      *      Expansion Coefficients          *
C      *
C      *****

    WRITE(6,*) ' '
    WRITE(6,*) 'Computing current on the monopole.....'
    WRITE(7,*) 'Listing the Current on the Monopole'
    DeltaZ=(h-d)/(N1-1)
    WRITE(7,*) 'Position      Distance      I(z) (A)'
    WRITE(7,*) ' Number      (Meters)      Mag      Phase'
    y=d
    k=1
55  Sum=(0.,0.)
    DO 66 n=0,N1
      Sum=Sum+(B(n+1)*Ja(n,3)*cos(n*Pi*y/l))
66  CONTINUE
    IZ(k)=2.0*Pi*a*Sum
    CM=CABS(IZ(k))
    CR=REAL(IZ(k))
    CI=AIMAG(IZ(k))
    CP=180.*ATAN2(CI,CR)/pi
    WRITE(7,200) k,y,CM,CP
    y=y+DeltaZ
    k=k+1
    IF(y.LE.(h+1.E-6)) GO TO 55
    WRITE(6,*) 'Complete.'

C      *****
C      *
C      *      Computing Input Impedance      *
C      *
C      *****

    Zin=(1.0,0.0)/IZ(1)

```


SUBROUTINE ALOAD(Ja,Pmk,Amk)
(Revision 8.1)

97


```

WRITE(6,100) Nmax
DO 11 n=0,Nmax
  R1=K2-((n*Pi/q)*(n*Pi/q))
  R2=K2-((n*Pi/l)*(n*Pi/l))
  un=CSR(R1)
  vn=CSR(R2)
  zu=un*a
  zv=vn*a
  Call BES1(zu,J0n,J1n)
  Call HAN1(zv,H0n,H1n)
  Ja(n,1) = Un*J0n
  Ja(n,2) = J1n
  Ja(n,3) = Vn*H1n
  Ja(n,4) = Vn*Vn*H0n
11 Continue
  WRITE(6,*) '      Completed.'
  WRITE(6,*) '      '
  WRITE(6,200) N1,Nmax
C
C Loading the Pmk Matrix (size N1 x Nmax)
C
  DO 22 m=0,N1
    WRITE(6,300) m,cr
    DO 22 k=0,Nmax
      Pmk(m,k)=(0.0,0.0)
      DO 33 n=0,N2
        S1=(Ja(n,1)*T(m,n)*T(k,n))/(l(n,2)*Ja(n,2))
        Pmk(m,k)=Pmk(m,k)+S1
      33 CONTINUE
    22 CONTINUE
  22 CONTINUE
  WRITE(6,*) '      Completed.'
  DO 44 m=0,N1
    DO 44 k=0,N1
      If(m.EQ.k) Then
        Amk(m+1,k+1)=Ja(k,3)*Pmk(m,m)-Ja(k,4)*I(m,1)
      ELSE
        Amk(m+1,k+1)=Ja(k,3)*Pmk(m,k)
      ENDIF
    44 CONTINUE
  100 FORMAT('      Loading Ja matrix of size',I3,' x 4.....')
  200 FORMAT('      Loading Pmk Matrix of size',I3,' x ',I3,'.....')
  300 FORMAT('      Calculating row',i3,a,\)
  RETURN
END

C
C *****
C

FUNCTION CSR(R)
REAL R
COMPLEX CSR
C Evaluating SQRT(R) with special consideration to neg. reals
IF(R.GE.0.0) THEN
  CSR=SQRT(R)
ELSE
  CSR=(0.,-1.)*SQRT(-R)
END IF
RETURN
END

```

```

C
C *****
C
      SUBROUTINE BES1(Z,J0,J1)
C
C      Computing Bessel Functions for n=0,1 with
C      Complex Argument, 2. Direct Power Series Method for
C      CABS(Z) .LE. 6 and Hankel's Asymptotic Formula for
C      CABS(Z) .GT. 6. Written 11/5/87 by M.A. Morgan
C
      INTEGER M,M2
      REAL C(34),DM,F(34),G0,P(34),PI,P2
      COMPLEX Z,Z2,Z3,Z4,J0,J1,AM,CL,P0,P1,Q0,Q1,C0,C1,S0,S1
      PI=3.1415927
      P2=2.0/PI
      IF(CABS(Z).LE.6.0) THEN
C
C      Utilizing the Direct Power Series Method
C
          G0= 1.781072
          Z2=0.5*Z
          CL=CLOG(G0*Z2)
C
C      Computing F(m) = m! and P(m) = 1 + 1/2 + 1/3 + ....+ 1/m
C
          F(1)=1.0
          P(1)=1.0
          DO 11 M=2,34
              F(M)=M*F(M-1)
              P(M)=P(M-1)+1.0/M
11          CONTINUE
C
C      Computing Power Series Coefficients
C
          DM=-1.0
          DO 22 M=1,34
              C(M)=DM/(F(M)*F(M))
              DM=-DM
22          CONTINUE
C
C      Computing J0 and J1
C
          J0=(1.,0.)
          J1=(0.,0.)
          M=0
33          M=M+1
          M2=2*M
          AM=C(M)*(Z2**M2)
          J0=J0+AM
          J1=J1-M*AM
          IF((CABS(AM).GT.1.0E-10).AND.(M.LT.34)) GO TO 33
          J1=J1/Z2
          return
      ELSE
C
C      Hankel' Asymptotic Formula (Abram. & Stegun p. 364)
C
          Z2=Z*Z
          Z3=Z*Z2
          Z4=Z*Z3
          P0=1.0-.0703125/Z2+.1121521/Z4
          Q0=-.125/Z+.0732422/Z3
      
```

```

P1=1.0+.1171875/Z2-.1441956/Z4
Q1=.375/Z-.10253906/Z3
C0=CCOS(Z-.25*P1)
S0=CSIN(Z-.25*P1)
C1=CCOS(Z-.75*P1)
S1=CSIN(Z-.75*P1)
AM=CSORT(P2/Z)
J0=AM*(P0*C0-Q0*S0)
J1=AM*(P1*C1-Q1*S1)
ENDIF
RETURN
END

C
C *****
C
SUBROUTINE MAN1(Z,H0,H1)
C
C   Computing Hankel Functions for n=0,1 with
C   Complex Argument, Z.   Direct Power Series Method for
C   CABS(Z) .LE. 5   and Hankel's Asymptotic Formula for
C   CABS(Z) .GT. 5.   Written 11/6/87 by M.A. Morgan
C
INTEGER M,M2
REAL C(34),DM,F(34),G0,P(34),Pi,P2
COMPLEX Z,Z2,Z3,Z4,J0,J1,Y0,Y1,AM,CL,P0,P1,Q0,Q1
COMPLEX E0,E1,X0,X1,H0,H1,j
P1=3.1415927
P2=2.0/PI
j=(0.,1.)
IF(CABS(Z).LE.5.0) THEN
C
C   Direct Power Series Method
C
G0= 1.78072
Z2=0.5*Z
CL=CLOG(G0*Z2)
C
C   Computing F(m) = m !   and P(m) = 1 + 1/2 + 1/3 + ..... + 1/m
C
F(1)=1.0
P(1)=1.0
DO 11 M=2,34
F(M)=M*F(M-1)
P(M)=P(M-1)+1.0/M
11 CONTINUE
C
C   Computing Power Series Coefficients
C
DM=-1.0
DO 22 M=1,34
C(M)=DM/(F(M)*F(M))
DM=-DM
22 CONTINUE
C
C   Computing J0 and J1
C
J0=(1.,0.)
J1=(0.,0.)
M=0
33 M=M+1
M2=2*M
AM=C(M)*(Z2**M2)

```

```

      J0=J0+AM
      J1=J1-M*AM
      IF((CABS(AM).GT.1.0E-10).AND.(M.LT.34)) GO TO 33
      J1=J1/Z2
C
C   Computing Y0 and Y1
C
      M=0
      Y0=CL*J0
      Y1=Z2*CL*J1-0.5*J0
44    M=M+1
      M2=2*M
      AM=C(M)*P(M)*(Z2**M2)
      Y0=Y0-AM
      Y1=Y1+M*AM
      IF((CABS(AM).GT.1.0E-10).AND.(M.LT.34)) GO TO 44
      Y0=P2*Y0
      Y1=P2*Y1/Z2
      H0=J0-j*Y0
      H1=J1-j*Y1
      RETURN
    ELSE
C
C   Hankel' Asymptotic Formula (Abram. & Stegun p. 364)
C
      Z2=Z*Z
      Z3=Z*Z2
      Z4=Z*Z3
      P0=1.0-.0703125/Z2+.1121521/Z4
      Q0=-.125/Z+.0732422/Z3
      P1=1.0+.1171875/Z2-.1441956/Z4
      Q1=.375/Z-.10253906/Z3
      X0=(Z-.25*P1)
      X1=(Z-.75*P1)
      E0=CEXP(-j*X0)
      E1=CEXP(-j*X1)
      AM=CSORT(P2/Z)
      H0=AM*(P0-j*Q0)*E0
      H1=AM*(P1-j*Q1)*E1
    ENDIF
    RETURN
  END

C
C *****
C
      SUBROUTINE FACTOR (A,P,N,NMX)
      PERFORMING LU-DECOMPOSITION WITH PIVOTING ON THE A-MATRIX
C
      INTEGER I,J,JP1,K,P(NMX),PJ,PR,R,RM1,RP1
      REAL DMAX,ELMAG
      COMPLEX A(NMX,NMX),D(120)
      DO 60 R=1,N
        DO 10 K=1,N
          D(K)=A(K,R)
10       RM1=R-1
          IF(RM1.LT.1) GO TO 31
          DO 30 J=1,RM1
            PJ=P(J)
            A(J,R)=D(PJ)
            D(PJ)=D(J)
            JP1=J+1
            DO 20 I=JP1,N

```

```

20          D(I)=D(I)-A(I,J)*A(J,R)
30      CONTINUE
31      CONTINUE
          DMAX=CABS(D(R))
          P(R)=R
          RP1=R+1
          IF(RP1.GT.N) GO TO 41
          DO 40 I=RP1,N
              ELMAG=CABS(D(I))
              IF(ELMAG.LT.DMAX) GO TO 40
              DMAX=ELMAG
          P(R)=I
40      CONTINUE
41      PR=P(R)
          A(R,R)=D(PR)
          D(PR)=D(R)
          IF(RP1.GT.N) GO TO 51
          DO 50 I=RP1,N
              A(I,R)=D(I)/A(R,R)
50      CONTINUE
51      CONTINUE
60      RETURN
      END

C *****
C
      SUBROUTINE SOLVE (A,B,P,N,NMX)
C      BACK SUBSTITUTION TO INVERT THE LINEAR SYSTEM
      COMPLEX A(NMX,NMX),B(NMX),Y(120),SUM
      INTEGER I,IP1,J,K,P(NMX),PPI
      DO 20 I=1,N
          PPI=P(I)
          Y(I)=B(PPI)
          B(PPI)=B(I)
          IP1=I+1
          IF(IP1.GT.N) GO TO 11
          DO 10 J=IP1,N
              B(J)=B(J)-A(J,I)*Y(I)
10      CONTINUE
11      CONTINUE
20      CONTINUE
          DO 40 K=1,N
              I=N-K+1
              SUM=(0.,0.)
              IP1=I+1
              IF(IP1.GT.N) GO TO 31
              DO 30 J=IP1,N
                  SUM=SUM+A(I,J)*B(J)
30      CONTINUE
31      CONTINUE
          B(I)=(Y(I)-SUM)/A(I,I)
40      CONTINUE
      RETURN
      END

```

APPENDIX E

SAMPLE INPUT/OUTPUT DATA FILES USED WITH MONO

This Appendix lists the input and output data file structures used within MONO. There are two different types of input data files, one that is entered at the keyboard at run time and one which allows unattended processing of a number of runs without user intervention. In each case, the data fields may be either arranged in column format with one entry per line, or all on one line separated by commas. Additionally, a variable type is set by the program which allows a real variable to read both an input of "1" or "1." as the same.

A. INPUT DATA FILE STRUCTURE

This data file may be adjusted to allow the user the option of selecting either the output file name or, for the case of MONO8, the calculation of the electric field along the antenna at run time. Below is a commented data set that could be used. Note the comments are NOT to be entered in the data set as errors would occur.

Data File Entry	Comment
w	This identifies the basis for all physical measurements of the antenna. Using a "w" or "W" signifies all measurements are in terms of wavelength, while a "m" or "M" indicates measurements are in terms of meters.
299.8	Driving source frequency in MHz
.24	Antenna height, h . Can be entered as "0.24".
.01	Antenna radius, a .
.02	Gap distance, q .
2.17	Ground plate spacing, l .
30	Number of modes for Region I, N_1 .
30	Number of modes for Region II, N_2 .
60	Number of modes for Gap expansion, M_1 . Not used for MON08.
30	Number of points to calculate the current along the antenna.
d:\file.out	DOS path and name to assign to output file. Maximum length is 25 characters. This entry may also be entered at the keyboard at run time.
"y" or "n"	Indicates whether to calculate the electric field along the antenna. Test is NOT case sensitive. If yes, data is stored as 'EZ.DAT' in the current directory in format for PLOT.FOR found in Appendix B. This may be entered via the keyboard at run time.

The same data file can be arranged as follows:

w,299.8,.24,.01.02,2.17,30,30,60,30,d:\file.out,n

The data file is easily modified to allow the user to group a series of runs together to be batch processed later using the standard DOS redirection command. For example, to use input data file named 'RUN1' and to have the normal screen output redirected to a running log file named 'OUTPUT.LOG', the correct syntax would be:

```
MONO <[path]RUN1 >>[path]OUTPUT.LOG
```

where *path* is the DOS path where the individual files are stored. This parameter is optional and defaults to the current directory. A number of runs could then be completed without user input by combining a series of these commands in one batch file. The file structure is the same as that listed above except that an 'n' is inserted at the beginning of the file to indicate that a separate input file is not to be used. Therefore, the same data file used above would be modified as seen below:

```
n,w,299.8,.24,.01.02,2.17,30,30,60,30,d:\file.out,n
```

B. SAMPLE OUTPUT FILE

The output file generated by MONO7 for the inputs used above is listed below: (* indicates not included in output from MONO8)

Driving Frequency, 299.800 MHz
 Monopole Height, .240 meters (.240 Lambda)
 Monopole Radius, .010 meters (.010 Lambda)
 Feed Gap Distance, .010 meters (.010 Lambda)
 Upper Plane Height, 2.171 meters (2.170 Lambda)
 Region I Coeffs. (N1): 30
 Region II Coeffs. (N2): 30
 * No. Gap Coeffs. (M1): 60
 No. Points for I(z): 30

Listing the Expansion Coefficients
N and B(N):

0	(-9.259474E-05,-3.712934E-04)
1	(-1.716743E-04,-7.285348E-04)
2	(-1.250944E-04,-6.843712E-04)
3	(-8.932992E-06,-5.970440E-04)
4	(6.372479E-04,-3.034107E-04)
5	(-7.747178E-04,-5.976821E-04)
6	(-4.176759E-04,-5.106181E-04)
7	(-2.877242E-04,-4.189367E-04)
8	(-2.029108E-04,-3.268855E-04)
9	(-1.371401E-04,-2.384746E-04)
10	(-8.359972E-05,-1.573042E-04)
11	(-4.017067E-05,-8.621241E-05)
12	(-6.131331E-06,-2.729695E-05)
13	(1.893293E-05,1.824955E-05)
14	(3.552895E-05,5.013411E-05)
15	(4.440288E-05,6.891159E-05)
16	(4.656793E-05,7.587663E-05)
17	(4.326494E-05,7.290936E-05)
18	(3.588156E-05,6.228465E-05)
19	(2.588031E-05,4.649168E-05)
20	(1.465865E-05,2.799412E-05)
21	(3.497886E-06,9.087322E-06)
22	(-6.533222E-06,-8.273393E-06)
23	(-1.463069E-05,-2.258123E-05)
24	(-2.028524E-05,-3.284282E-05)
25	(-2.328759E-05,-3.859688E-05)
26	(-2.370753E-05,-3.988246E-05)
27	(-2.185403E-05,-3.717663E-05)
28	(-1.821469E-05,-3.127903E-05)
29	(-1.339421E-05,-2.322528E-05)
30	(-8.037723E-06,-1.412969E-05)

Listing the Current on the Monopole

Position Number	Distance (Meters)	I(z) (A)	
		Mag	Phase
1	.010	2.316E-02	-15.04
2	.018	2.309E-02	-15.98
3	.026	2.299E-02	-17.24
4	.034	2.284E-02	-18.58
5	.042	2.262E-02	-19.80
6	.050	2.234E-02	-20.78

7	.058	2.200E-02	-21.49
8	.066	2.161E-02	-21.97
9	.073	2.121E-02	-22.34
10	.081	2.082E-02	-22.72
11	.089	2.044E-02	-23.19
12	.097	2.007E-02	-23.78
13	.105	1.970E-02	-24.44
14	.113	1.929E-02	-25.11
15	.121	1.881E-02	-25.70
16	.129	1.822E-02	-26.16
17	.137	1.752E-02	-26.50
18	.145	1.669E-02	-26.74
19	.153	1.574E-02	-26.95
20	.161	1.467E-02	-27.19
21	.169	1.349E-02	-27.49
22	.177	1.222E-02	-27.86
23	.185	1.088E-02	-28.27
24	.193	9.485E-03	-28.64
25	.200	8.069E-03	-28.91
26	.208	6.671E-03	-29.03
27	.216	5.331E-03	-28.99
28	.224	4.091E-03	-28.84
29	.232	2.987E-03	-28.72
30	.240	2.042E-03	-28.84
Input Resistance =		41.703650	
Input Reactance =		11.206850	

APPENDIX F

SAMPLE INPUT/OUTPUT DATA FILES USED WITH NEC

This Appendix lists an input data file used NEC and the corresponding output file. The run selected was for an antenna with the following physical characteristics using one reflection:

Driving Frequency	299.8 MHz
Antenna Height	0.48 wavelengths
Antenna Radius	0.01 wavelengths
Gap Distance	0.02 wavelengths
Ground Plate Spacing	1.4 wavelengths

```
CE      Run 11: Monopole Antenna of Height .48,Radius .01,.02,1.40
GW 1, 24, 0, 0, 0, 0, 0, .48, .01
GW 2, 48, 0, 0, 2.32, 0, 0, 3.28, .01
GE 1
GN 1
EK
EX 0   1   1   0   1.0
EX 0   2  24   0  -1.0
EX 0   2  25   0  -1.0
XQ
EN
```

Sample output file from the above data is shown below:

NUMERICAL ELECTROMAGNETICS CODE

- - - - COMMENTS - - - -

Run 11: Monopole Antenna of Height .48,Radius .01,.02,1.40

- - - STRUCTURE SPECIFICATION - - -

COORDINATES MUST BE INPUT IN
METERS OR BE SCALED TO METERS
BEFORE STRUCTURE INPUT IS ENDED

WIRE LAST NO. SEG.	TAG X1 Y1 Z1 X2 Y2 Z2 RADIUS	NO. OF SEG.	FIRST SEG.
1	.00000 .00000 .00000 .00000 .00000 .48000 .01000	24	1
24	1		
2	.00000 .00000 2.32000 .00000 .00000 3.28000 .01000	48	25
72	2		

GROUND PLANE SPECIFIED.

WHERE WIRE ENDS TOUCH GROUND, CURRENT WILL BE INTERPOLATED TO IMAGE IN GROUND PLANE.

TOTAL SEGMENTS USED= 72 NO. SEG. IN A SYMMETRIC CELL= 72 SYMMETRY FLAG= 0

- MULTIPLE WIRE JUNCTIONS -
JUNCTION SEGMENTS (- FOR END 1, + FOR END 2)
NONE

- - - - SEGMENTATION DATA - - - -

COORDINATES IN METERS

I+ AND I- INDICATE THE SEGMENTS BEFORE AND AFTER I

SEG. NO.	COORDINATES OF SEG. CENTER X Y Z	SEG. LENGTH	ORIENTATION ALPHA	ANGLES BETA	WIRE RADIUS	CONNECTION DATA I- I I+	TAG NO.
1	.00000 .00000 .01000	.02000	90.00000	.00000	.01000	1 1 2	1
2	.00000 .00000 .03000	.02000	90.00000	.00000	.01000	1 2 3	1
3	.00000 .00000 .05000	.02000	90.00000	.00000	.01000	2 3 4	1
4	.00000 .00000 .07000	.02000	90.00000	.00000	.01000	3 4 5	1
5	.00000 .00000 .09000	.02000	90.00000	.00000	.01000	4 5 6	1
6	.00000 .00000 .11000	.02000	90.00000	.00000	.01000	5 6 7	1
7	.00000 .00000 .13000	.02000	90.00000	.00000	.01000	6 7 8	1
8	.00000 .00000 .15000	.02000	90.00000	.00000	.01000	7 8 9	1
9	.00000 .00000 .17000	.02000	90.00000	.00000	.01000	8 9 10	1
10	.00000 .00000 .19000	.02000	90.00000	.00000	.01000	9 10 11	1
11	.00000 .00000 .21000	.02000	90.00000	.00000	.01000	10 11 12	1
12	.00000 .00000 .23000	.02000	90.00000	.00000	.01000	11 12 13	1
13	.00000 .00000 .25000	.02000	90.00000	.00000	.01000	12 13 14	1

14	.00000	.00000	.27000	.02000	90.00000	.00000	.01000	13	14	15	1
15	.00000	.00000	.29000	.02000	90.00000	.00000	.01000	14	15	16	1
16	.00000	.00000	.31000	.02000	90.00000	.00000	.01000	15	16	17	1
17	.00000	.00000	.33000	.02000	90.00000	.00000	.01000	16	17	18	1
18	.00000	.00000	.35000	.02000	90.00000	.00000	.01000	17	18	19	1
19	.00000	.00000	.37000	.02000	90.00000	.00000	.01000	18	19	20	1
20	.00000	.00000	.39000	.02000	90.00000	.00000	.01000	19	20	21	1
21	.00000	.00000	.41000	.02000	90.00000	.00000	.01000	20	21	22	1
22	.00000	.00000	.43000	.02000	90.00000	.00000	.01000	21	22	23	1
23	.00000	.00000	.45000	.02000	90.00000	.00000	.01000	22	23	24	1
24	.00000	.00000	.47000	.02000	90.00000	.00000	.01000	23	24	0	1
25	.00000	.00000	2.33000	.02000	90.00000	.00000	.01000	0	25	26	2
26	.00000	.00000	2.35000	.02000	90.00000	.00000	.01000	25	26	27	2
27	.00000	.00000	2.37000	.02000	90.00000	.00000	.01000	26	27	28	2
28	.00000	.00000	2.39000	.02000	90.00000	.00000	.01000	27	28	29	2
29	.00000	.00000	2.41000	.02000	90.00000	.00000	.01000	28	29	30	2
30	.00000	.00000	2.43000	.02000	90.00000	.00000	.01000	29	30	31	2
31	.00000	.00000	2.45000	.02000	90.00000	.00000	.01000	30	31	32	2
32	.00000	.00000	2.47000	.02000	90.00000	.00000	.01000	31	32	33	2
33	.00000	.00000	2.49000	.02000	90.00000	.00000	.01000	32	33	34	2
34	.00000	.00000	2.51000	.02000	90.00000	.00000	.01000	33	34	35	2
35	.00000	.00000	2.53000	.02000	90.00000	.00000	.01000	34	35	36	2
36	.00000	.00000	2.55000	.02000	90.00000	.00000	.01000	35	36	37	2
37	.00000	.00000	2.57000	.02000	90.00000	.00000	.01000	36	37	38	2
38	.00000	.00000	2.59000	.02000	90.00000	.00000	.01000	37	38	39	2
39	.00000	.00000	2.61000	.02000	90.00000	.00000	.01000	38	39	40	2
40	.00000	.00000	2.63000	.02000	90.00000	.00000	.01000	39	40	41	2
41	.00000	.00000	2.65000	.02000	90.00000	.00000	.01000	40	41	42	2
42	.00000	.00000	2.67000	.02000	90.00000	.00000	.01000	41	42	43	2
43	.00000	.00000	2.69000	.02000	90.00000	.00000	.01000	42	43	44	2
44	.00000	.00000	2.71000	.02000	90.00000	.00000	.01000	43	44	45	2
45	.00000	.00000	2.73000	.02000	90.00000	.00000	.01000	44	45	46	2
46	.00000	.00000	2.75000	.02000	90.00000	.00000	.01000	45	46	47	2
47	.00000	.00000	2.77000	.02000	90.00000	.00000	.01000	46	47	48	2
48	.00000	.00000	2.79000	.02000	90.00000	.00000	.01000	47	48	49	2
49	.00000	.00000	2.81000	.02000	90.00000	.00000	.01000	48	49	50	2
50	.00000	.00000	2.83000	.02000	90.00000	.00000	.01000	49	50	51	2
51	.00000	.00000	2.85000	.02000	90.00000	.00000	.01000	50	51	52	2
52	.00000	.00000	2.87000	.02000	90.00000	.00000	.01000	51	52	53	2
53	.00000	.00000	2.89000	.02000	90.00000	.00000	.01000	52	53	54	2
54	.00000	.00000	2.91000	.02000	90.00000	.00000	.01000	53	54	55	2
55	.00000	.00000	2.93000	.02000	90.00000	.00000	.01000	54	55	56	2
56	.00000	.00000	2.95000	.02000	90.00000	.00000	.01000	55	56	57	2
57	.00000	.00000	2.97000	.02000	90.00000	.00000	.01000	56	57	58	2
58	.00000	.00000	2.99000	.02000	90.00000	.00000	.01000	57	58	59	2
59	.00000	.00000	3.01000	.02000	90.00000	.00000	.01000	58	59	60	2
60	.00000	.00000	3.03000	.02000	90.00000	.00000	.01000	59	60	61	2
61	.00000	.00000	3.05000	.02000	90.00000	.00000	.01000	60	61	62	2
62	.00000	.00000	3.07000	.02000	90.00000	.00000	.01000	61	62	63	2
63	.00000	.00000	3.09000	.02000	90.00000	.00000	.01000	62	63	64	2
64	.00000	.00000	3.11000	.02000	90.00000	.00000	.01000	63	64	65	2
65	.00000	.00000	3.13000	.02000	90.00000	.00000	.01000	64	65	66	2
66	.00000	.00000	3.15000	.02000	90.00000	.00000	.01000	65	66	67	2
67	.00000	.00000	3.17000	.02000	90.00000	.00000	.01000	66	67	68	2
68	.00000	.00000	3.19000	.02000	90.00000	.00000	.01000	67	68	69	2
69	.00000	.00000	3.21000	.02000	90.00000	.00000	.01000	68	69	70	2
70	.00000	.00000	3.23000	.02000	90.00000	.00000	.01000	69	70	71	2
71	.00000	.00000	3.25000	.02000	90.00000	.00000	.01000	70	71	72	2
72	.00000	.00000	3.27000	.02000	90.00000	.00000	.01000	71	72	0	2

```

***** DATA CARD NO. 1  GN 1 0 0 0 0.00000E+00 0.00000E+00 0.00000E+00 0.00000E+00
0.00000E+00 0.00000E+00
***** DATA CARD NO. 2  EK 0 0 0 0 0.00000E+00 0.00000E+00 0.00000E+00 0.00000E+00
0.00000E+00 0.00000E+00
***** DATA CARD NO. 3  EX 0 1 1 0 1.00000E+00 0.00000E+00 0.00000E+00 0.00000E+00
0.00000E+00 0.00000E+00
***** DATA CARD NO. 4  EX 0 2 24 0 -1.00000E+00 0.00000E+00 0.00000E+00 0.00000E+00
0.00000E+00 0.00000E+00
***** DATA CARD NO. 5  EX 0 2 25 0 -1.00000E+00 0.00000E+00 0.00000E+00 0.00000E+00
0.00000E+00 0.00000E+00

```

***** DATA CARD NO. 6 XQ 0 0 0 0 0.00000E+00 0.00000E+00 0.00000E+00 0.00000E+00
0.00000E+00 0.00000E+00

- - - - - FREQUENCY - - - - -

FREQUENCY= 2.9980E+02 MHZ
WAVELENGTH= 1.0000E+00 METERS

APPROXIMATE INTEGRATION EMPLOYED FOR SEGMENTS MORE THAN 1.000 WAVELENGTHS APART
THE EXTENDED THIN WIRE KERNEL WILL BE USED

- - - STRUCTURE IMPEDANCE LOADING - - -

THIS STRUCTURE IS NOT LOADED

- - - ANTENNA ENVIRONMENT - - -

PERFECT GROUND

- - - MATRIX TIMING - - -

FILL= 1.500 MIN., FACTOR= .364 MIN.

- - - ANTENNA INPUT PARAMETERS - - -

TAG NO.	SEG. NO.	VOLTAGE (VOLTS)		CURRENT (AMPS)		IMPEDANCE (OHMS)		ADMITTANCE
		REAL	IMAG.	REAL	IMAG.	REAL	IMAG.	REAL
1	1	1.00000E+00	0.00000E+00	2.43054E-03	2.78753E-03	1.77698E+02	-2.03799E+02	2.43054E-03
2.78753E-03	1.21527E-03							
2	48	1.00000E+00	0.00000E+00	-2.42866E-03	-2.79143E-03	1.77398E+02	-2.03896E+02	2.42866E-03
2.79143E-03	1.21433E-03							
2	49	1.00000E+00	0.00000E+00	-2.42265E-03	-2.79230E-03	1.77274E+02	-2.04322E+02	2.42265E-03
2.79230E-03	1.21132E-03							

- - - CURRENTS AND LOCATION - - -

DISTANCES IN WAVELENGTHS

SEG. NO.	TAG NO.	COORD. OF SEG. CENTER			SEG. LENGTH	CURRENT (AMPS)			PHASE
		X	Y	Z		REAL	IMAG.	MAG.	
1	1	.0000	.0000	.0100	.02000	2.4305E-03	2.7875E-03	3.6984E-03	48.914
2	1	.0000	.0000	.0300	.02000	2.4147E-03	1.0516E-03	2.6338E-03	23.534
3	1	.0000	.0000	.0500	.02000	2.3833E-03	-8.5797E-05	2.3848E-03	-2.062
4	1	.0000	.0000	.0700	.02000	2.3366E-03	-9.8162E-04	2.5344E-03	-22.787
5	1	.0000	.0000	.0900	.02000	2.2754E-03	-1.7685E-03	2.8819E-03	-37.856
6	1	.0000	.0000	.1100	.02000	2.2004E-03	-2.4668E-03	3.3055E-03	-48.267
7	1	.0000	.0000	.1300	.02000	2.1125E-03	-3.0847E-03	3.7387E-03	-55.585
8	1	.0000	.0000	.1500	.02000	2.0130E-03	-3.6240E-03	4.1456E-03	-60.950
9	1	.0000	.0000	.1700	.02000	1.9031E-03	-4.0841E-03	4.5058E-03	-65.016
10	1	.0000	.0000	.1900	.02000	1.7842E-03	-4.4630E-03	4.8065E-03	-68.209
11	1	.0000	.0000	.2100	.02000	1.6579E-03	-4.7588E-03	5.0394E-03	-70.792
12	1	.0000	.0000	.2300	.02000	1.5258E-03	-4.9697E-03	5.1987E-03	-72.932
13	1	.0000	.0000	.2500	.02000	1.3895E-03	-5.0945E-03	5.2806E-03	-74.744
14	1	.0000	.0000	.2700	.02000	1.2508E-03	-5.1325E-03	5.2827E-03	-76.304
15	1	.0000	.0000	.2900	.02000	1.1113E-03	-5.0841E-03	5.2041E-03	-77.670
16	1	.0000	.0000	.3100	.02000	9.7278E-04	-4.9502E-03	5.0449E-03	-78.882

17	1	.0000	.0000	.3300	.02000	8.3692E-04	-4.7327E-03	4.8061E-03	-79.972
18	1	.0000	.0000	.3500	.02000	7.0529E-04	-4.4340E-03	4.4897E-03	-80.982
19	1	.0000	.0000	.3700	.02000	5.7941E-04	-4.0569E-03	4.0981E-03	-81.872
20	1	.0000	.0000	.3900	.02000	4.6064E-04	-3.6044E-03	3.6337E-03	-82.717
21	1	.0000	.0000	.4100	.02000	3.5018E-04	-3.0785E-03	3.0983E-03	-83.510
22	1	.0000	.0000	.4300	.02000	2.4894E-04	-2.4785E-03	2.4909E-03	-84.264
23	1	.0000	.0000	.4500	.02000	1.5733E-04	-1.7963E-03	1.8032E-03	-84.995
24	1	.0000	.0000	.4700	.02000	7.2003E-05	-9.5821E-04	9.6081E-04	-85.703
25	2	.0000	.0000	2.3300	.02000	-8.2718E-05	9.5969E-04	9.6325E-04	94.926
26	2	.0000	.0000	2.3500	.02000	-1.7730E-04	1.7990E-03	1.8077E-03	95.629
27	2	.0000	.0000	2.3700	.02000	-2.7635E-04	2.4819E-03	2.4972E-03	96.353
28	2	.0000	.0000	2.3900	.02000	-3.8402E-04	3.0826E-03	3.1064E-03	97.101
29	2	.0000	.0000	2.4100	.02000	-5.0002E-04	3.6090E-03	3.6434E-03	97.888
30	2	.0000	.0000	2.4300	.02000	-6.2347E-04	4.0618E-03	4.1094E-03	98.727
31	2	.0000	.0000	2.4500	.02000	-7.5316E-04	4.4391E-03	4.5025E-03	99.629
32	2	.0000	.0000	2.4700	.02000	-8.8769E-04	4.7379E-03	4.8203E-03	100.612
33	2	.0000	.0000	2.4900	.02000	-1.0256E-03	4.9554E-03	5.0604E-03	101.693
34	2	.0000	.0000	2.5100	.02000	-1.1652E-03	5.0891E-03	5.2208E-03	102.896
35	2	.0000	.0000	2.5300	.02000	-1.3049E-03	5.1373E-03	5.3004E-03	104.252
36	2	.0000	.0000	2.5500	.02000	-1.4430E-03	5.0989E-03	5.2992E-03	105.801
37	2	.0000	.0000	2.5700	.02000	-1.5778E-03	4.9737E-03	5.2180E-03	107.600
38	2	.0000	.0000	2.5900	.02000	-1.7076E-03	4.7623E-03	5.0582E-03	109.726
39	2	.0000	.0000	2.6100	.02000	-1.8308E-03	4.4659E-03	4.8266E-03	112.292
40	2	.0000	.0000	2.6300	.02000	-1.9460E-03	4.0864E-03	4.5261E-03	115.464
41	2	.0000	.0000	2.6500	.02000	-2.0515E-03	3.6256E-03	4.1658E-03	119.502
42	2	.0000	.0000	2.6700	.02000	-2.1461E-03	3.0856E-03	3.7585E-03	124.820
43	2	.0000	.0000	2.6900	.02000	-2.2286E-03	2.4669E-03	3.3245E-03	132.094
44	2	.0000	.0000	2.7100	.02000	-2.2979E-03	1.7679E-03	2.8993E-03	142.427
45	2	.0000	.0000	2.7300	.02000	-2.3532E-03	9.8018E-04	2.5492E-03	157.387
46	2	.0000	.0000	2.7500	.02000	-2.3937E-03	8.3523E-05	2.3952E-03	178.002
47	2	.0000	.0000	2.7700	.02000	-2.4190E-03	-1.0547E-03	2.6369E-03	-156.441
48	2	.0000	.0000	2.7900	.02000	-2.4287E-03	-2.7914E-03	3.7001E-03	-131.025
49	2	.0000	.0000	2.8100	.02000	-2.4226E-03	-2.7923E-03	3.6968E-03	-130.945
50	2	.0000	.0000	2.8300	.02000	-2.4010E-03	-1.0573E-03	2.6235E-03	-156.235
51	2	.0000	.0000	2.8500	.02000	-2.3641E-03	7.9330E-05	2.3655E-03	178.078
52	2	.0000	.0000	2.8700	.02000	-2.3124E-03	9.7436E-04	2.5083E-03	157.151
53	2	.0000	.0000	2.8900	.02000	-2.2466E-03	1.7605E-03	2.8542E-03	141.917
54	2	.0000	.0000	2.9100	.02000	-2.1675E-03	2.4580E-03	3.2772E-03	131.406
55	2	.0000	.0000	2.9300	.02000	-2.0762E-03	3.0752E-03	3.7104E-03	124.025
56	2	.0000	.0000	2.9500	.02000	-1.9738E-03	3.6139E-03	4.1178E-03	118.642
57	2	.0000	.0000	2.9700	.02000	-1.8617E-03	4.0734E-03	4.4786E-03	114.562
58	2	.0000	.0000	2.9900	.02000	-1.7413E-03	4.4518E-03	4.7803E-03	111.362
59	2	.0000	.0000	3.0100	.02000	-1.6141E-03	4.7472E-03	5.0141E-03	108.779
60	2	.0000	.0000	3.0300	.02000	-1.4819E-03	4.9578E-03	5.1745E-03	106.641
61	2	.0000	.0000	3.0500	.02000	-1.3461E-03	5.0823E-03	5.2575E-03	104.834
62	2	.0000	.0000	3.0700	.02000	-1.2084E-03	5.1202E-03	5.2609E-03	103.280
63	2	.0000	.0000	3.0900	.02000	-1.0707E-03	5.0718E-03	5.1836E-03	101.921
64	2	.0000	.0000	3.1100	.02000	-9.3452E-04	4.9381E-03	5.0257E-03	100.716
65	2	.0000	.0000	3.1300	.02000	-8.0147E-04	4.7209E-03	4.7884E-03	99.635
66	2	.0000	.0000	3.1500	.02000	-6.7310E-04	4.4227E-03	4.4736E-03	98.654
67	2	.0000	.0000	3.1700	.02000	-5.5087E-04	4.0463E-03	4.0836E-03	97.753
68	2	.0000	.0000	3.1900	.02000	-4.3609E-04	3.5946E-03	3.6210E-03	96.917
69	2	.0000	.0000	3.2100	.02000	-3.2990E-04	3.0698E-03	3.0875E-03	96.134
70	2	.0000	.0000	3.2300	.02000	-2.3317E-04	2.4712E-03	2.4822E-03	95.390
71	2	.0000	.0000	3.2500	.02000	-1.4630E-04	1.7909E-03	1.7969E-03	94.670
72	2	.0000	.0000	3.2700	.02000	-6.6339E-05	9.5517E-04	9.5747E-04	93.973

- - - POWER BUDGET - - -

INPUT POWER = 3.6409E-03 WATTS
 RADIATED POWER= 3.6409E-03 WATTS
 STRUCTURE LOSS= 0.0000E+00 WATTS
 NETWORK LOSS = 0.0000E+00 WATTS
 EFFICIENCY = 100.00 PERCENT

***** DATA CARD NO. 7 EN 0 0 0 0 0.00000E+00 0.00000E+00 0.00000E+00 0.00000E+00
 0.00000E+00 0.00000E+00

RUN TIME = 1.952

LIST OF REFERENCES

1. Stutzman, W. L., Thiele, G. A., *Antenna Theory and Design*, John Wiley and Sons, Inc., 1981
2. Morgan, M. A., *Notes on the Unloaded Monopole Antenna Solution via Cylindrical Harmonic Expansions*, dated 5 May 1988 and 6 July 1988
3. Harrington, R. F., *Time-Harmonic Electromagnetic Fields*, McGraw-Hill Book Company, Inc., 1961
4. Ramo, S., Whinnery, J. R., Van Duzer, T., *Fields and Waves in Communication Electronics*, John Wiley and Sons, Inc., 1984
5. Strum, R. D., Kirk, D. E., *First Principles of Discrete Systems and Digital Signal Processing*, Addison-Wesley Publishing Company, Inc., 1988
6. Burke, G. J., Poggio, A. J., *Numerical Electromagnetic Code (NEC) -- Method of Moments; Part III: Users Guide*, Lawrence Livermore National Laboratory, 1981
7. Bringham, E. O., *The Fast Fourier Transform*, Prentice-Hall, Inc., 1971

INITIAL DISTRIBUTION LIST

		No. Copies
1.	Defense Technical Information Center Cameron Station Alexandria, VA 22304-6145	2
2.	Library, Code 0142 Naval Postgraduate School Monterey, CA 93943-5002	2
3.	Department Chairman, Code 62 Department of Electrical and Computer Engineering Naval Postgraduate School Monterey, CA 93943-5000	1
4.	Professor M. A. Morgan, Code 62Mw Department of Electrical and Computer Engineering Naval Postgraduate School Monterey, CA 93943-5000	10
5.	Professor Richard W. Adler, Code 62Ab Department of Electrical and Computer Engineering Naval Postgraduate School Monterey, CA 93943-5000	1
6.	Dr. Arthur Jordan Code 1114SE Office of Naval Research 800 N. Quincy St. Arlington, VA 22217	1
7.	Dr. David Lewis AST Office Defense Advanced Research Projects Agency 1400 Wilson Blvd. Arlington, VA 22209	1
8.	Dr. Felix Schwering ATTN: AMSEL-RD-C3-TA1 Myer Center for C3 Systems Fort Monmouth, NJ 07703	2

9. Dr. James W. Mink 1
Electronics Division
Army Research Office
P.O. Box 12211
Research Triangle Park, NC 27709
10. LT Robert Hurley 2
c/o Naval Education Training Center
Department Head Class 107
Newport, RI 02840